Appendix A.19:

Aldershot St – CPT 5261

Table 1: Site Description for Aldershot St (CPT 5261 – CC LIQ 9).

Attribute	Yes/No			Description/Date	Symbol in Figure 1
	10-m Buffer	20-m Buffer	50-m Buffer		
Near a body of surface water or other free face features?	No	No	No	Situated on the inside of the meander of the Avon River. The center of the site is 910 m away from the nearest free-face feature that is ~2.0 m high and stretches NW-SE.	NA
Lateral spreading observed during the CES?	No	No	No	Absence of ground cracks indicates no lateral spreading, as observed by the mapping team.[1]	NA
Nearby buildings or structures?	Yes	Yes	Yes	Building coverage of the 10-m, 20-m, and 50-m buffers is 19%, 22%, and 20%, respectively. Buildings are in the NW, NE, and SW quadrants of the 10-m and 20-m buffers and in all quadrants of the 50-m buffer.	White Fill + Brown Outline
Sloping land?	No	No	No	Flat land, residential area.	NA
Step changes in the ground surface?	No	No	No	NA	NA
Retaining walls?	No	No	No	NA	NA
Vegetation?	Yes	Yes	Yes	Trees and bushes cover 22% of the 10-m buffer, 15% of the 20-m buffer and 24% of the 50-m buffer and spread through all quadrants.	White Fill + Green Outline
Anthropogenic changes to the site between the LiDAR surveys?	Yes	Yes	Yes	Building addition in the NW quadrant of the 50-m buffer between Feb 2006 and Mar 2009. Building removal at the N rim of the 50-m buffer between Mar 2014 and Jun 2015. Between Jan 2015 and Apr 2015, removal of one building in the N half of all the buffers and two more buildings in the N half of the 50-m buffer. Outside of the 50-m buffer, 11 buildings were removed between Mar 2014 and Jun 2015, and six new buildings were constructed at these properties by Jun 2015.	Addition of Building by 2009: Yellow Crossline; Removal and Addition of Buildings in 2014 and 2015: Orange Crossline
Other important factors?	Yes	Yes	Yes	Low-motor-vehicle-volume roadway occupies 2%, 18%, and 9% of the 10-m, 20-m, and 50-m buffers, respectively, affecting the SE quadrant of the 10-m buffer and the NE, SE, and SW quadrants of the 20-m and 50-m buffers.	Road: Gray Fill + Red Outline

Note: Buffer is the area within a circle of a specified radius with CPT investigations done at its center (172.697064°, -43.510579°).

[1] Canterbury Geotechnical Database. (2012). "Observed Ground Crack Locations", Map Layer CGD0400 - 23 July 2012, retrieved July 09, 2018 from https://canterburygeotechnicaldatabase.projectorbit.com/

Figure 1: Site plan with areas where LiDAR survey data is considered.

Note 1: Eight patches (outlined in red) in free field were initially selected for settlement assessment as areas free of vegetation and structures. Further analyses such as proximity of a patch to a CPT, proximity of a patch to a property subjected to addition and/or demolition of a structure, front yard/backyard alterations (e.g., ploughing, rubble, scrap), aerial distribution of sediment ejecta, and density of LiDAR points for 2003 resulted in Patches A and B being selected for detailed settlement assessment and other patches being discarded in detailed settlement assessment. In addition, since significant amounts of ejecta were observed on roads in the CES, the entire portion of the road was analyzed for settlement. Roads as hard, relatively flat surfaces provide many ground-classified points. Therefore, it is very useful to compare settlement estimates on roads with settlement estimates for the unpaved patches.

Table 2: LiDAR flight error adjustments, global adjustments for the difference between average LiDAR point elevations and benchmark survey elevations, and vertical tectonic movement adjustments.

	Adjustments (mm)		
Earthquake Event(s)	LiDAR Flight Error	Global Offset[2]	Tectonic Vertical Movement
Sep-10	0	-3	0
Feb-11	0	16	-30
Jun-11	0	38	-50
Dec-11	0	-65	10
CES	0	-14	-70
Any LiDAR survey affected by ejecta?*			Yes

Notes: The negative sign indicates the subtraction from the ground surface subsidence, while the positive sign indicates the addition to the ground surface subsidence; * indicates the presence of ejecta at the site at the time of the March 2011 LiDAR survey (and potentially May 2011 LiDAR survey) hence the total ground surface subsidence will be increased by 50 mm for the Feb-11 EQ and reduced by the same amount for the Jun-11 EQ.

Table 3a: LiDAR Measurement Error for Patch A.

Surveys	Buffer	Area Averaged Difference Indicating Repeat Measurement Error (mm)	$\sigma^*_{\text{individual LiDAR points}}$ (mm)	%Reduction in σ due to Area Averaging of LiDAR Points
Post Feb 2011: Mar 2011 and May 2011	10-m	65	59	[110,110]
	20-m	65		
	50-m	65		
Post Dec 2011: Feb 2012 and Oct 2015	10-m	7	70	[10,10]
	20-m	7		
	50-m	7		

*Standard deviation.

[2] Russell, J., & van Ballegooy, S. (2015). *Canterbury Earthquake Sequence: Increased liquefaction vulnerability assessment methodology*. New Zealand: Tonkin & Taylor Ltd.

Table 3b: LiDAR Measurement Error for Patch B.

Surveys	Buffer	Area Averaged Difference Indicating Repeat Measurement Error (mm)	$\sigma^*_{\text{individual LiDAR points}}$ (mm)	%Reduction in σ due to Area Averaging of LiDAR Points
Post Feb 2011: Mar 2011 and May 2011	10-m	NA	59	[110,110]
	20-m	NA		
	50-m	65		
Post Dec 2011: Feb 2012 and Oct 2015	10-m	NA	70	[7,7]
	20-m	NA		
	50-m	5		

*Standard deviation.

Table 3c: LiDAR Measurement Error for Road.

Surveys	Buffer	Area Averaged Difference Indicating Repeat Measurement Error (mm)	$\sigma^*_{\text{individual LiDAR points}}$ (mm)	%Reduction in σ due to Area Averaging of LiDAR Points
Post Feb 2011: Mar 2011 and May 2011	10-m	137	59	[139,147]
	20-m	82		
	50-m	87		
Post Dec 2011: Feb 2012 and Oct 2015	10-m	19	70	[4,6]
	20-m	4		
	50-m	3		

*Standard deviation.

Table 4a: Ground surface subsidence adjustments due to LiDAR measurement error for Patch A.

Earthquake Event(s)	$\sigma_{\text{pre-EQ LiDAR survey}}$ (mm)	$\sigma_{\text{post-EQ LiDAR survey}}$ (mm)	σ_{total} (mm)	Area Average Adjusted σ (mm)**
Sep-10	158	56	134	±148
Feb-11	56	59	59	±65
Jun-11	59	61	62	±69
Dec-11	61	70	87	±95
CES	158	70	124	±137

**Based on the highest %Reduction in Table 3a.

Table 4b: Ground surface subsidence adjustments due to LiDAR measurement error for Patch B.

Earthquake Event(s)	$\sigma_{\text{pre-EQ LiDAR survey}}$ (mm)	$\sigma_{\text{post-EQ LiDAR survey}}$ (mm)	σ_{total} (mm)	Area Average Adjusted σ (mm) **
Sep-10	158	56	134	±148
Feb-11	56	59	59	±65
Jun-11	59	61	62	±69
Dec-11	61	70	87	±95
CES	158	70	124	±137

**Based on the highest %Reduction in Table 3b.

Table 4c: Ground surface subsidence adjustments due to LiDAR measurement error for Road.

Earthquake Event(s)	$\sigma_{\text{pre-EQ LiDAR survey}}$ (mm)	$\sigma_{\text{post-EQ LiDAR survey}}$ (mm)	σ_{total} (mm)	Area Average Adjusted σ (mm) **
Sep-10	158	56	134	±198
Feb-11	56	59	59	±87
Jun-11	59	61	62	±92
Dec-11	61	70	87	±128
CES	158	70	124	±184

**Based on the highest %Reduction in Table 3c.

Table 5a: Raw liquefaction-related ground surface subsidence using original LiDAR points for Patch A.

	Average Ground Surface Subsidence (mm)		
Earthquake Event(s)	10-m Buffer	20-m Buffer	50-m Buffer
Sep-10	30	30	30
Feb-11	242	242	242
Jun-11	110	110	110
Dec-11	75	75	75
CES	457	457	457

Table 5b: Raw liquefaction-related ground surface subsidence using original LiDAR points for Patch B.

	Average Ground Surface Subsidence (mm)		
Earthquake Event(s)	10-m Buffer	20-m Buffer	50-m Buffer
Sep-10	NA	NA	41
Feb-11	NA	NA	259
Jun-11	NA	NA	76
Dec-11	NA	NA	63
CES	NA	NA	440

Table 5c: Raw liquefaction-related ground surface subsidence using original LiDAR points for Road.

	Average Ground Surface Subsidence (mm)		
Earthquake Event(s)	10-m Buffer	20-m Buffer	50-m Buffer
Sep-10	74	48	26
Feb-11	70	82	90
Jun-11	146	99	90
Dec-11	58	77	69
CES	348	306	275

Table 6a: Corrected liquefaction-related ground surface subsidence using original LiDAR points for Patch A with the calculated adjustments in Table 2.

	Average Calculated Ground Surface Subsidence (mm)		
Earthquake Event(s)	10-m Buffer	20-m Buffer	50-m Buffer
Sep-10	27±150	27±150	27±150
Feb-11	278±75	278±75	278±75
Jun-11	47±75	47±75	47±75
Dec-11	20±100	20±100	20±100
CES	372±125	372±125	372±125

Notes: Plus/minus values are same as those in Table 4a, but rounded to the nearest 25; Positive overall values indicate ground surface subsidence, while negative overall values indicate ground surface uplift.

Table 6b: Corrected liquefaction-related ground surface subsidence using original LiDAR points for Patch B with the calculated adjustments in Table 2.

	Average Calculated Ground Surface Subsidence (mm)		
Earthquake Event(s)	10-m Buffer	20-m Buffer	50-m Buffer
Sep-10	NA	NA	38±150
Feb-11	NA	NA	295±75
Jun-11	NA	NA	14±75
Dec-11	NA	NA	8±100
CES	NA	NA	356±125

Notes: Plus/minus values are same as those in Table 4b, but rounded to the nearest 25; Positive overall values indicate ground surface subsidence, while negative overall values indicate ground surface uplift.

Table 6c: Corrected liquefaction-related ground surface subsidence using original LiDAR points for Road with the calculated adjustments in Table 2.

	Average Calculated Ground Surface Subsidence (mm)		
Earthquake Event(s)	10-m Buffer	20-m Buffer	50-m Buffer
Sep-10	71±200	45±200	23±200
Feb-11	106±75	118±75	126±75
Jun-11	84±100	37±100	28±100
Dec-11	3±125	22±125	14±125
CES	264±175	222±175	191±175

Notes: Plus/minus values are same as those in Table 4c, but rounded to the nearest 25; Positive overall values indicate ground surface subsidence, while negative overall values indicate ground surface uplift.

Table 7a: Corrected liquefaction-related ground surface subsidence for Patch A using LiDAR DEMs.

	Estimated Ground Surface Subsidence (mm)								
	10-m Buffer			20-m Buffer			50-m Buffer		
Earthquake Event(s)	16th %ile	50th %ile	84th %ile	16th %ile	50th %ile	84th %ile	16th %ile	50th %ile	84th %ile
Sep-10	50	50	50	50	50	50	50	50	50
Feb-11	300	300	350	300	300	350	300	300	350
Jun-11	<50	<50	<50	<50	<50	<50	<50	<50	<50
Dec-11	50	50	50	50	50	50	50	50	50
CES	350	350	450	350	350	450	350	350	450

Note: These percentiles are not the exact statistical measures; they indicate the spatial variability of ground surface subsidence.

Table 7b: Corrected liquefaction-related ground surface subsidence for Patch B using LiDAR DEMs.

	Estimated Ground Surface Subsidence (mm)								
	10-m Buffer			20-m Buffer			50-m Buffer		
Earthquake Event(s)	16th %ile	50th %ile	84th %ile	16th %ile	50th %ile	84th %ile	16th %ile	50th %ile	84th %ile
Sep-10	NA	NA	NA	NA	NA	NA	50	50	50
Feb-11	NA	NA	NA	NA	NA	NA	200	200	200
Jun-11	NA	NA	NA	NA	NA	NA	<50	<50	<50
Dec-11	NA	NA	NA	NA	NA	NA	50	50	50
CES	NA	NA	NA	NA	NA	NA	300	350	400

Note: These percentiles are not the exact statistical measures; they indicate the spatial variability of ground surface subsidence.

Table 7c: Corrected liquefaction-related ground surface subsidence for Road using LiDAR DEMs.

	Estimated Ground Surface Subsidence (mm)								
	10-m Buffer			20-m Buffer			50-m Buffer		
Earthquake Event(s)	16th %ile	50th %ile	84th %ile	16th %ile	50th %ile	84th %ile	16th %ile	50th %ile	84th %ile
Sep-10	50	50	50	50	50	50	50	50	50
Feb-11	100	100	150	100	150	200	150	200	200
Jun-11	<50	<50	<50	<50	<50	<50	<50	<50	<50
Dec-11	50	50	50	50	50	100	50	50	100
CES	250	250	350	250	250	350	250	350	350

Note: These percentiles are not the exact statistical measures; they indicate the spatial variability of ground surface subsidence.

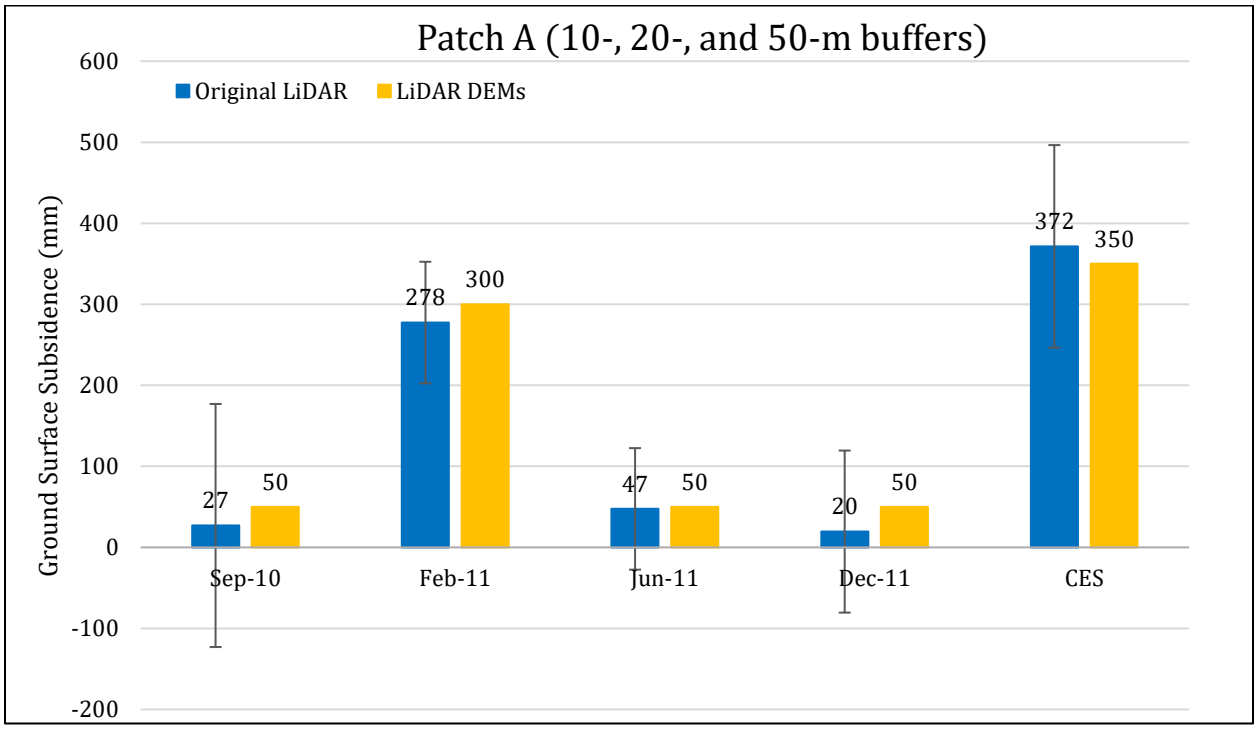

Figure 2: Comparison between ground surface subsidence determined from original LiDAR survey points and ground surface subsidence (50th %ile) estimated using LiDAR DEMs for Patch A.

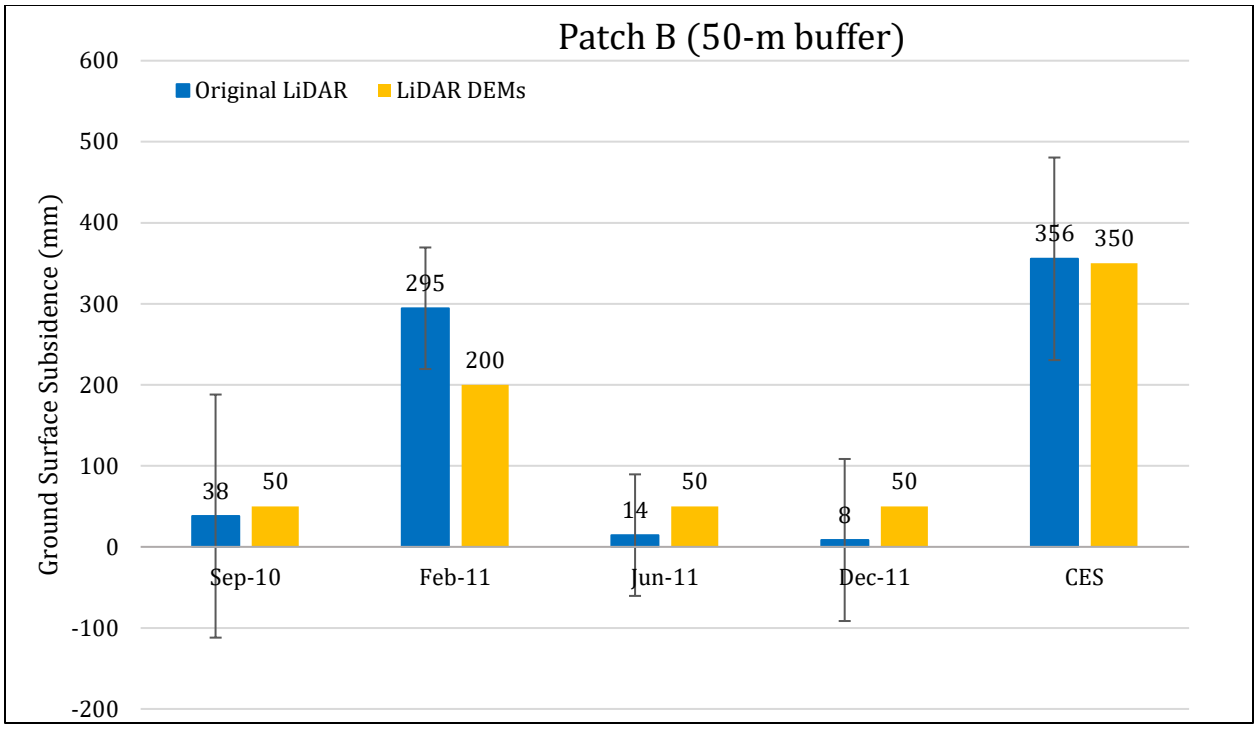

Figure 3: Comparison between ground surface subsidence determined from original LiDAR survey points and ground surface subsidence (50th %ile) estimated using LiDAR DEMs for Patch B.

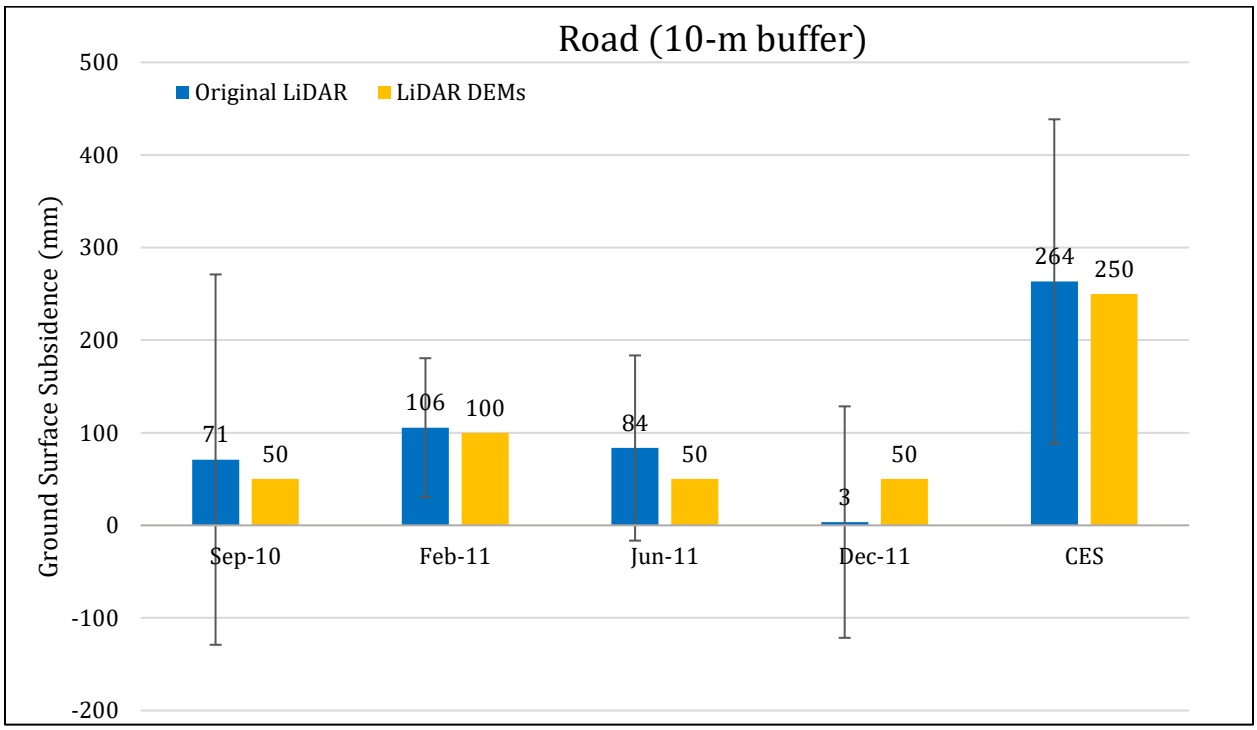

Figure 4: Comparison between ground surface subsidence determined from original LiDAR survey points and ground surface subsidence (50th %ile) estimated using LiDAR DEMs for Road for the 10-m buffer.

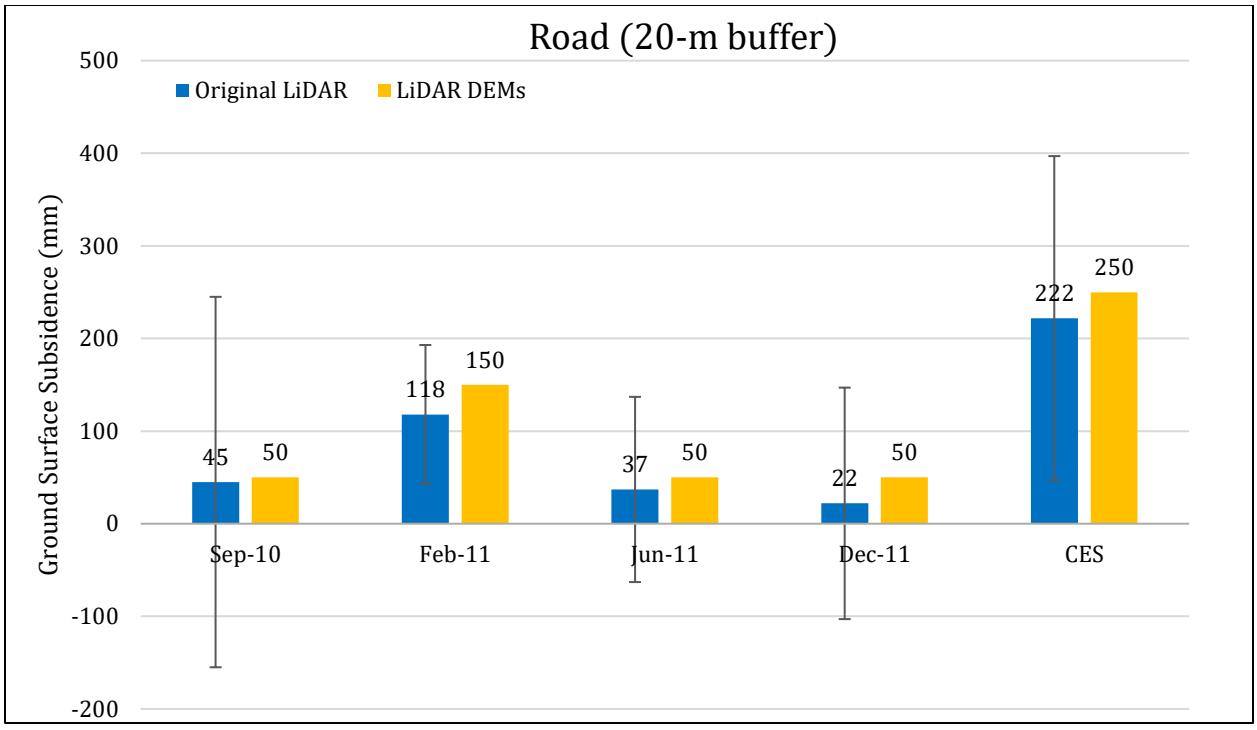

Figure 5: Comparison between ground surface subsidence determined from original LiDAR survey points and ground surface subsidence (50th %ile) estimated using LiDAR DEMs for Road for the 20-m buffer.

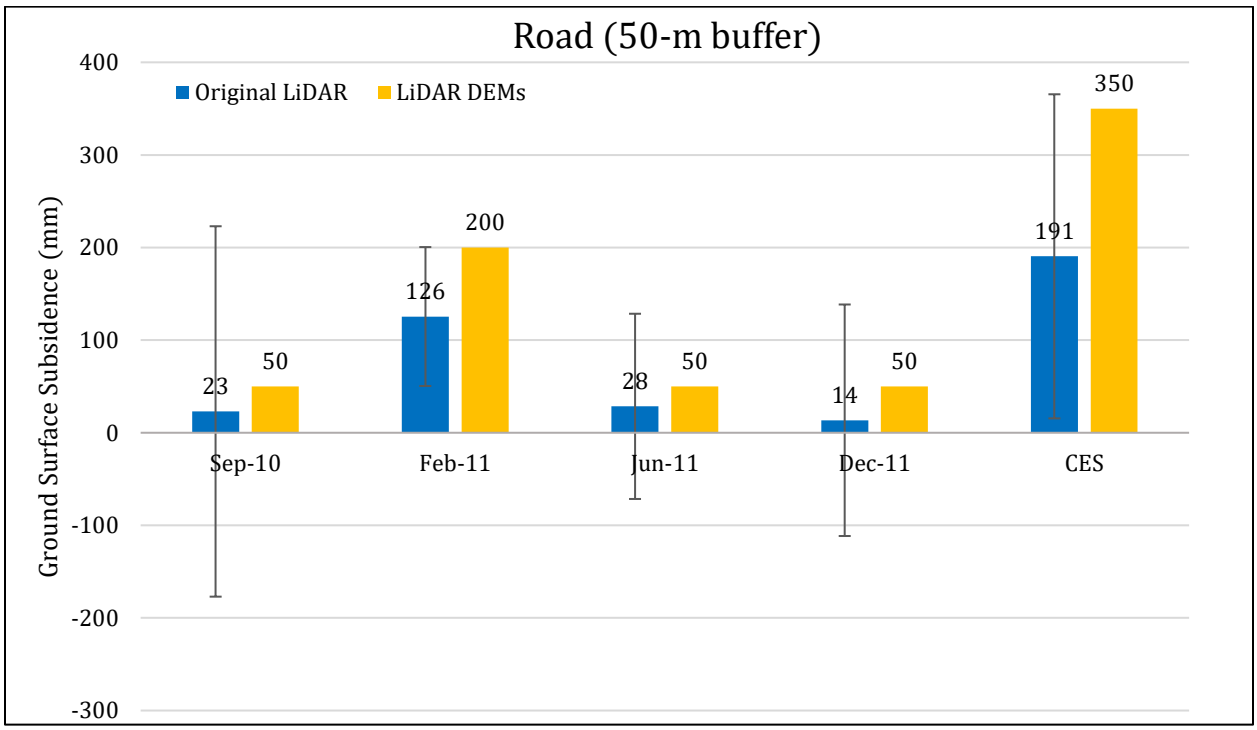

Figure 6: Comparison between ground surface subsidence determined from original LiDAR survey points and ground surface subsidence (50th %ile) estimated using LiDAR DEMs for Road for the 50-m buffer.

Note 2: The ground surface subsidence values determined from original LiDAR survey points are similar to the ground surface subsidence values estimated using LiDAR DEMs for all earthquake events.

Table 8a: Ejecta-Induced settlement for the top 20 m of the soil profile for Patch A for the 50th %ile PGA, P_L=50%, and C_{FC}=0.13 using BI-2014, ZRB-2002, and I_C cutoff of 2.6.

Earthquake Event(s)	M_W	PGA (g)	Depth to Groundwater (m)	S_T(mm)	S_{V1D} (mm)	$S_{E,L}$ (mm)
Sep-10	7.1	0.18	1.8	27±150	19±20	8±151
Feb-11	6.2	0.42	1.8	278±75	132±50	146±90
Jun-11	6.2	0.28	1.5	47±75	74±25	-27±79
Dec-11	6.1	0.31	1.5	20±100	88±50	-68±112

Notes: S_T = Total settlement (Table 6); S_{V1D} = Average vertical settlement due to volumetric compression using Boulanger and Idriss (2014) (BI-2014), Zhang et al. (2002) (ZRB-2002) procedures and de Greef and Lengkeek (2018) thin-layer correction; $S_{E,L}$ = Ejecta-induced settlement as the difference between the LiDAR-based S_T and S_{V1D}.

Table 8b: Ejecta-Induced settlement for the top 20 m of the soil profile for Patch B for the 50th %ile PGA, P_L=50%, and C_{FC}=0.13 using BI-2014, ZRB-2002, and I_C cutoff of 2.6.

Earthquake Event(s)	M_W	PGA (g)	Depth to Groundwater (m)	S_T(mm)	S_{V1D} (mm)	$S_{E,L}$ (mm)
Sep-10	7.1	0.18	1.8	38±150	5±25	33±151
Feb-11	6.2	0.42	1.8	295±75	83±50	212±90
Jun-11	6.2	0.28	1.5	14±75	32±40	-18±79
Dec-11	6.1	0.31	1.5	8±100	42±50	-34±112

Notes: S_T = Total settlement (Table 6); S_{V1D} = Average vertical settlement due to volumetric compression using Boulanger and Idriss (2014) (BI-2014), Zhang et al. (2002) (ZRB-2002) procedures and de Greef and Lengkeek (2018) thin-layer correction; $S_{E,L}$ = Ejecta-induced settlement as the difference between the LiDAR-based S_T and S_{V1D}.

Table 8c: Ejecta-Induced settlement for the top 20 m of the soil profile for Road within the 50-m buffer for the 50th %ile PGA, P_L=50%, and C_{FC}=0.13 using BI-2014, ZRB-2002, and I_c cutoff of 2.6.

Earthquake Event(s)	M_W	PGA (g)	Depth to Groundwater (m)	S_T(mm)	S_{V1D} (mm)	$S_{E,L}$ (mm)
Sep-10	7.1	0.18	1.8	23±200	14±20	9±201
Feb-11	6.2	0.42	1.8	126±75	115±50	11±90
Jun-11	6.2	0.28	1.5	28±100	60±25	-32±103
Dec-11	6.1	0.31	1.5	14±125	73±50	-59±135

Notes: S_T = Total settlement (Table 6); S_{V1D} = Average vertical settlement due to volumetric compression using Boulanger and Idriss (2014) (BI-2014), Zhang et al. (2002) (ZRB-2002) procedures and de Greef and Lengkeek (2018) thin-layer correction; $S_{E,L}$ = Ejecta-induced settlement as the difference between the LiDAR-based S_T and S_{V1D}.

Note 3: The uncertainty for volumetric settlement was derived based on the sensitivity of volumetric settlement to PGA, C_{FC}, and P_L for each earthquake event for VsVp 57203 *Shirley Intermediate School* and CC LIQ 1 – CPT 5586 – *Vivian St* sites. Taking the 50th percentile as the baseline case, the minimum and maximum values corresponding to the difference between the 25th percentile and the 50th percentile and the 75th percentile and the 50th percentile were determined. The arithmetic mean of the range of the minimum and maximum difference was evaluated for each patch at the two sites. The maximum arithmetic mean for each earthquake event was rounded to the nearest five and used as the uncertainty value. Accordingly, the 1-D volumetric settlement uncertainties of ±20, ±50, ±25, and ±50 mm for the Sep-10, Feb-11, Jun-11, and Dec-11 earthquake events, respectively, were used for all sites in this study.

Table 9a: Coverage area and height of ejecta estimates for Patch A using photographs.

Earthquake Event	$A_{E,thick}$ (m^2)	$H_{E,thick}$ (mm)	$A_{E,thin}$ (m^2)	$H_{E,thin}$ (mm)	A_T (m^2)
Sep-10	0	0	0	0	54.0
Feb-11	30.4	40-60	21.9	20-40	52.3*
Jun-11	NA	NA	NA	NA	54.0
Dec-11	0	0	0	0	54.0

Notes: $A_{E,thick/thin}$ = Coverage area of thick/thin ejecta layers; $H_{E,thick/thin}$ = Lower-upper estimate of height of thick/thin ejecta layers; A_T = Total assessment area of a buffer being considered; Thin and thick layers correspond to light gray and dark gray colors of ejecta observed in aerial photographs; NA = Not available due to the presence of shadows within the assessment area; * indicates reduction in A_T due to the presence of objects within the assessment area.

Table 9b: Coverage area and height of ejecta estimates for Patch B using photographs.

Earthquake Event	$H_{E,thin1}$ (mm)	$A_{E,thin1}$ (m^2)	$H_{E,thin2}$ (mm)	$A_{E,thin2}$ (m^2)	$H_{E,thick}$ (mm)	$A_{E,thick}$ (m^2)	A_T (m^2)
Sep-10	0	0	0	0	0	0	81.2
Feb-11	40-60	22.9	60-80	21.4	100-160	36.9	81.2
Jun-11*	0	0	40-100	23.2	0	0	81.9
Dec-11	0	0	5-10	9.1	20-40	72.8	81.9

Notes: $A_{E,thick/thin}$ = Coverage area of thick/thin ejecta layers; $H_{E,thick/thin}$ = Lower-upper estimate of height of thick/thin ejecta layers; A_T = Total assessment area of a buffer being considered; Thin and thick layers correspond to light gray and dark gray colors of ejecta observed in aerial photographs; * indicates uncertainty in the estimate due to the presence of shadows within the assessment area in the aerial photographs.

Table 9c: Coverage area and height of ejecta estimates for Road within the 50-m buffer using photographs.

Earthquake Event	$H_{E,thin}$ (mm)	$A_{E,thin}$ (m^2)	$H_{E,thick}$ (mm)	$A_{E,thick}$ (m^2)	$H_{E,prism/pyr}$ (mm)	$V_{E,prism+pyr}$ (m^3)	A_T (m^2)
Sep-10	0	0	0	0	0	0	730
Feb-11	0	0	5-15	88.6	10-300	41-65	698
Jun-11	3-6	149	0	0	23-260	26-45	717
Dec-11	0	0	5-10	21.7	7-260	14-20	730

Notes: $A_{E,thick/thin}$ = Coverage area of thick/thin ejecta layers; $H_{E,thick/thin}$ = Lower-upper estimate of height of thick/thin ejecta layers; $H_{E,prism/pyr}$ = Lower-upper estimate of ejecta height near the curb based on 2-4% cross slope of normal crown; $V_{E,prism+pyr}$ = Lower-upper estimate of total volume of prismatic- and pyramidal-shape ejecta; A_T = Total assessment area of a buffer being considered; Thin and thick layers correspond to light gray and dark gray colors of ejecta observed in aerial photographs.

Note 4: The values in Table 9 correspond to the coverage area of ejecta outlined in aerial photographs (Figures 88 through 92) and the lower and upper estimates of ejecta height based on geometry, ground photographs (Figure 93 and 95), and EQC LDAT property inspection notes (Figures 94 and 96) and reports from Sep 2011. The ejecta-induced settlement using photographs and engineering judgment, $S_{E,P}$, is estimated as

$$S_{E,P} = \frac{\sum_{i=1}^{a} A_{E,thick,i} * H_{E,thick,i} + \sum_{j=1}^{b} A_{E,thin,j} * H_{E,thin,j} + \frac{1}{2}\sum_{n=1}^{f} W_{E,prism,n} * H_{E,prism,n} * L_{E,prism,n}}{A_T}$$
$$= \frac{\sum_{i=1}^{a} V_{E,thick,i} + \sum_{j=1}^{b} V_{E,thin,j} + \sum_{n=1}^{f} V_{E,prism,n}}{A_T}$$

where

- $A_{E,thick,i}$ and $H_{E,thick,i}$ are the area and the height of a thick ejecta layer, respectively;
- $A_{E,thin,j}$ and $H_{E,thin,j}$ are the area and the height of a thin ejecta layer, respectively;
- $W_{E,prism,n}$ and $L_{E,prism,n}$ are the width and the length of the coverage area of a prismatically shaped ejecta layer, respectively, and $H_{E,prism,n}$ is the height of a prism-like ejecta layer;
- A_T is the total assessment area for a buffer being considered (Figure 1).

Table 10: Ejecta-induced settlement estimates for Patches A and B and Road based on photographs.

EQ Event	Patch A (10-, 20-, and 50-m buffers)		Patch B (50-m buffer)		Road (50-m buffer)	
	$S_{E,P,lower}$ (mm)	$S_{E,P,upper}$ (mm)	$S_{E,P,lower}$ (mm)	$S_{E,P,upper}$ (mm)	$S_{E,P,lower}$ (mm)	$S_{E,P,upper}$ (mm)
Sep-10	0	0	0	0	0	0
Feb-11	32	52	73	111	60	95
Jun-11	NA	NA	11*	28*	37	64
Dec-11	0	0	18	37	19	28

Notes: $S_{E,P,lower}$ and $S_{E,P,upper}$ correspond to lower and upper estimates of $S_{E,P}$, respectively; NA = Not available due to the presence of shadows within the assessment area; * indicates uncertainty due to the presence of shadows.

Table 11: Best final estimates of ejecta-induced settlement for Patches A and B and Road.

EQ Event	Patch A (10-, 20-, and 50-m buffers)			Patch B (50-m buffer)			Road (50-m buffer)		
	$S_{E,L}$ (mm)	$S_{E,P}$ (mm)	$S_{E,final}$ (mm)	$S_{E,L}$ (mm)	$S_{E,P}$ (mm)	$S_{E,final}$ (mm)	$S_{E,L}$ (mm)	$S_{E,P}$ (mm)	$S_{E,final}$ (mm)
Sep-10	8±151	0	0	33±151	0	0	9±201	0	0
Feb-11	146±90	42±10	75±30	212±90	92±19	130±35	11±90	78±17	80±15
Jun-11	-27±79	NA	NA	-18±79	*20±8	20±10	-32±103	51±13	50±15
Dec-11	-68±112	0	0	-34±112	28±9	30±10	-59±135	24±4	25±5

Notes: $S_{E,L}$ = Ejecta-induced settlement based on LiDAR data reported in Table 8; $S_{E,P}$ = Median ejecta-induced settlement for the range of values reported in Table 10; $S_{E,final}$ = Best final estimate of ejecta-induced settlement rounded to the nearest 5; Final plus/minus values are also rounded to the nearest 5; NA = Not available due to the lack of visual evidence; * indicates uncertainty due to the presence of shadows.

Note 5:

- For Patch A, $S_{E,final}$ for the Sep-10, Jun-11, and Dec-11 EQs is based solely on $S_{E,P}$, while $S_{E,final}$ for the Feb-11 EQ is a weighted average of $S_{E,L}$ and $S_{E,P}$ with weights of 1/3 and 2/3, respectively.
- For Patch B, $S_{E,final}$ is equal to $S_{E,P}$ for the Sep-10, Jun-11, and Dec-11 EQs, whereas $S_{E,final}$ for the Feb-11 EQ is a weighted average of $S_{E,L}$ and $S_{E,P}$ with weights of 1/3 and 2/3, respectively.
- For Road, $S_{E,final}$ for is based solely on $S_{E,P}$ for all earthquake events.
- The uncertainty associated with $S_{E,final}$ is also a weighted average of uncertainties associated with $S_{E,L}$ and $S_{E,P}$ with the same corresponding weights.
- The weights are based on the LiDAR error bands, LPI prediction error (Maurer et al. 2014[3]), presence of ejecta at the time of LiDAR surveys, and completeness of visual evidence (i.e., ground and aerial photographs and EQC LDAT property inspection reports for the site). The Aldershot St site is not in the apparent zone of higher/lower ground surface subsidence for any earthquake event, but the ejecta was present at the site at the time of the Mar-2011 LiDAR survey and potentially May-2011 LiDAR survey. The site is in the zone of accurate LPI prediction of liquefaction severity for the Sep-10 EQ; it is in the zone of slight LPI

[3] Maurer, B. W., Green, R. A., Cubrinovski, M., & Bradley, B. A. (2014). Evaluation of the Liquefaction Potential Index for Assessing Liquefaction Hazard in Christchurch, New Zealand. *Journal of Geotechnical and Geoenvironmental Engineering*, 140(7), 04014032-1-11. doi:10.1061/(asce)gt.1943-5606.0001117

overprediction of liquefaction severity for the Feb-11 EQ. The LDAT property inspection report is available for Patches A and B. There are no ground photographs of the road.

Summary 1:

- **The best estimate of the ejecta-induced free-field ground settlement at the Aldershot St site for the SEP 2010 earthquake is 0 mm. For the FEB 2011 earthquake, about 55% of the site experienced ejecta-induced ground settlement that ranged from 75±30 mm to 130±35 mm. For the DEC 2011 earthquake, about 20% of the site had ejecta that induced 30±10 mm of ground settlement. The ejecta-induced free-field ground settlement for the JUN 2011 earthquake can be estimated as 20±10 mm although with less certainty due to the presence of shadows in the aerial photographs within the assessment areas and the site overall.**
- **The best estimate of the ejecta-induced free-field ground settlement of the road at the Aldershot St site for the SEP 2010, FEB 2011, JUN 2011, and DEC 2011 earthquake is 0 mm, 80±15 mm, 50±15 mm, and 25±5 mm, respectively.**

Note 7: CPT 5261 was initially named as CC LIQ9.

Note 8: The original outline of Patch A was changed to the one shown in Figure 1; however, the original outline still remains in some of the following figures.

Figure 7: Location of the site.

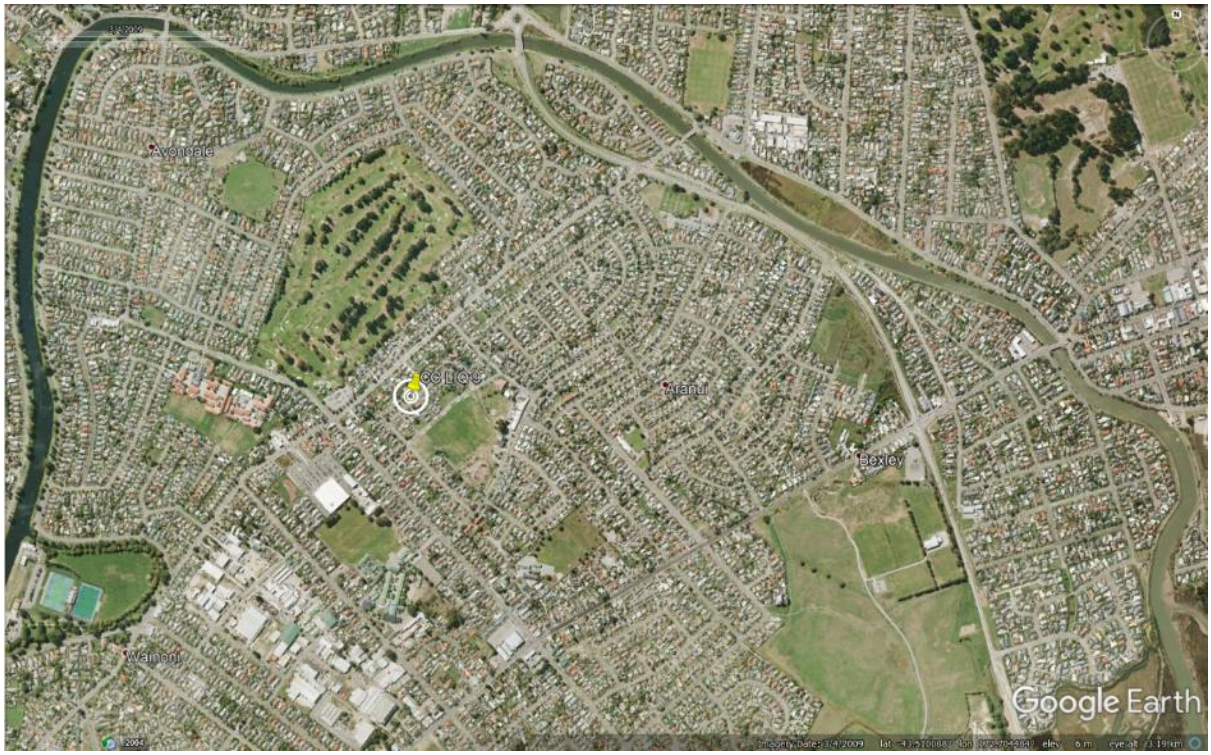

Figure 8: Position of the site relative to nearby buildings, vegetation, and free-face features.

Figure 9: Street view of the site showing flat land.

Figure 10: Satellite image of the site taken in Dec 2004.

Figure 11: Satellite image of the site taken in Feb 2006.

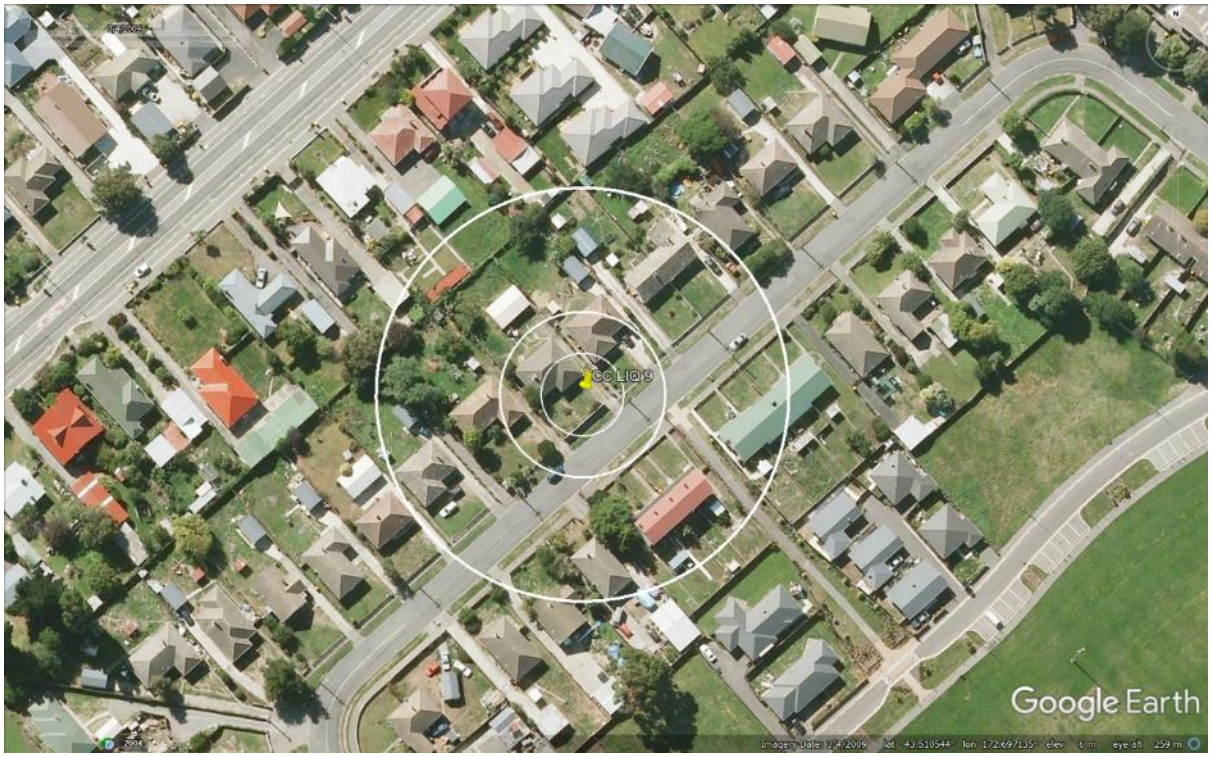

Figure 12: Satellite image of the site taken in Mar 2009.

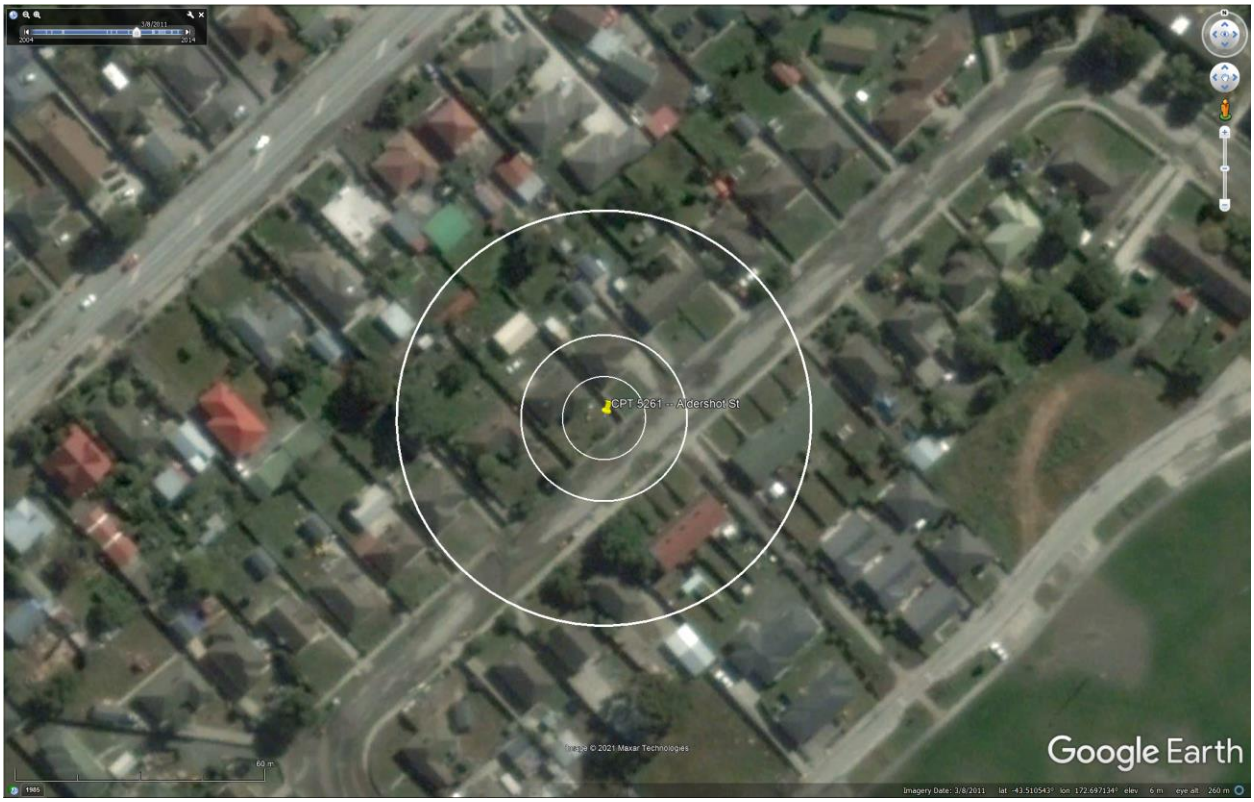

Figure 13: Satellite image acquired in Mar 2011 showing ejecta at the site.

Figure 14: Satellite image of the site taken in Apr 2012.

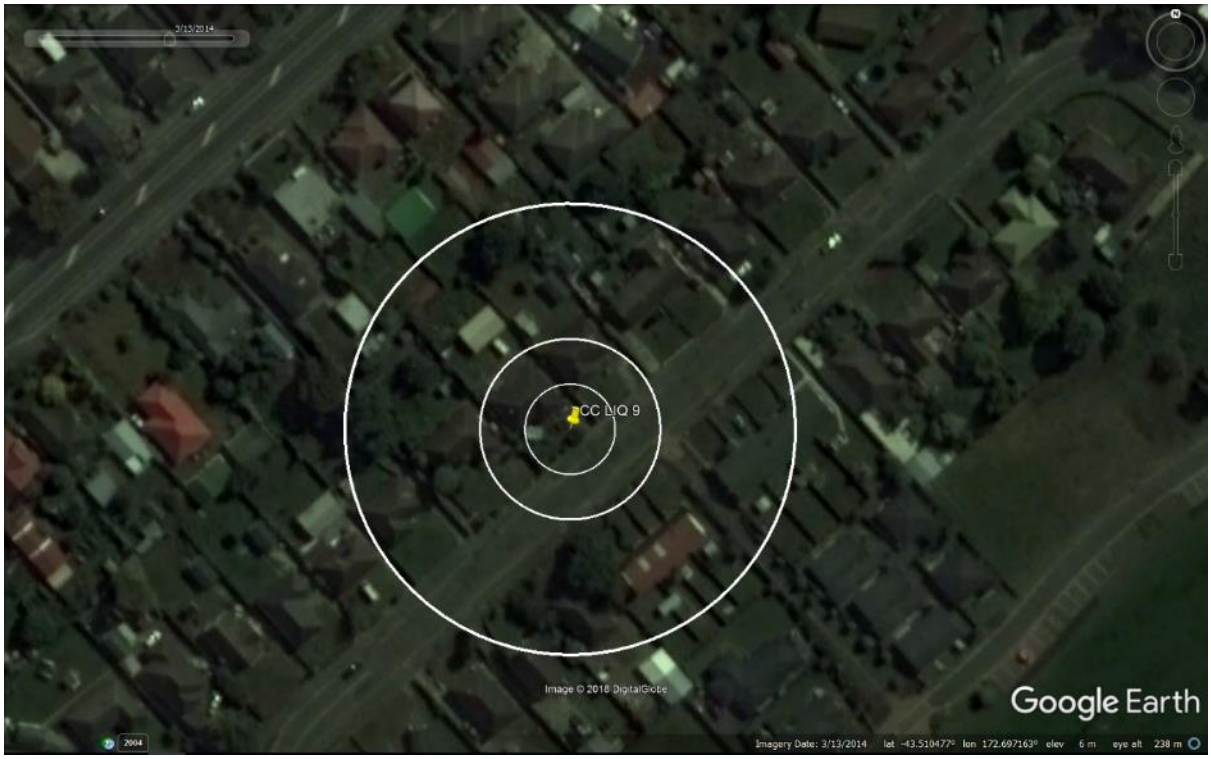

Figure 15: Satellite image of the site taken in Mar 2014.

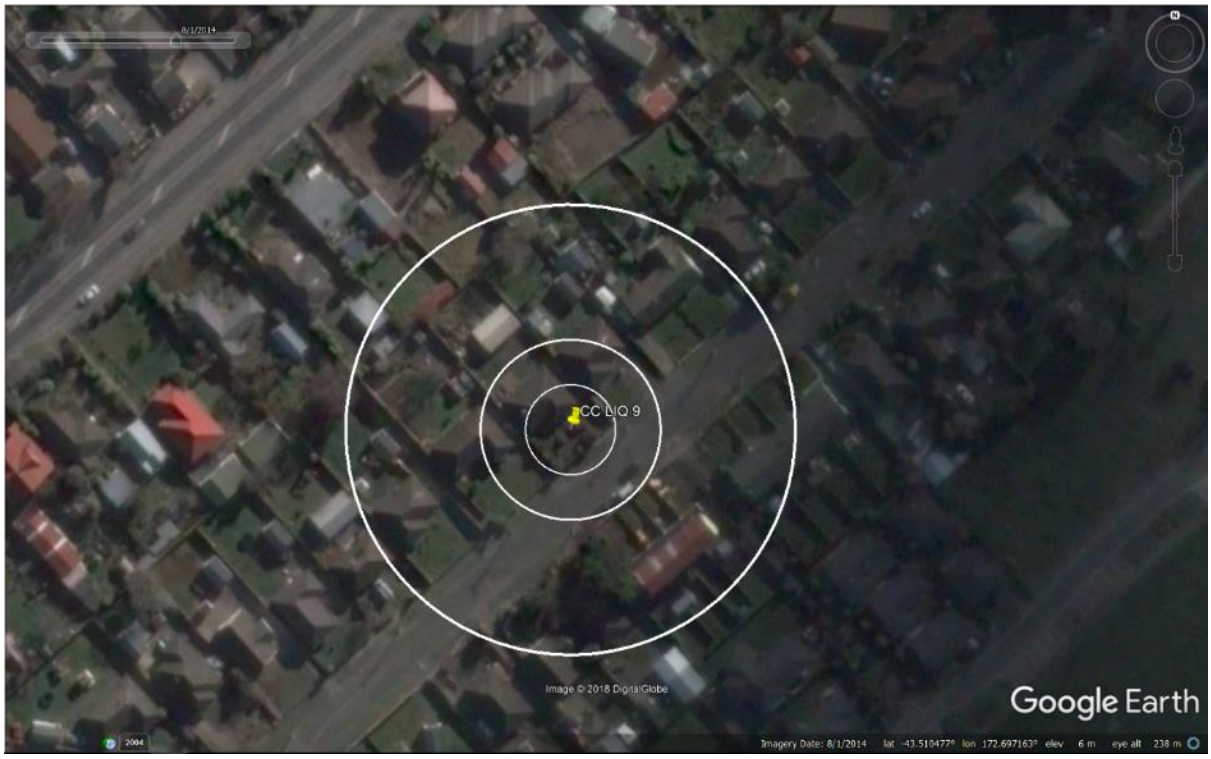

Figure 16: Satellite image of the site taken in Aug 2014.

Figure 17: Satellite image of the site taken in Sep 2014.

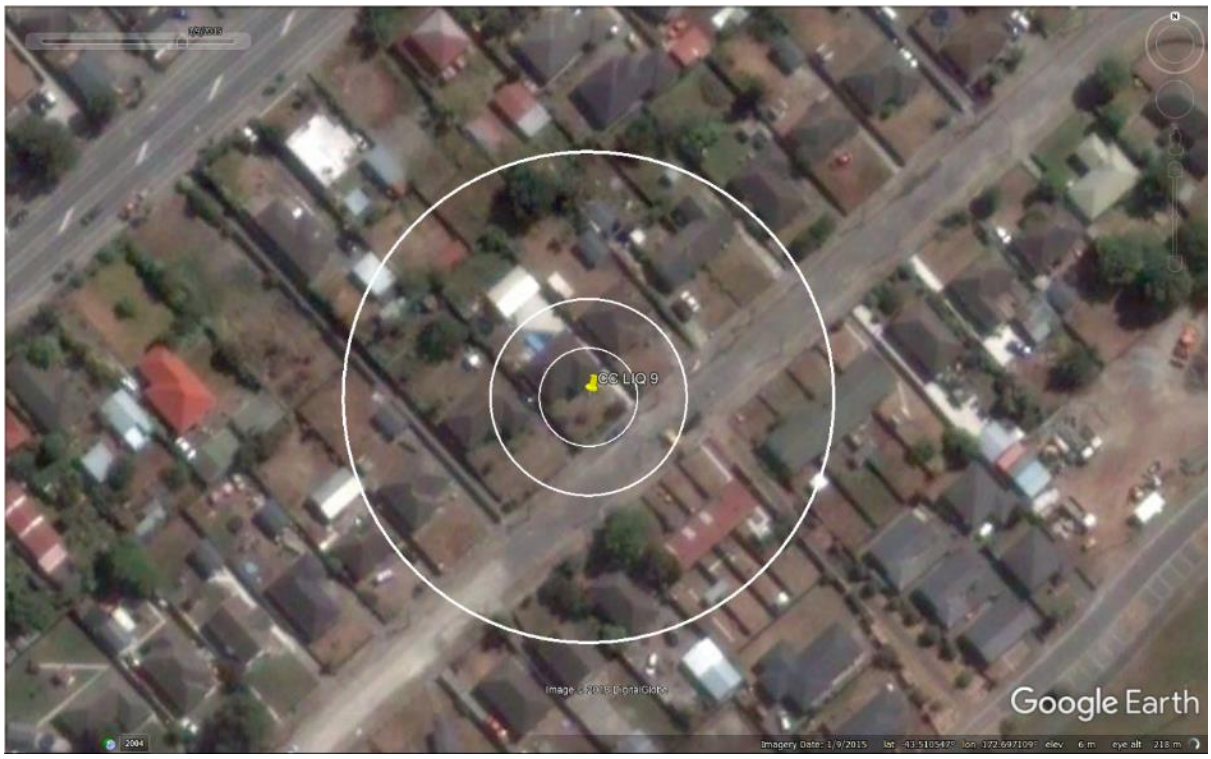

Figure 18: Satellite image of the site taken in Jan 2015.

Figure 19: Satellite image of the site taken in Apr 2015.

Figure 20: Satellite image of the site taken in Jun 2015.

Figure 21: Satellite image of the site taken in Sep 2015.

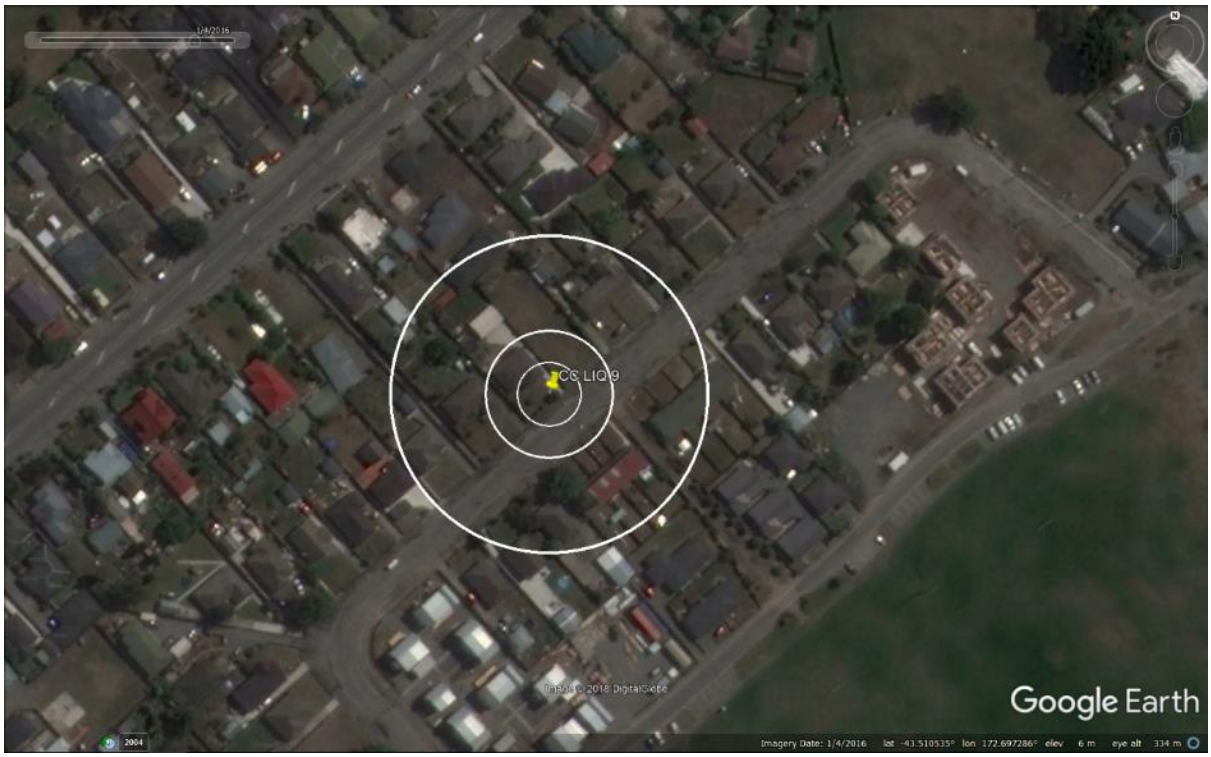

Figure 22: Satellite image of the site taken in Jan 2016.

Figure 23: Aerial photograph of the site taken on Sep 4, 2010.

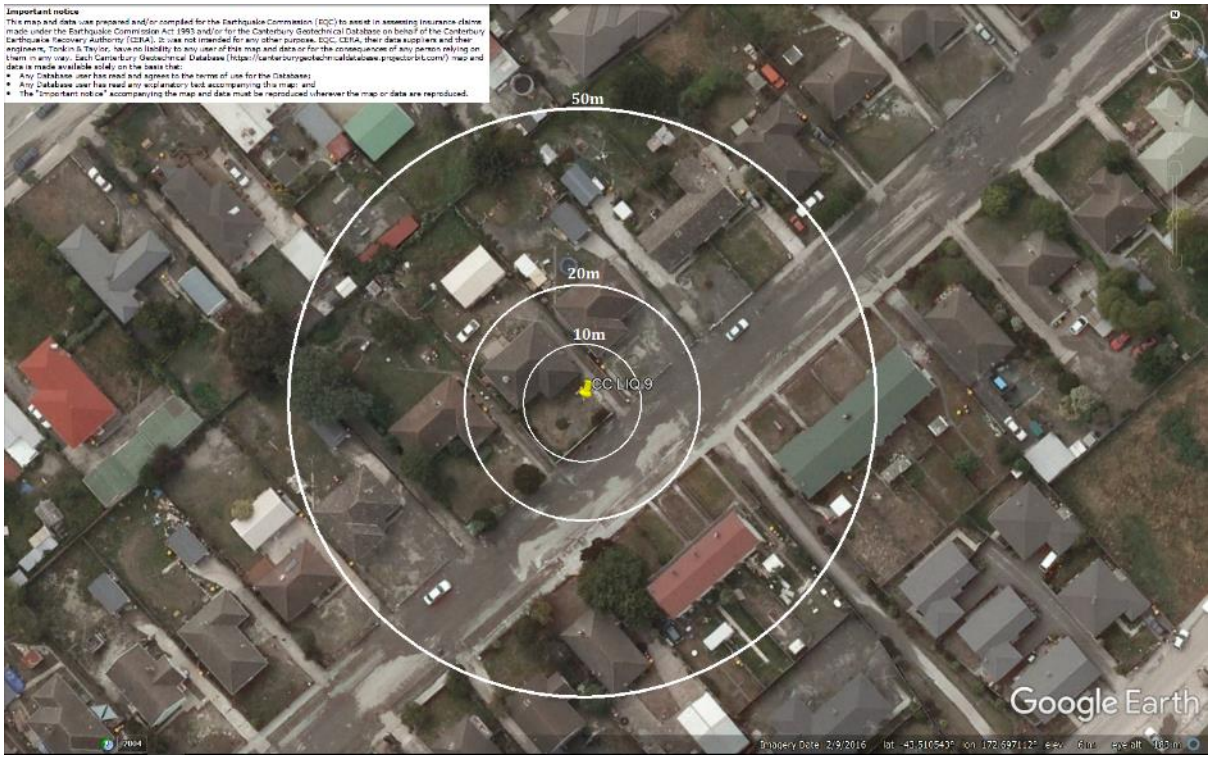

Figure 24: Aerial photograph of the site taken on Feb 24, 2011.

Figure 25: Aerial photograph of the site taken on June 16, 2011.

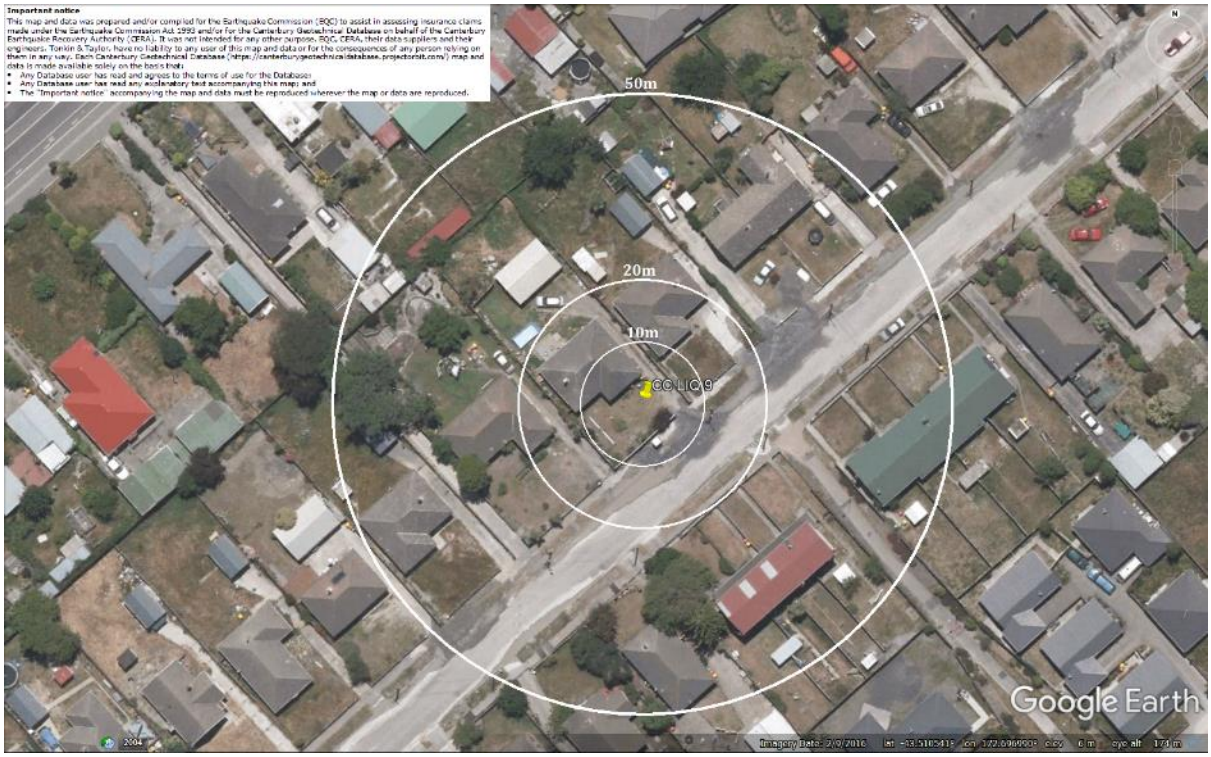

Figure 26: Aerial photograph of the site taken on Dec 24, 2012.

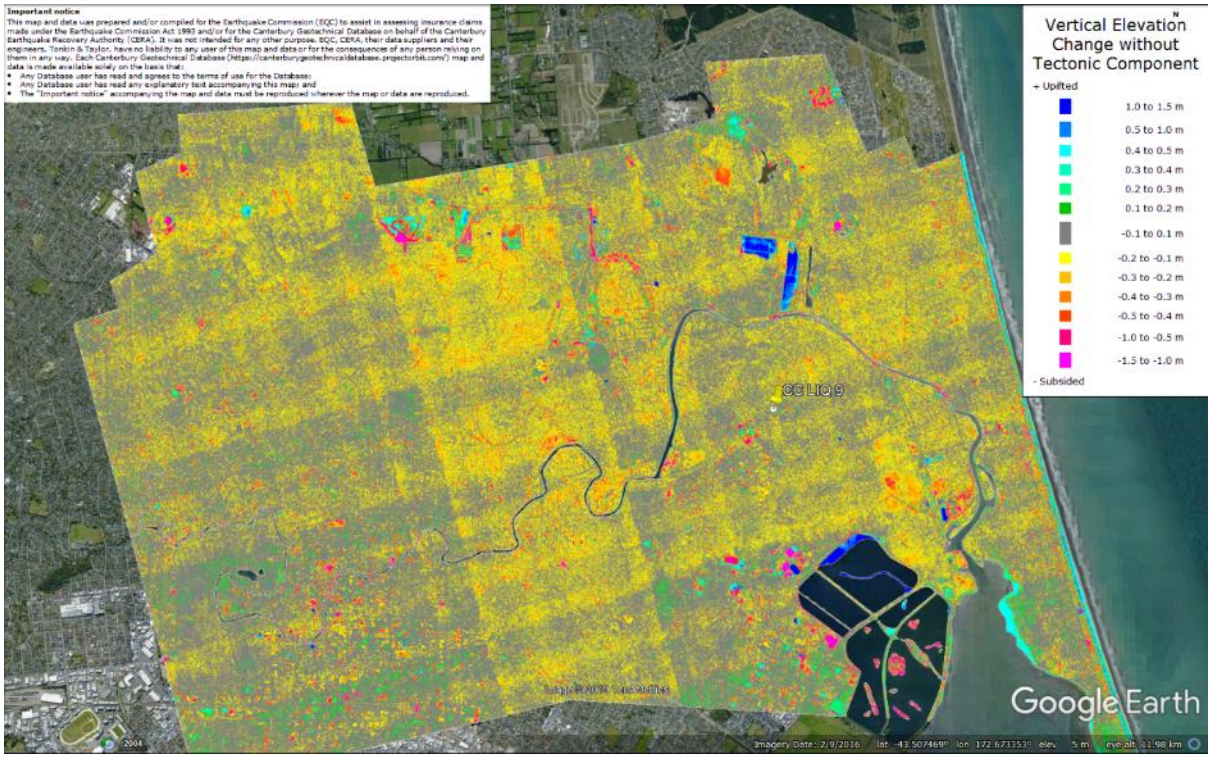

Figure 27: Vertical Ground Movements (Surface – Tectonic) for Sep 2010 Earthquake – the site is not in the apparent zone of overestimated ground surface subsidence.

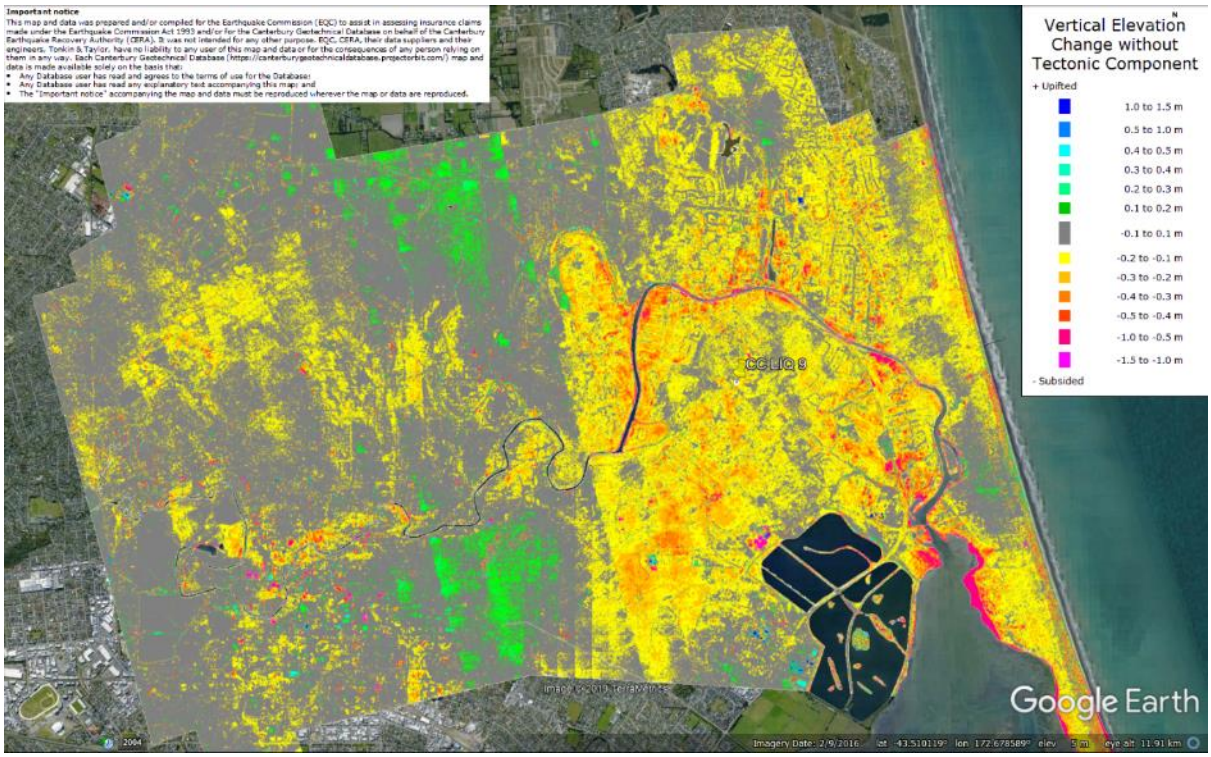

Figure 28: Vertical Ground Movements (Surface – Tectonic) for Feb 2011 Earthquake – the site is not in the apparent zone of underestimated ground surface subsidence.

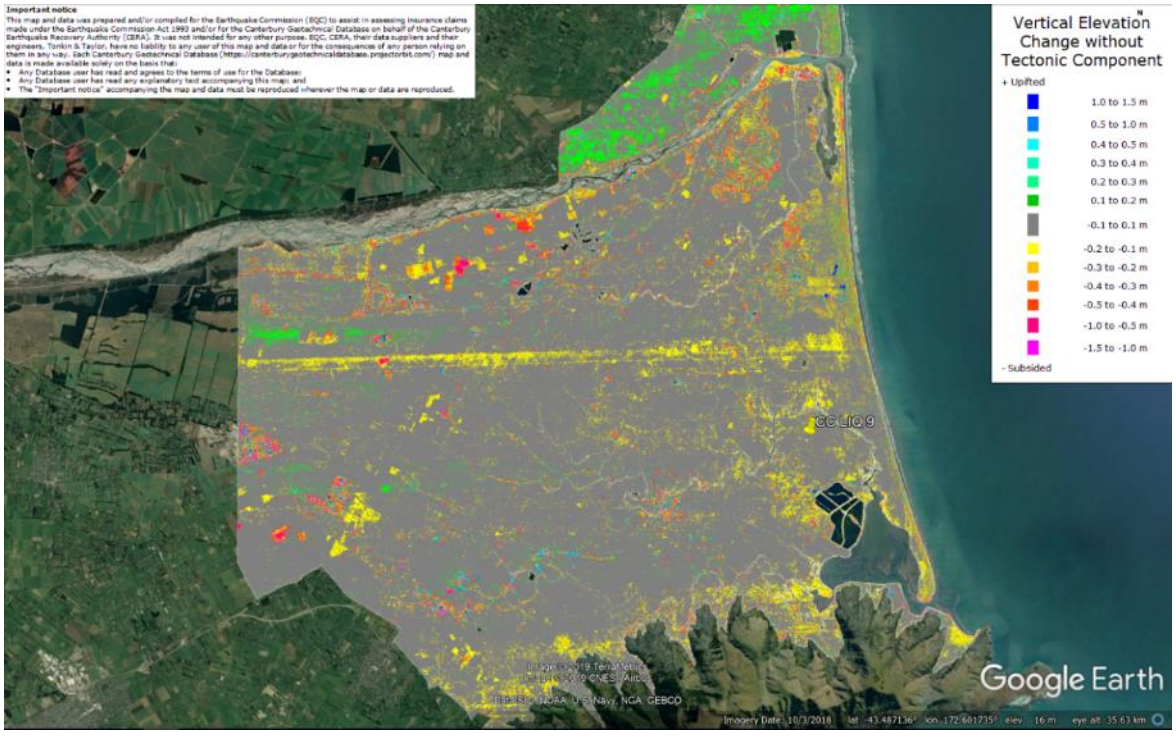

Figure 29: Vertical Ground Movements (Surface – Tectonic) for June 2011 Earthquake – the site is not in the apparent zone of overestimated or underestimated ground surface subsidence.

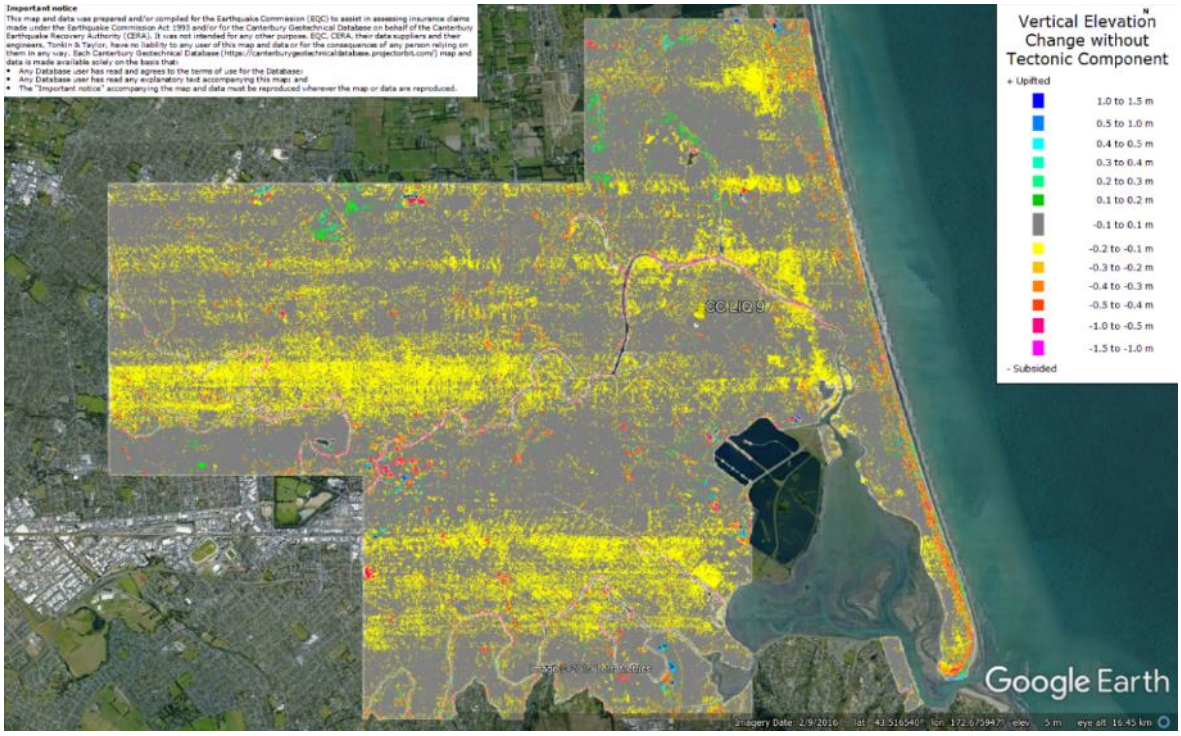

Figure 30: Vertical Ground Movements (Surface – Tectonic) for Dec 2011 Earthquake – the site is not in the apparent zone of overestimated or underestimated ground surface subsidence.

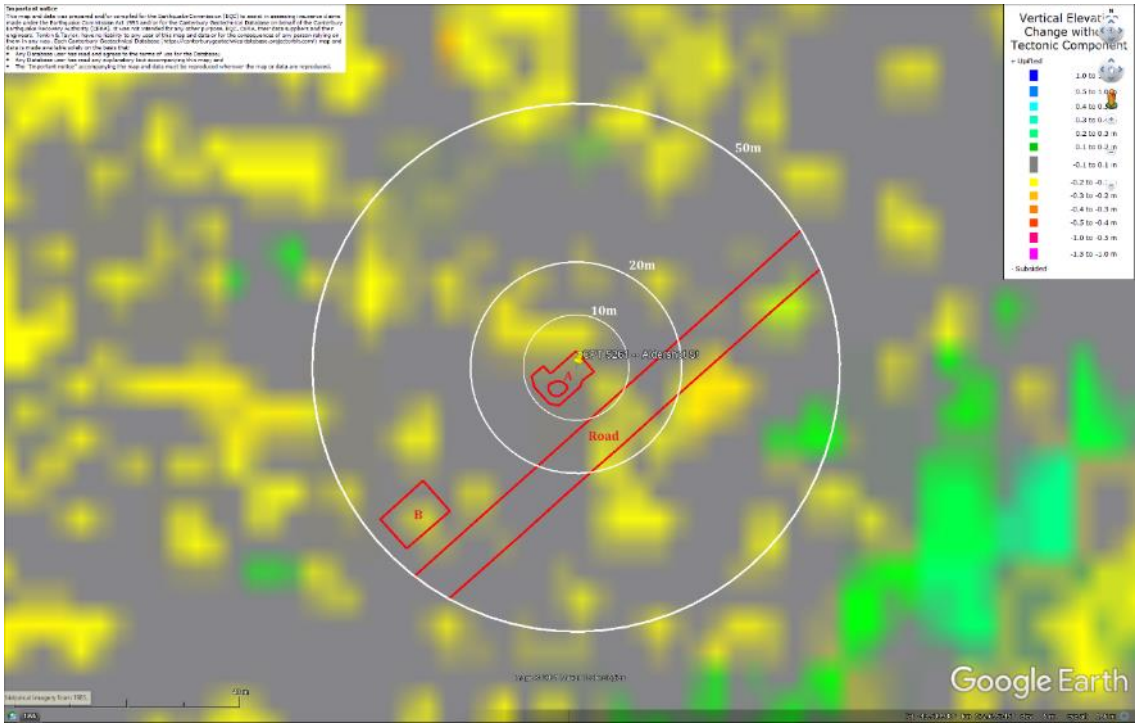

Figure 31: Ground surface subsidence without tectonic component for Sep 2010 Earthquake according to the LiDAR DEM.

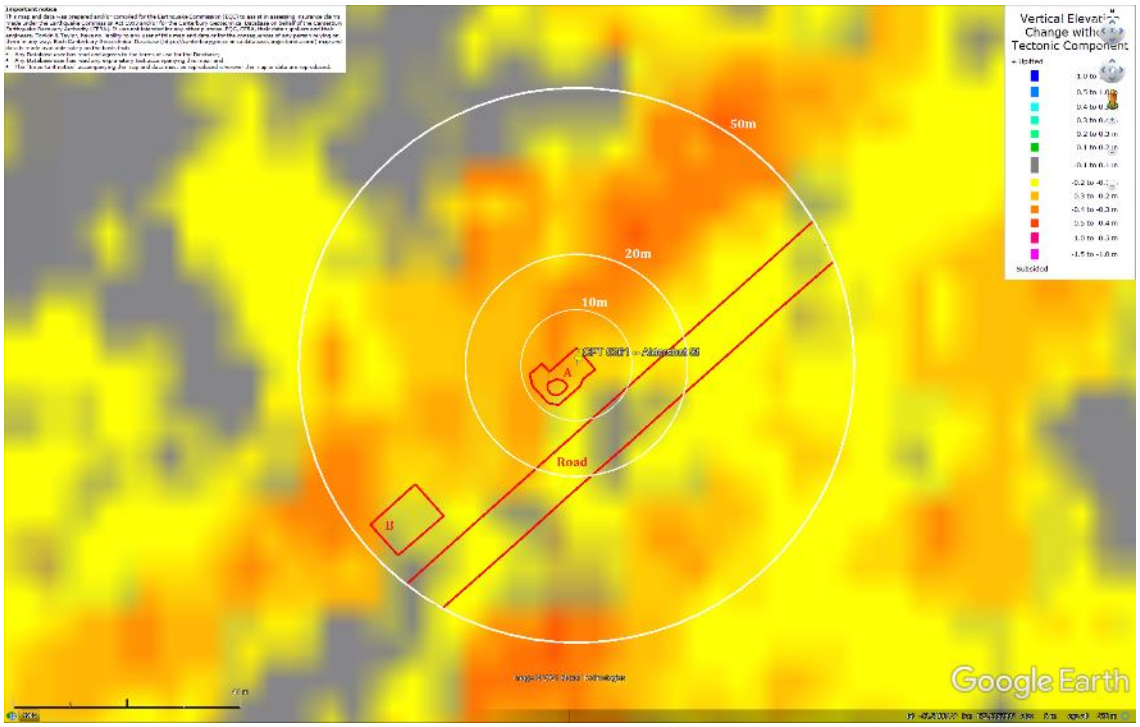

Figure 32: Ground surface subsidence without tectonic component for Feb 2011 Earthquake according to the LiDAR DEM.

Figure 33: Ground surface subsidence without tectonic component for June 2011 Earthquake according to the LiDAR DEM.

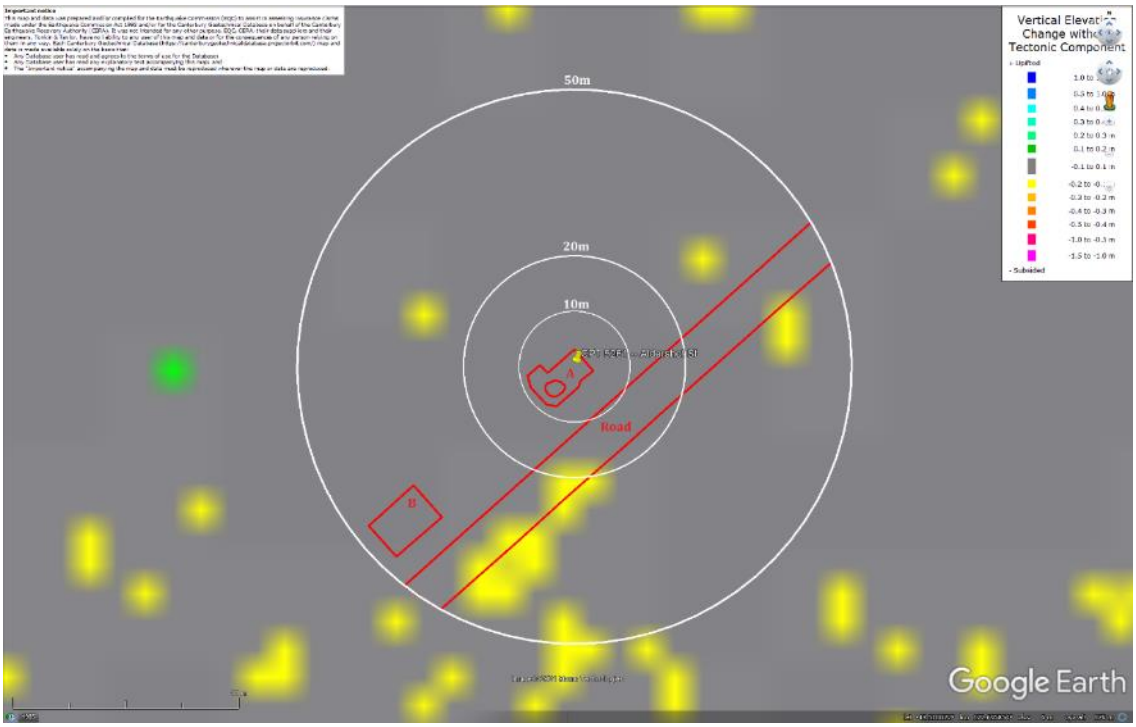

Figure 34: Ground surface subsidence without tectonic component for Dec 2011 Earthquake according to the LiDAR DEM.

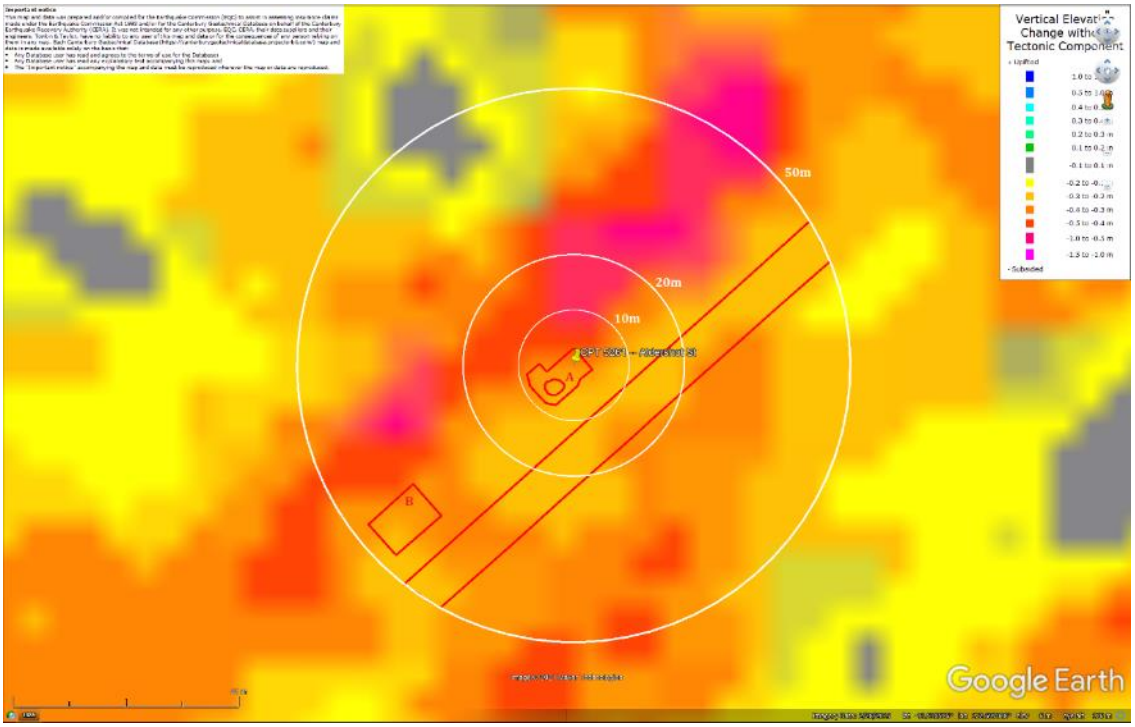

Figure 35: Ground surface subsidence without tectonic component for Canterbury Earthquake Sequence according to the LiDAR DEM.

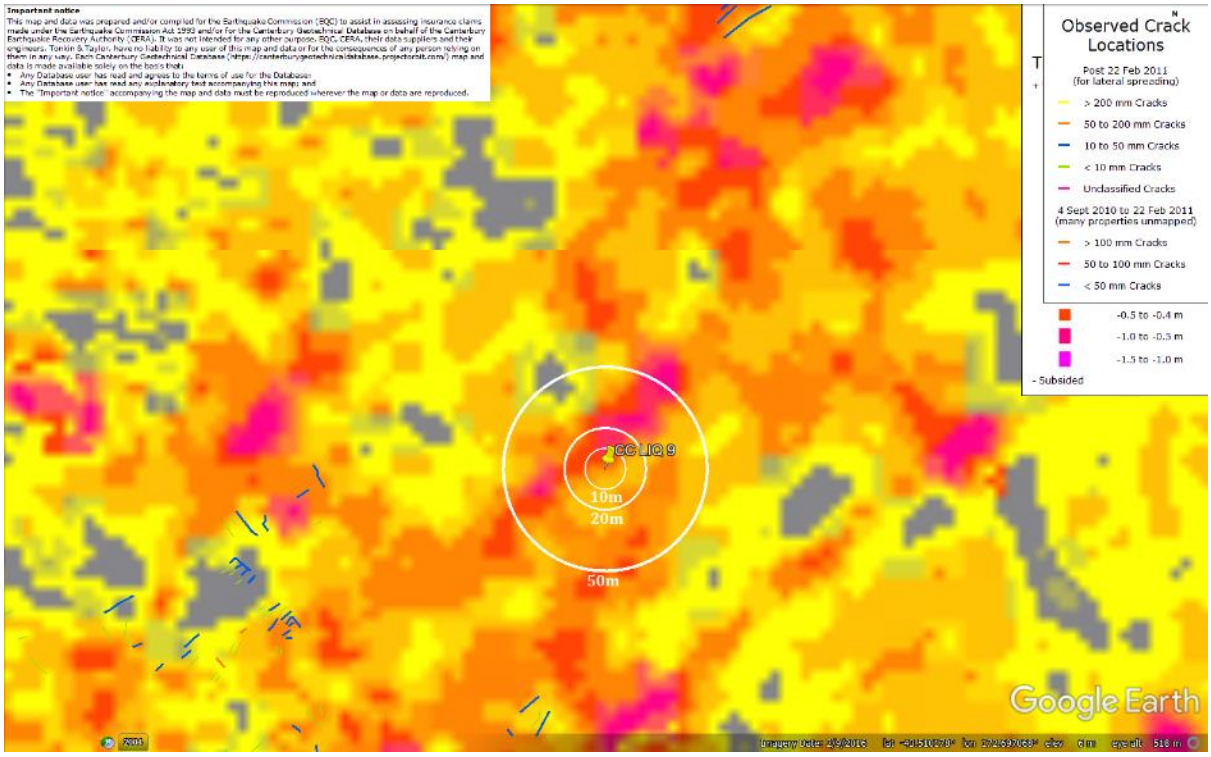

Figure 36: Absence of ground cracks indicates no lateral spreading for Canterbury Earthquake Sequence.

Figure 37: Vertical tectonic movements for Sep 2010 Earthquake.

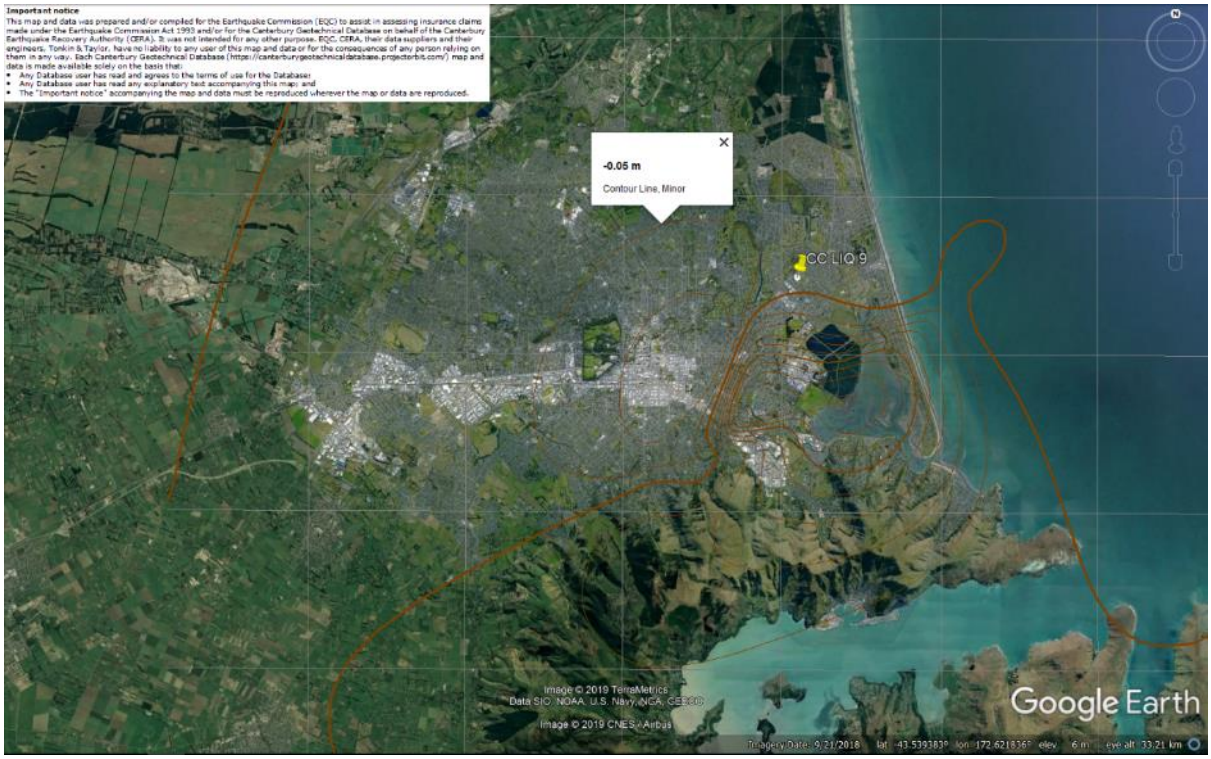

Figure 38: Vertical tectonic movements for Feb 2011 Earthquake.

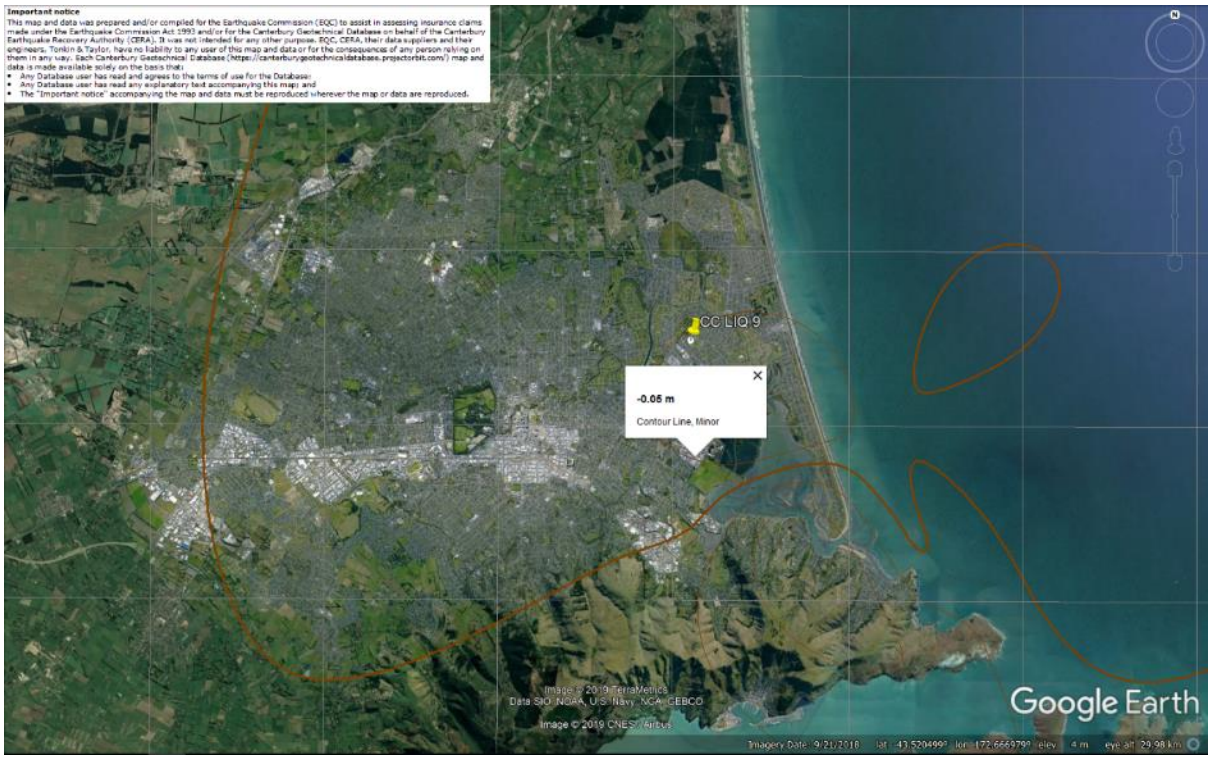

Figure 39: Vertical tectonic movements for June 2011 Earthquake.

Figure 40: Vertical tectonic movements for Dec 2011 Earthquake.

Figure 41: Vertical tectonic movements for Canterbury Earthquake Sequence.

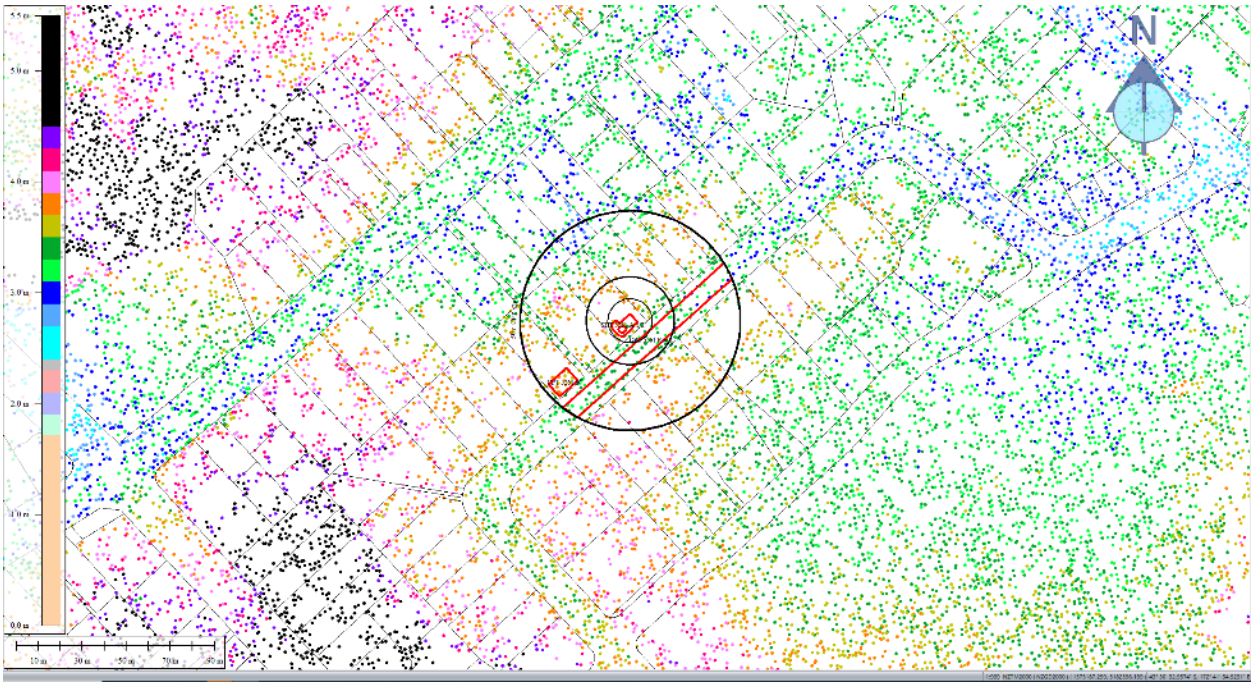

Figure 42: Jul 2003 LiDAR survey.

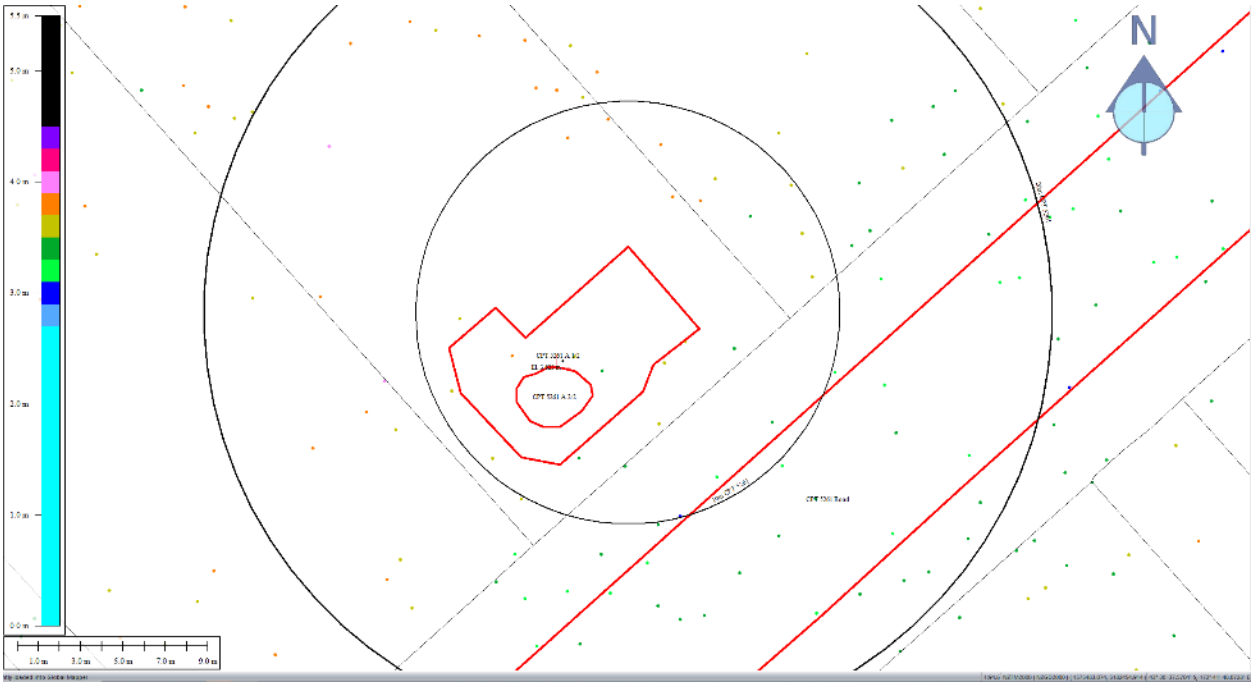

Figure 43: Ground surface elevation for Patch A for Jul 2003 LiDAR survey.

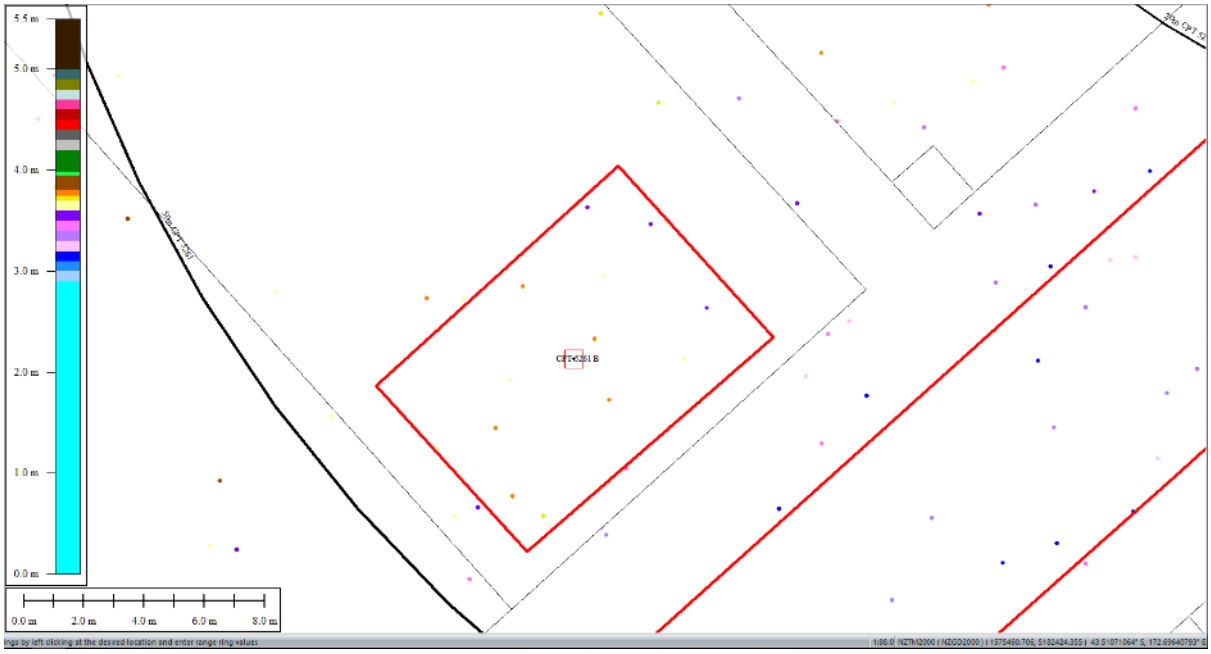

Figure 44: Ground surface elevation for Patch B for Jul 2003 LiDAR survey.

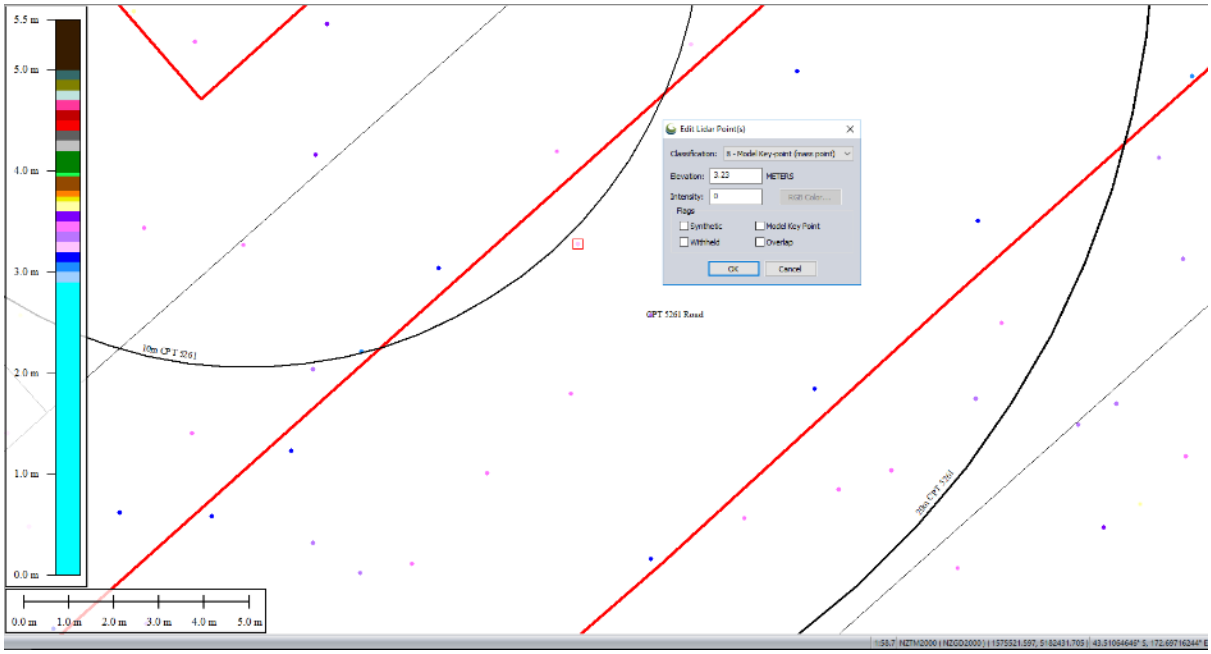

Figure 45: Ground surface elevation for the 10-m buffer for Road for Jul 2003 LiDAR survey.

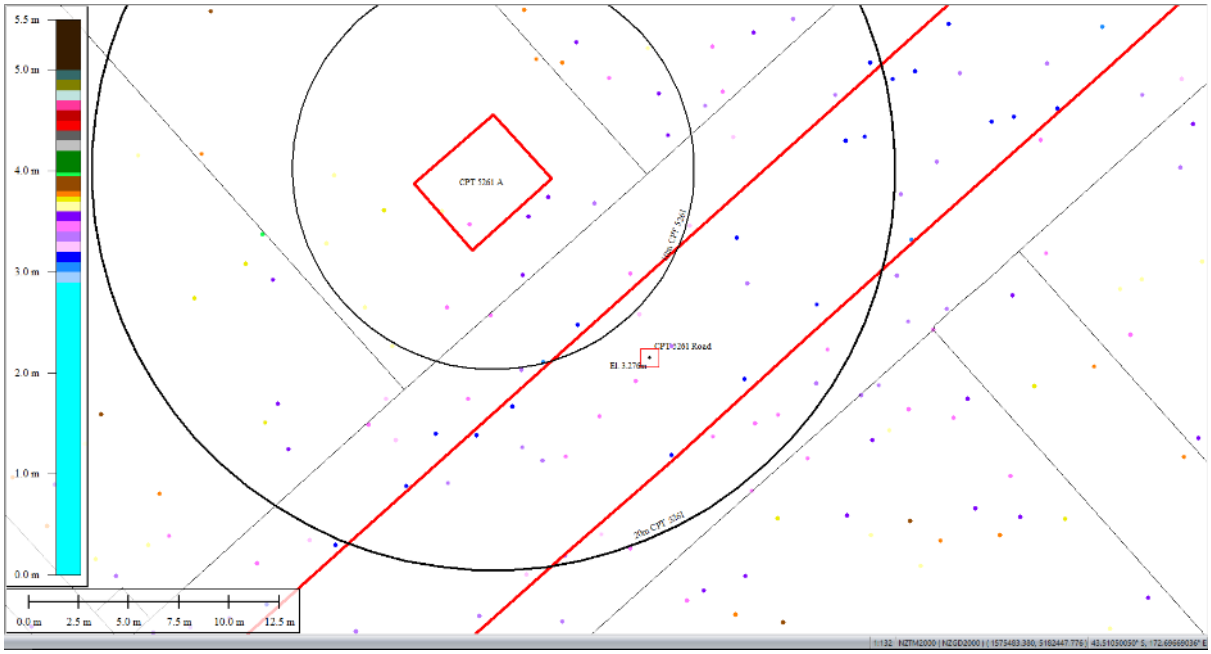

Figure 46: Ground surface elevation averaged over 20-m buffer for Road for Jul 2003 LiDAR survey.

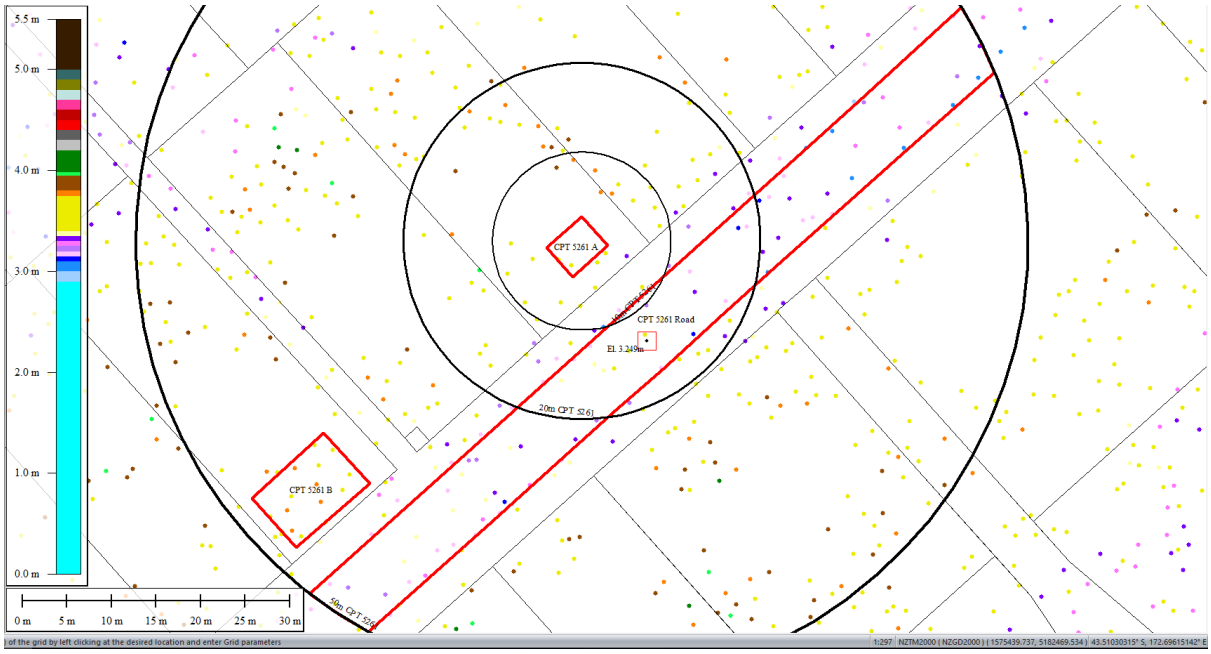

Figure 47: Ground surface elevation averaged over 50-m buffer for Road for Jul 2003 LiDAR survey.

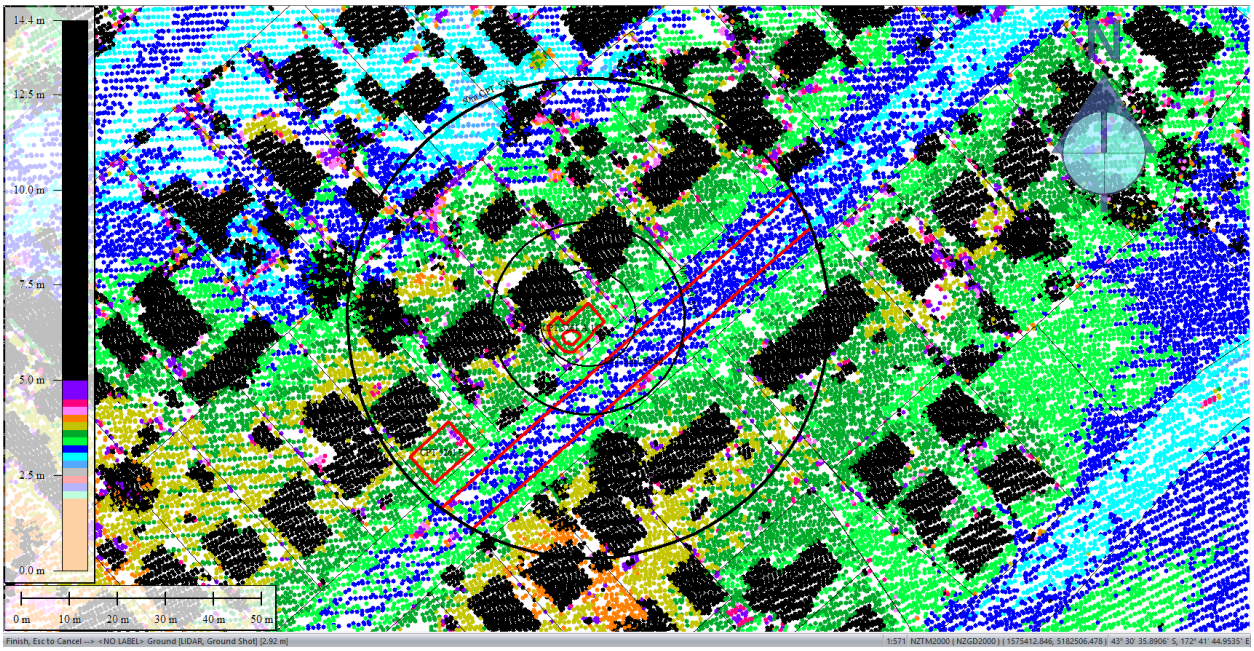

Figure 48: Sep 5, 2010 LiDAR survey.

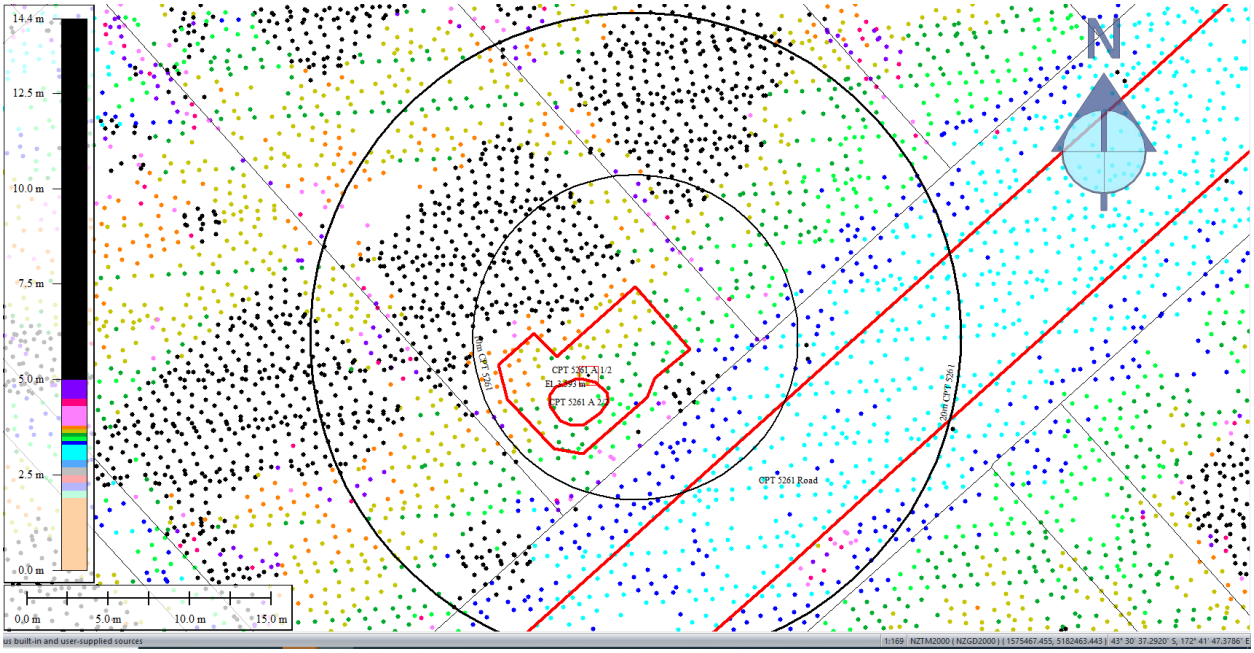

Figure 49: Ground surface elevation for Patch A for Sep 5, 2010 LiDAR survey.

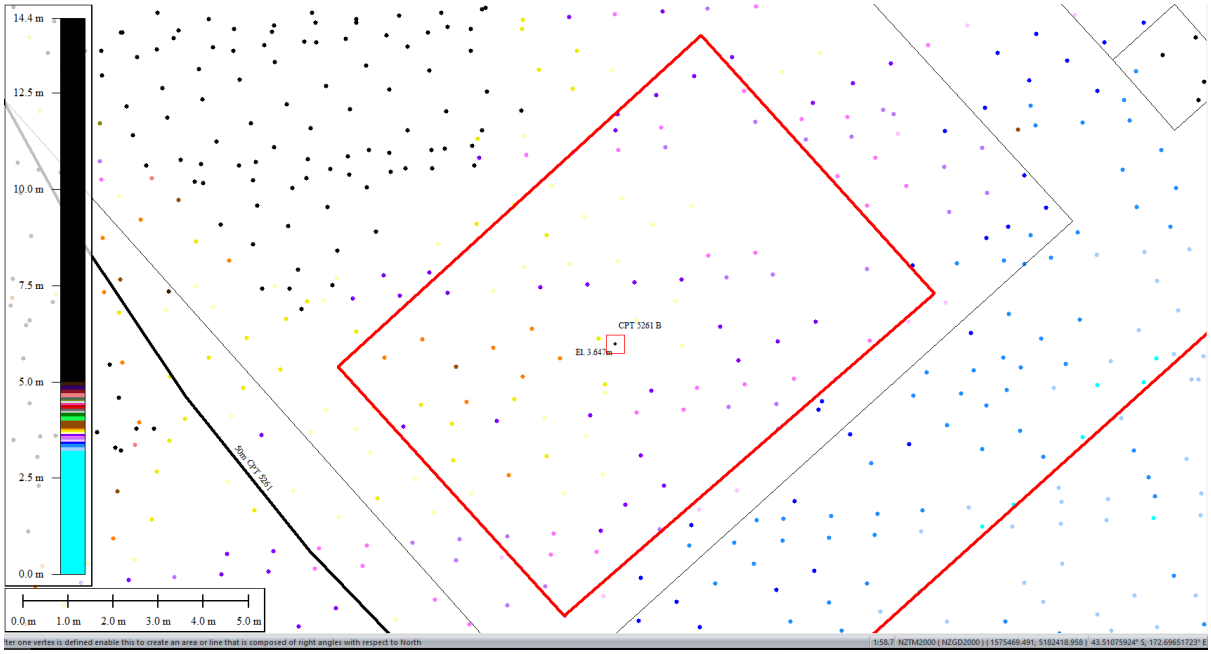

Figure 50: Ground surface elevation for Patch B for Sep 5, 2010 LiDAR survey.

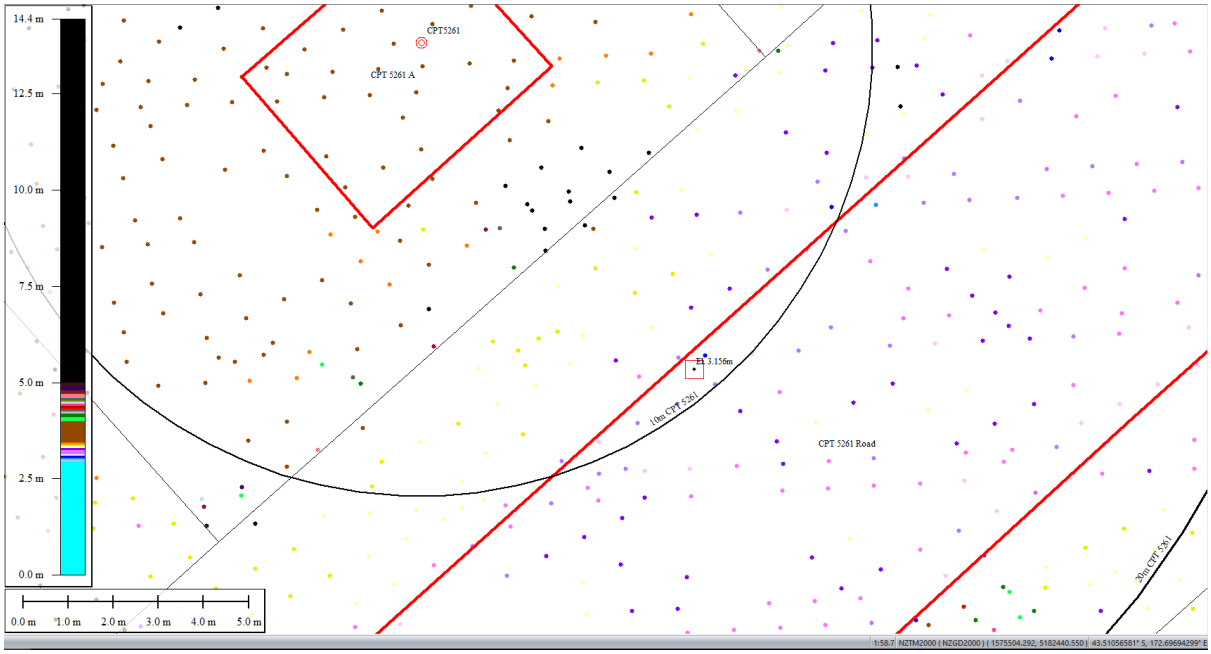

Figure 51: Ground surface elevation averaged over 10-m buffer for Road for Sep 5, 2010 LiDAR survey.

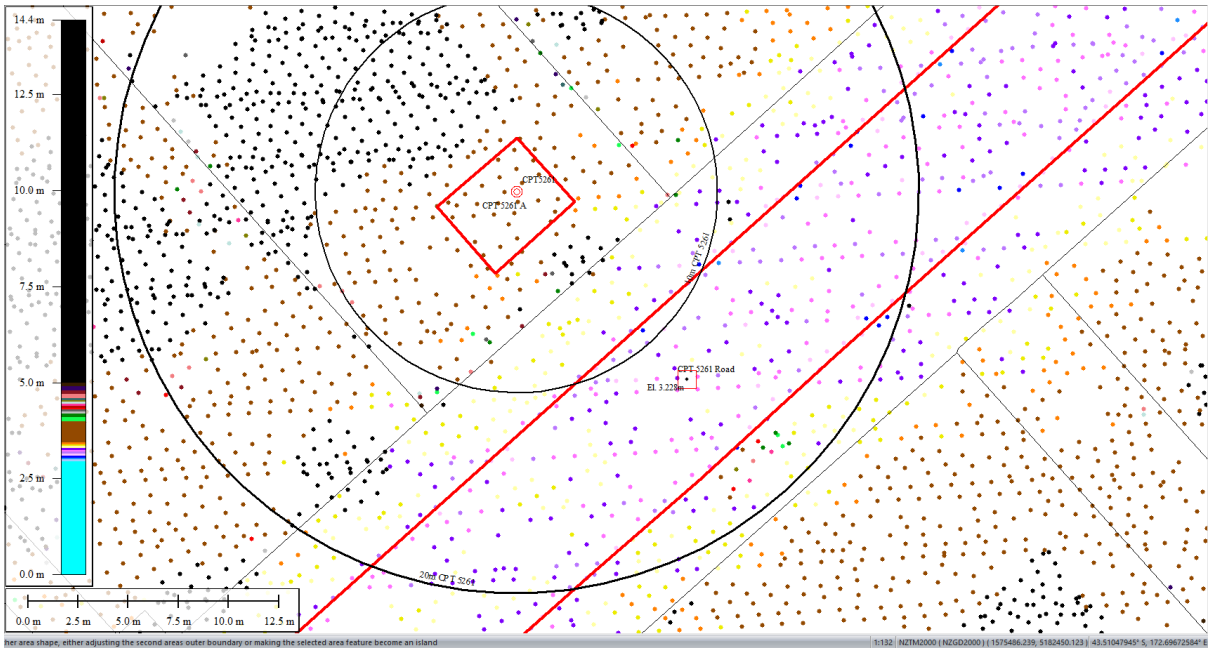

Figure 52: Ground surface elevation averaged over 20-m buffer for Road for Sep 5, 2010 LiDAR survey.

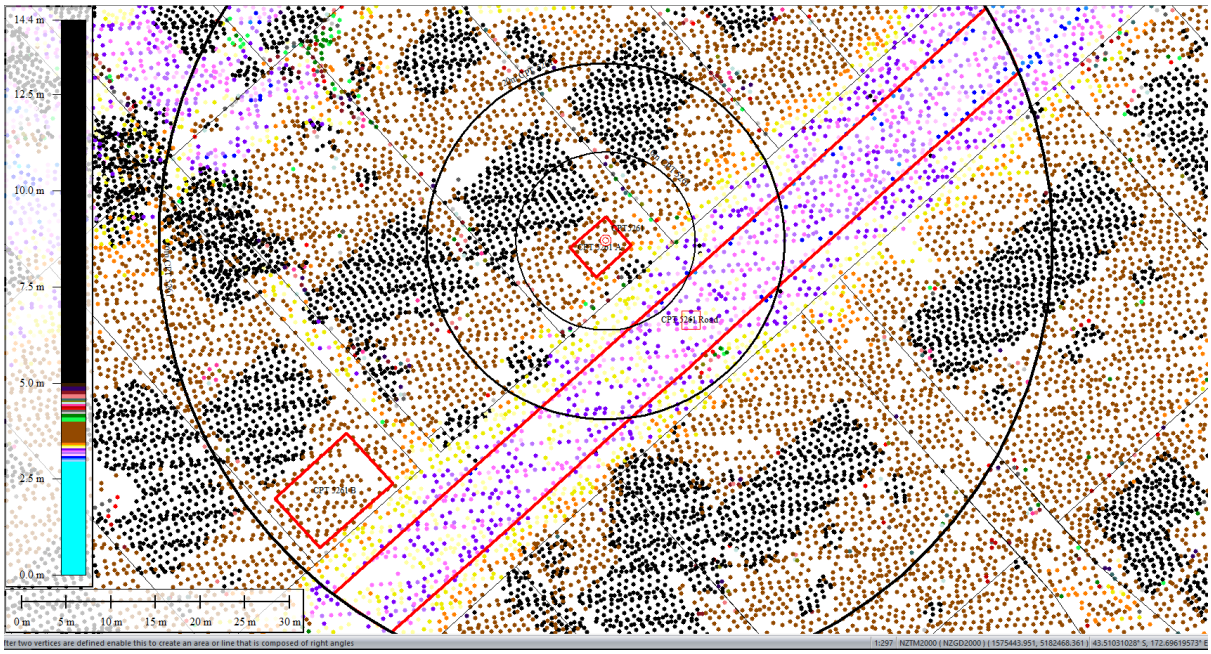

Figure 53: Ground surface elevation averaged over 50-m buffer for Road for Sep 5, 2010 LiDAR survey.

Figure 54: Mar 2011 LiDAR survey.

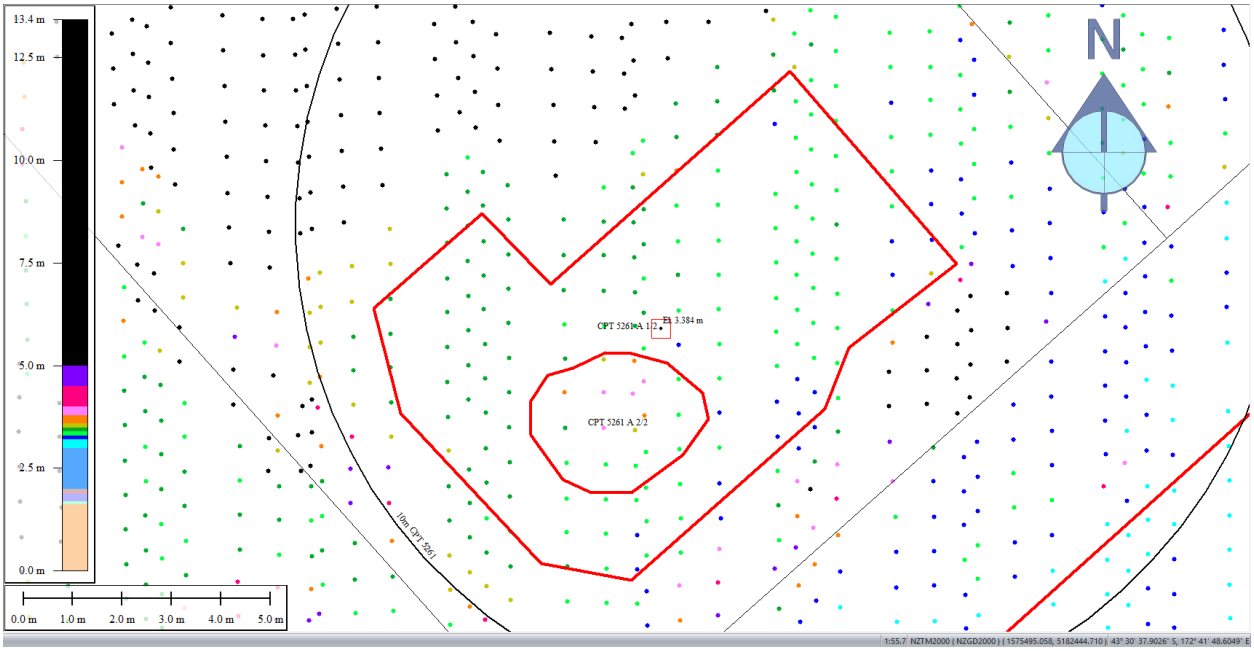

Figure 55: Ground surface elevation for Patch A for Mar 2011 LiDAR survey.

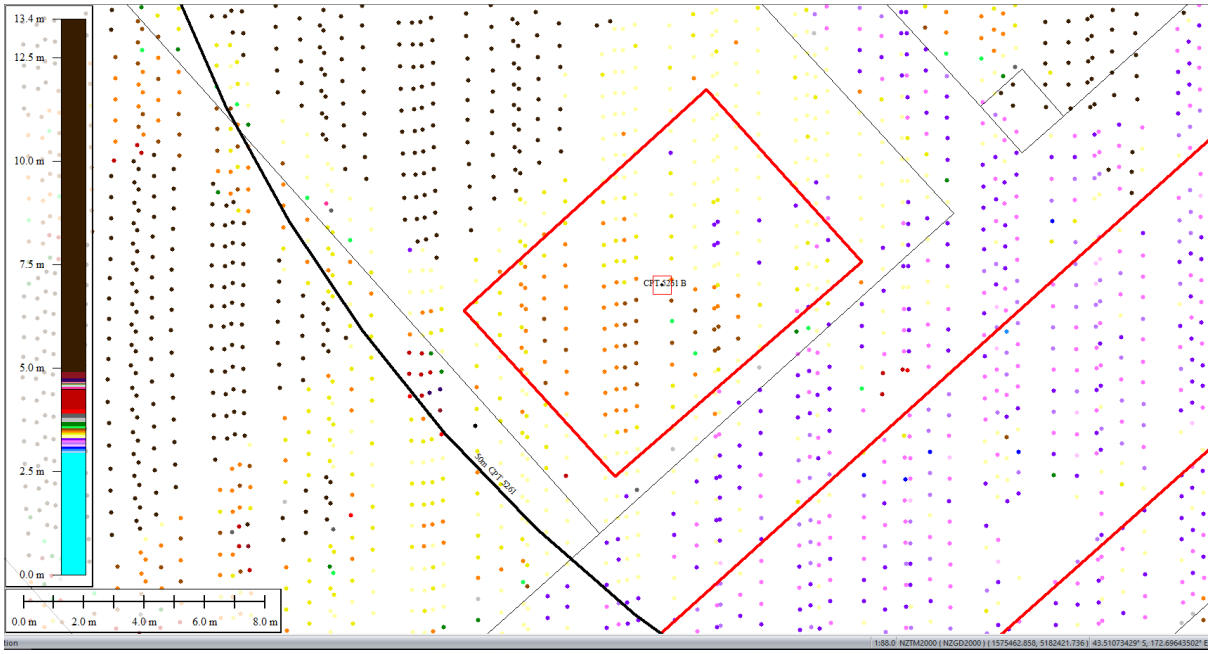

Figure 56: Ground surface elevation for Patch B for Mar 2011 LiDAR survey.

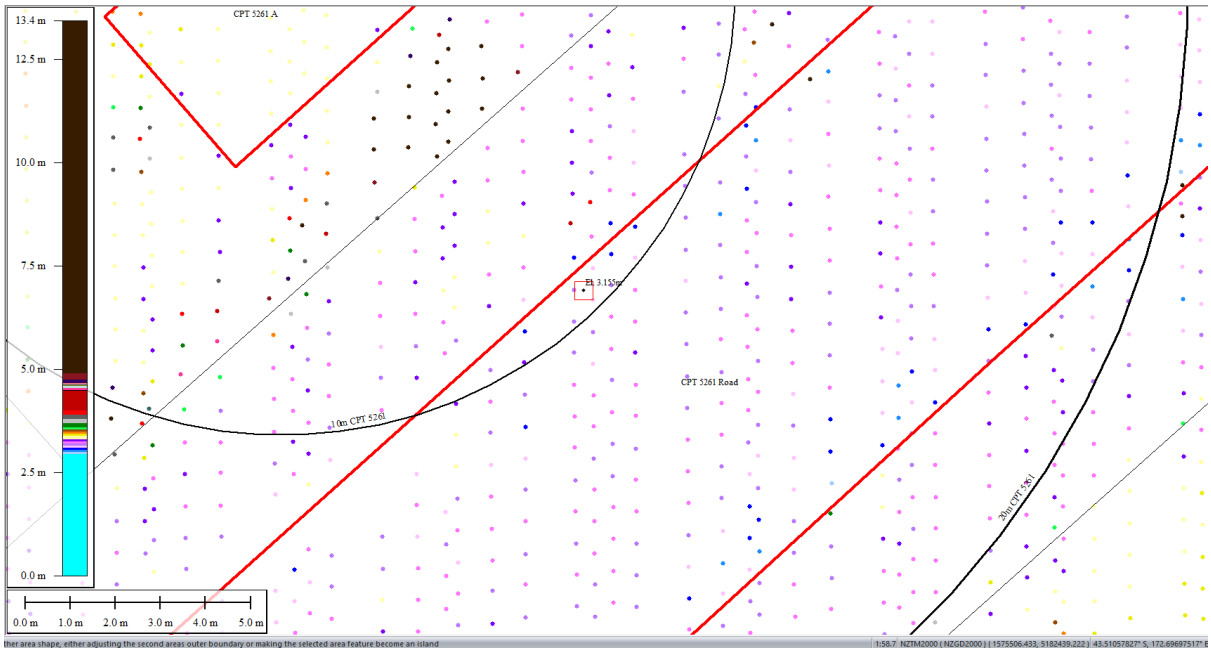

Figure 57: Ground surface elevation averaged over 10-m buffer for Road for Mar 2011 LiDAR survey.

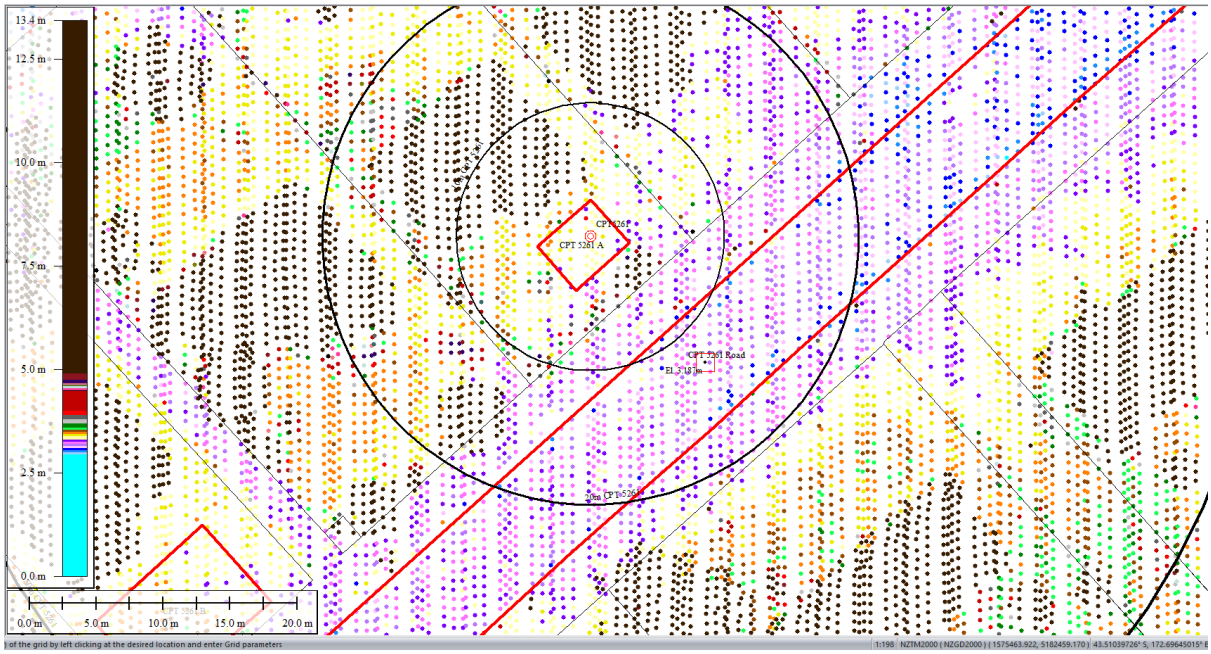

Figure 58: Ground surface elevation averaged over 20-m buffer for Road for Mar 2011 LiDAR survey.

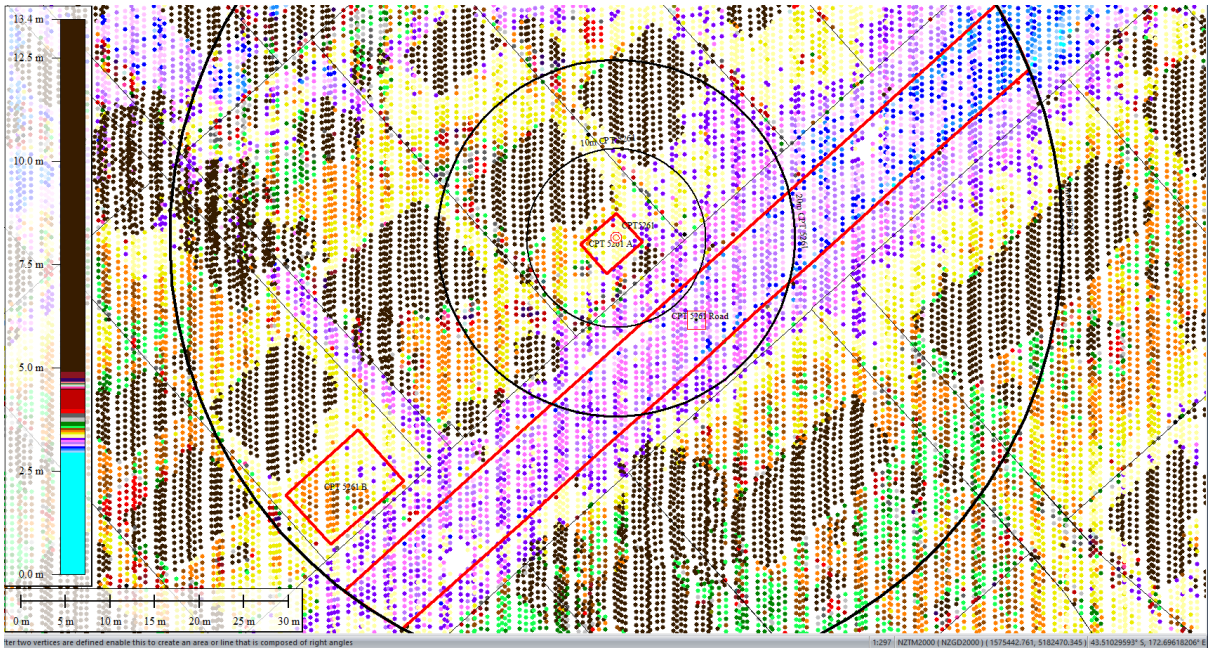

Figure 59: Ground surface elevation averaged over 50-m buffer for Road for Mar 2011 LiDAR survey.

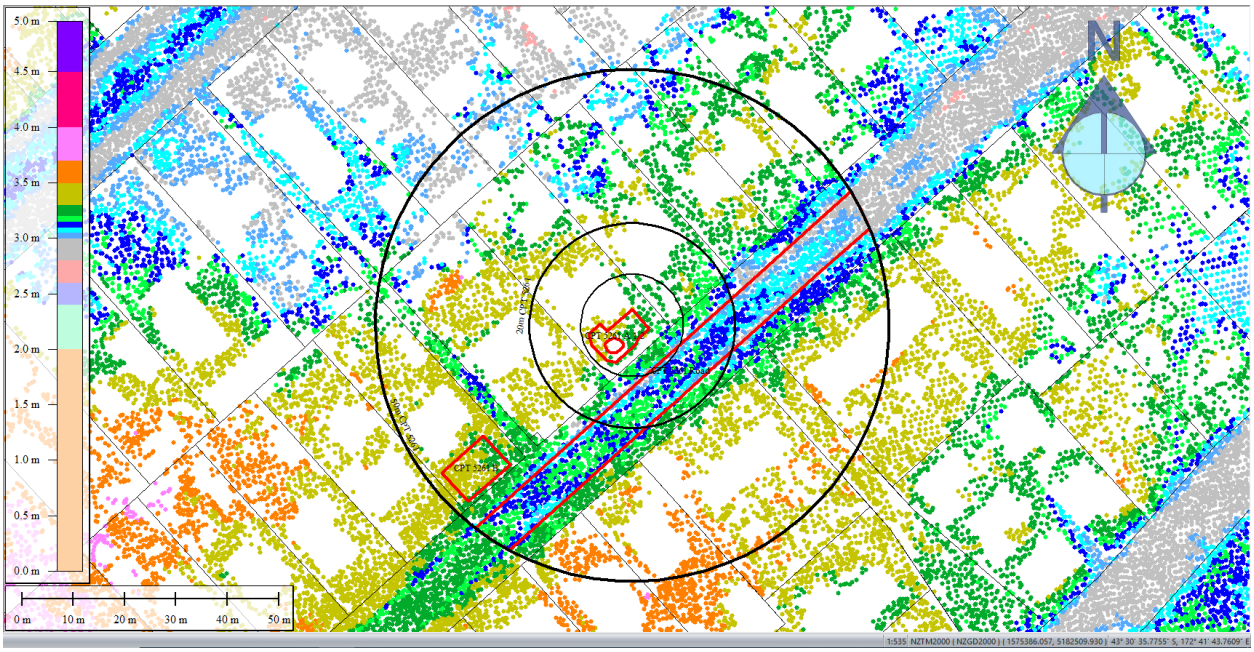

Figure 60: May 2011 LiDAR survey.

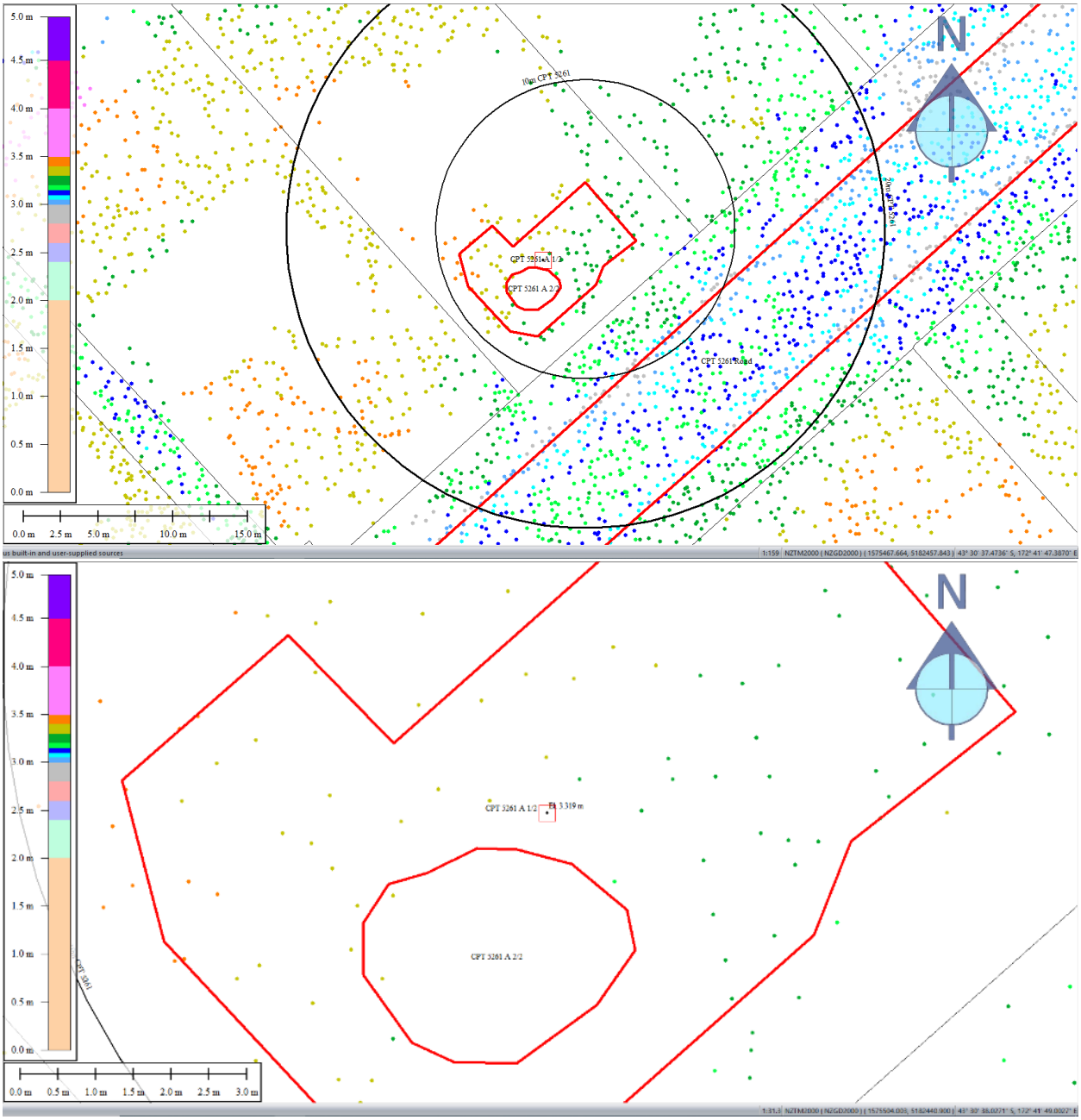

Figure 61: Ground surface elevation for Patch A for May 2011 LiDAR survey.

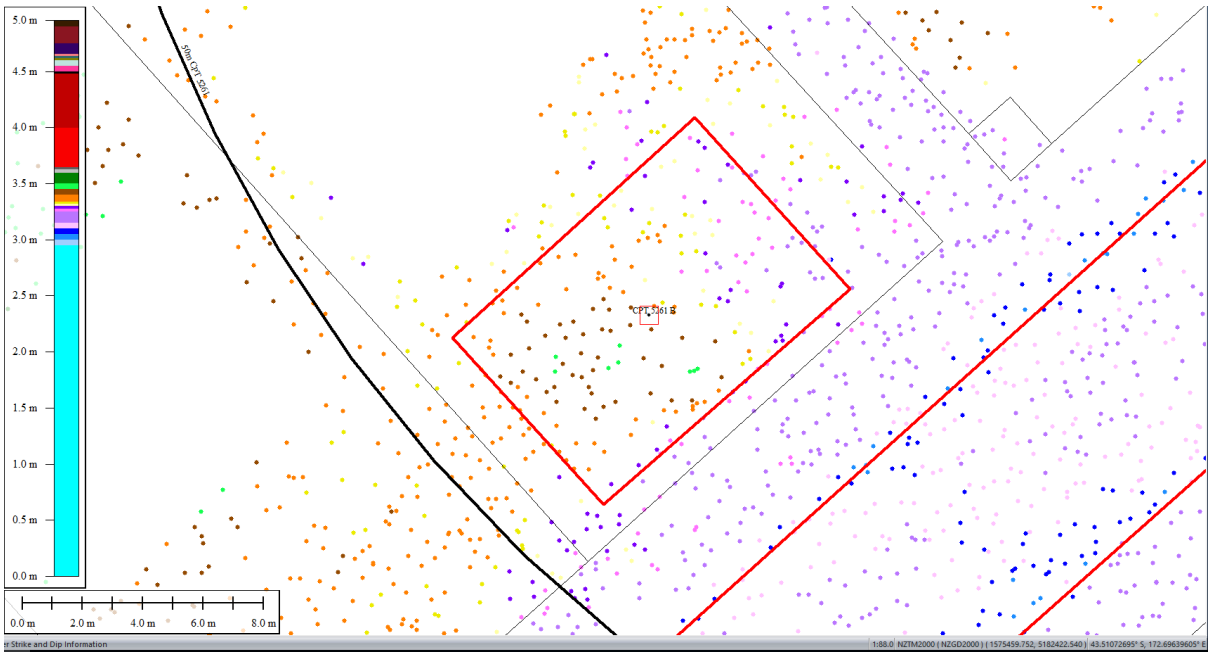

Figure 62: Ground surface elevation for Patch B for May 2011 LiDAR survey.

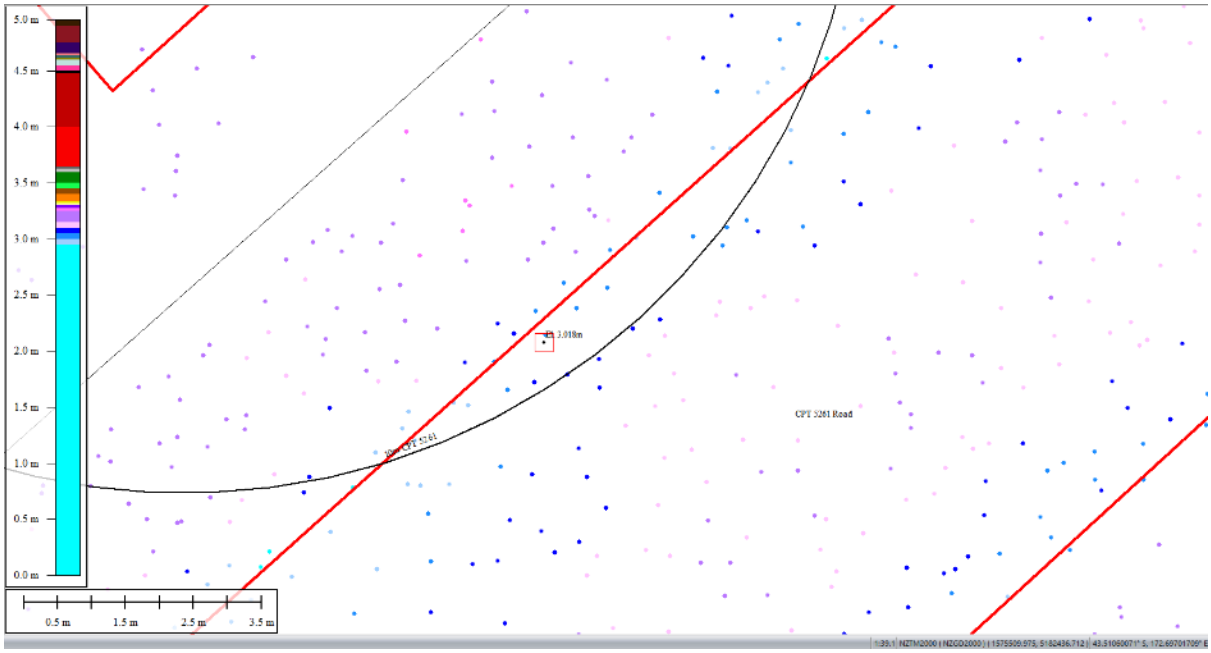

Figure 63: Ground surface elevation averaged over 10-m buffer for Road for May 2011 LiDAR survey.

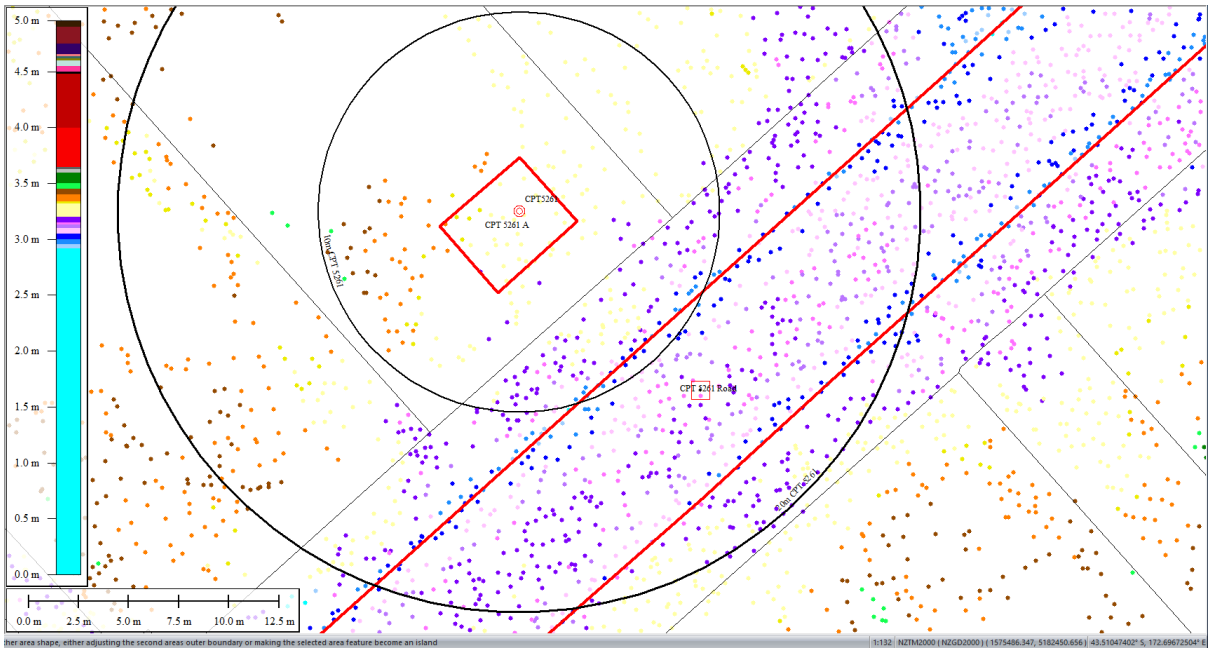

Figure 64: Ground surface elevation averaged over 20-m buffer for Road for May 2011 LiDAR survey.

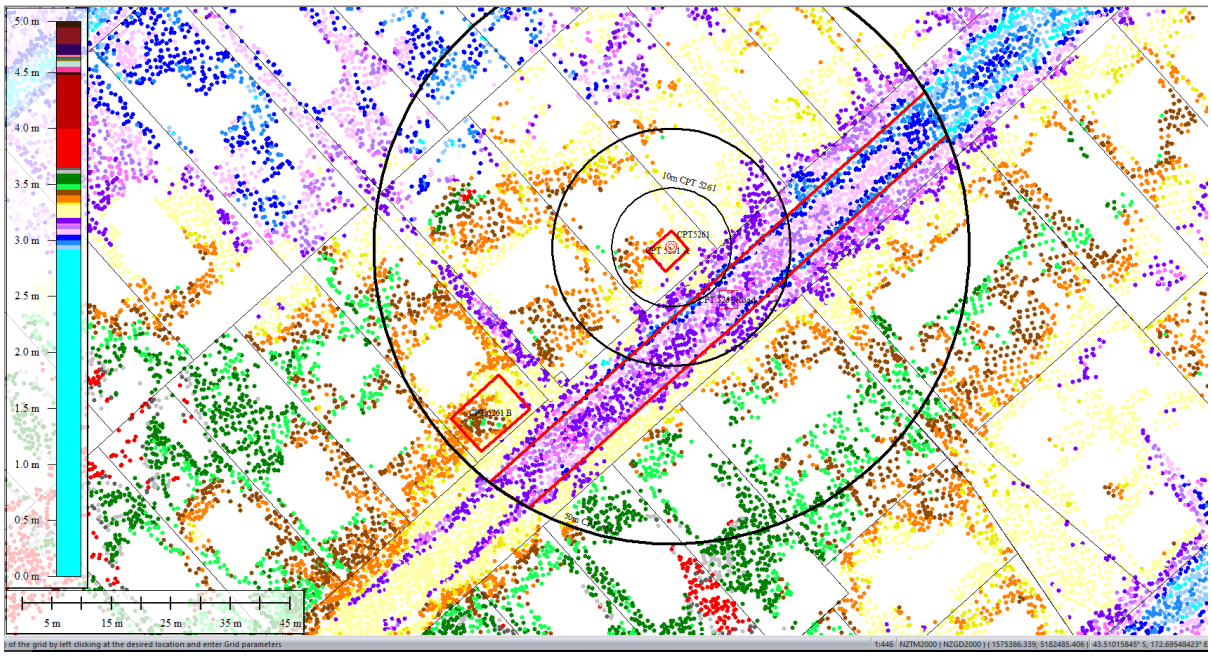

Figure 65: Ground surface elevation averaged over 50-m buffer for Road for May 2011 LiDAR survey.

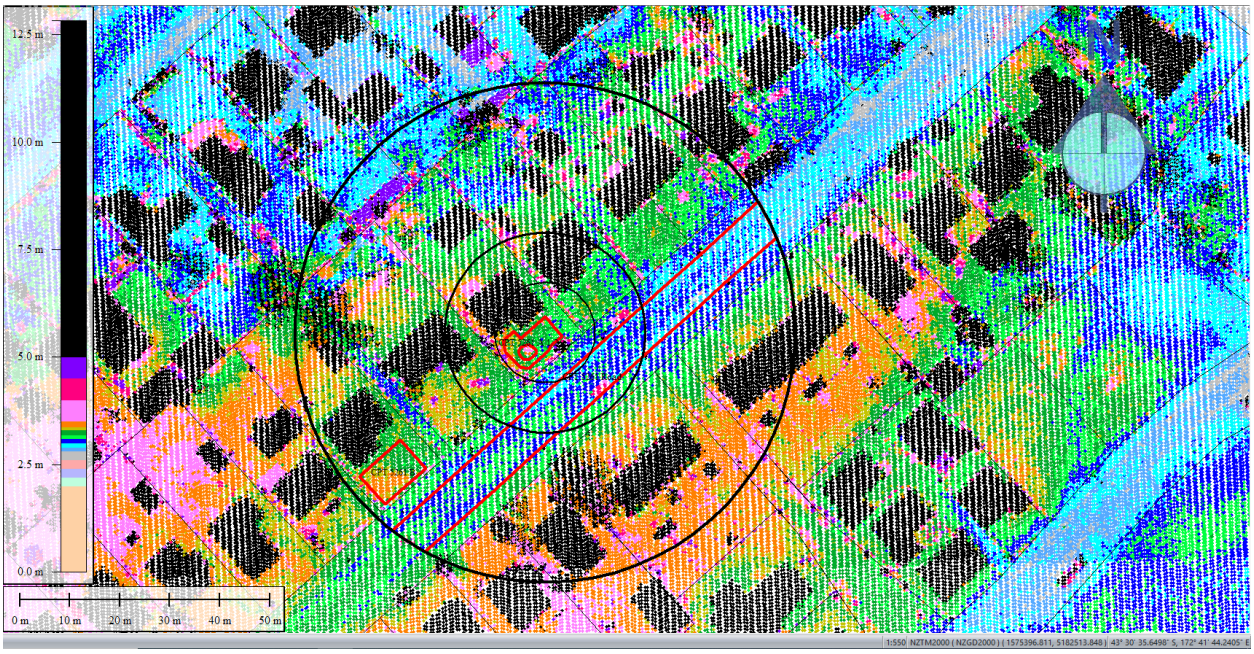

Figure 66: Sep 2011 LiDAR survey.

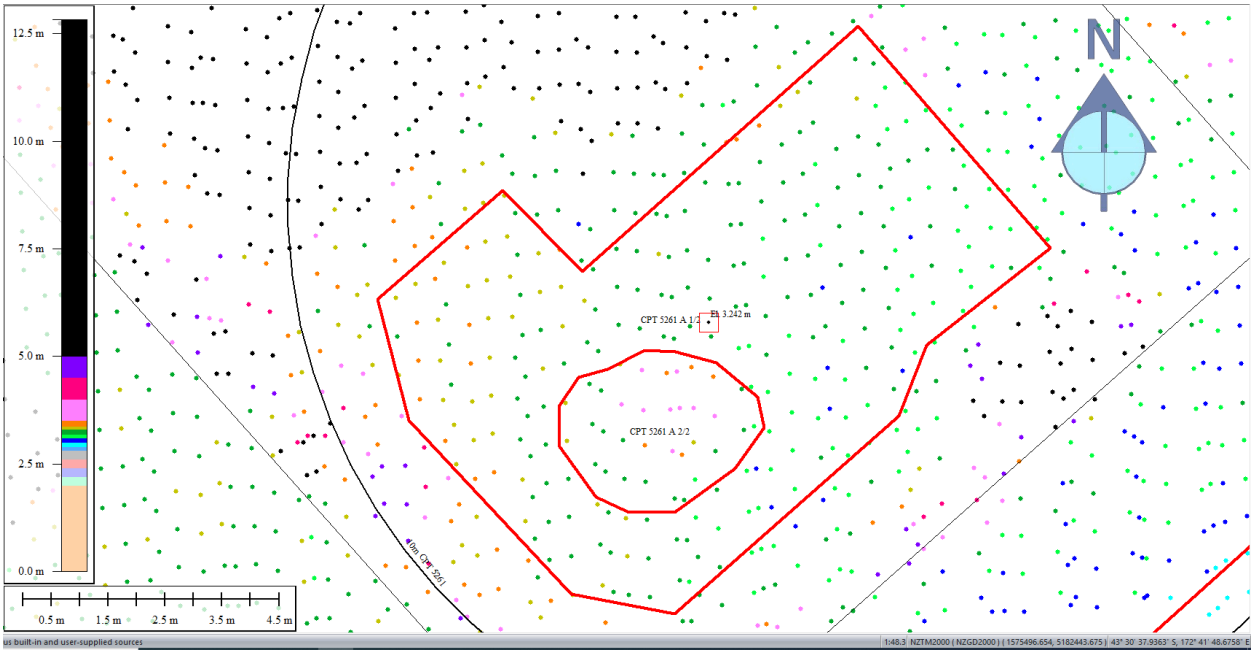

Figure 67: Ground surface elevation for Patch A for Sep 2011 LiDAR survey.

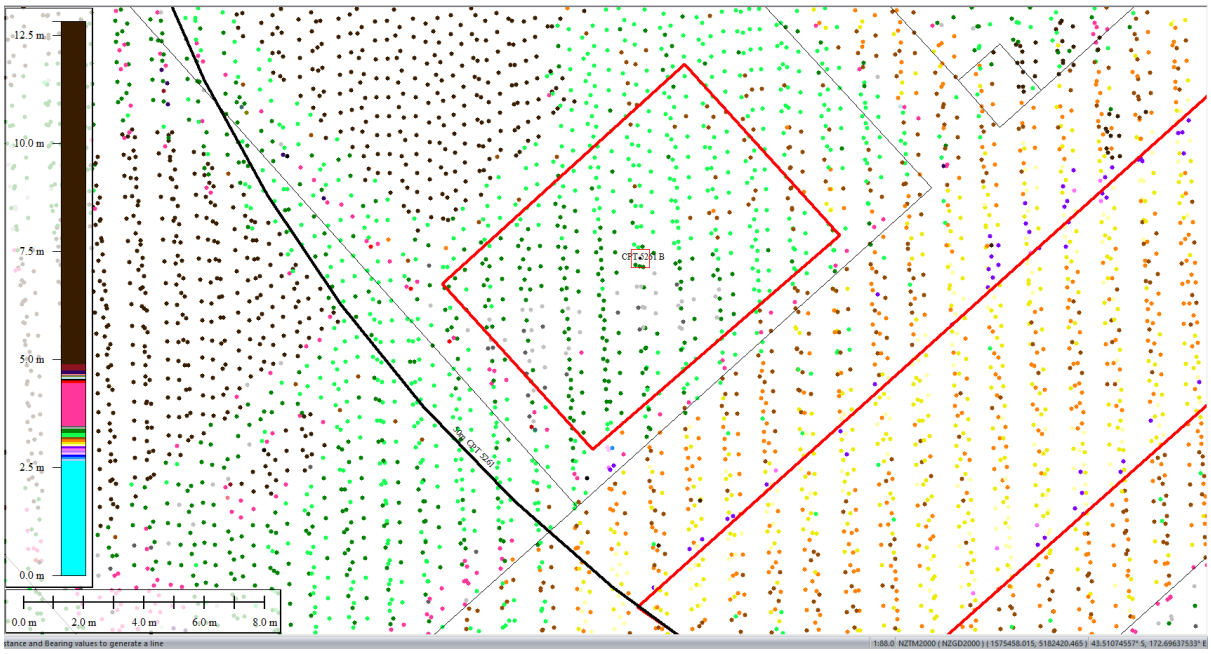

Figure 68: Ground surface elevation for Patch B for Sep 2011 LiDAR survey.

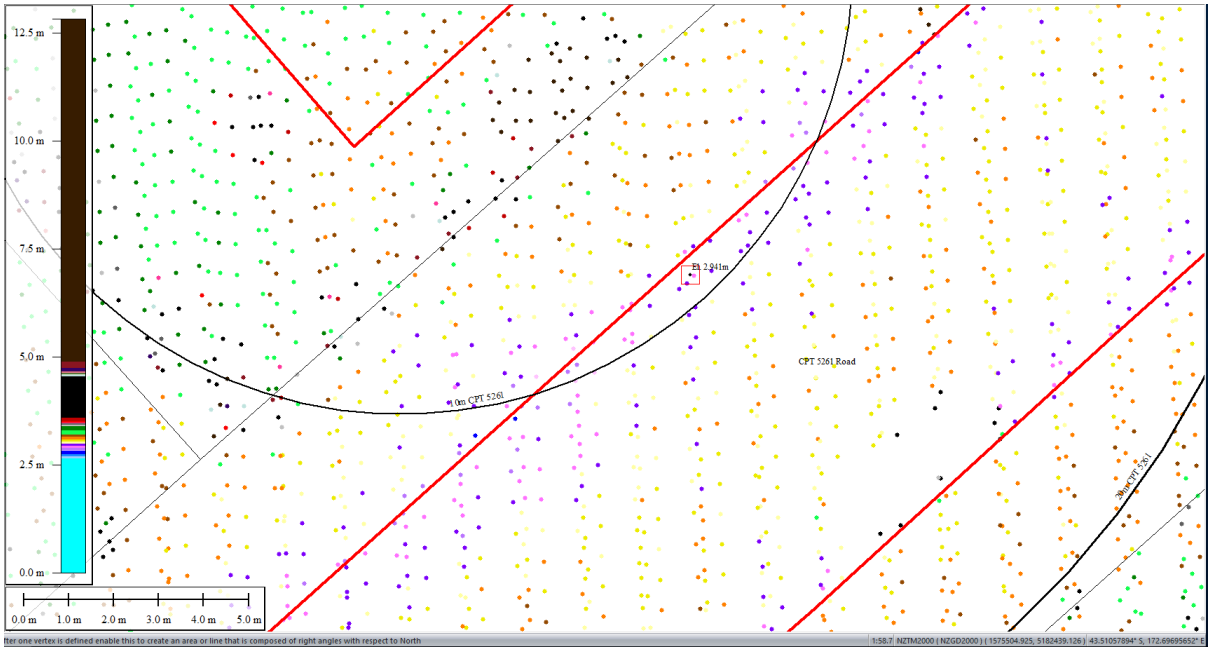

Figure 69: Ground surface elevation averaged over 10-m buffer for Road for Sep 2011 LiDAR survey.

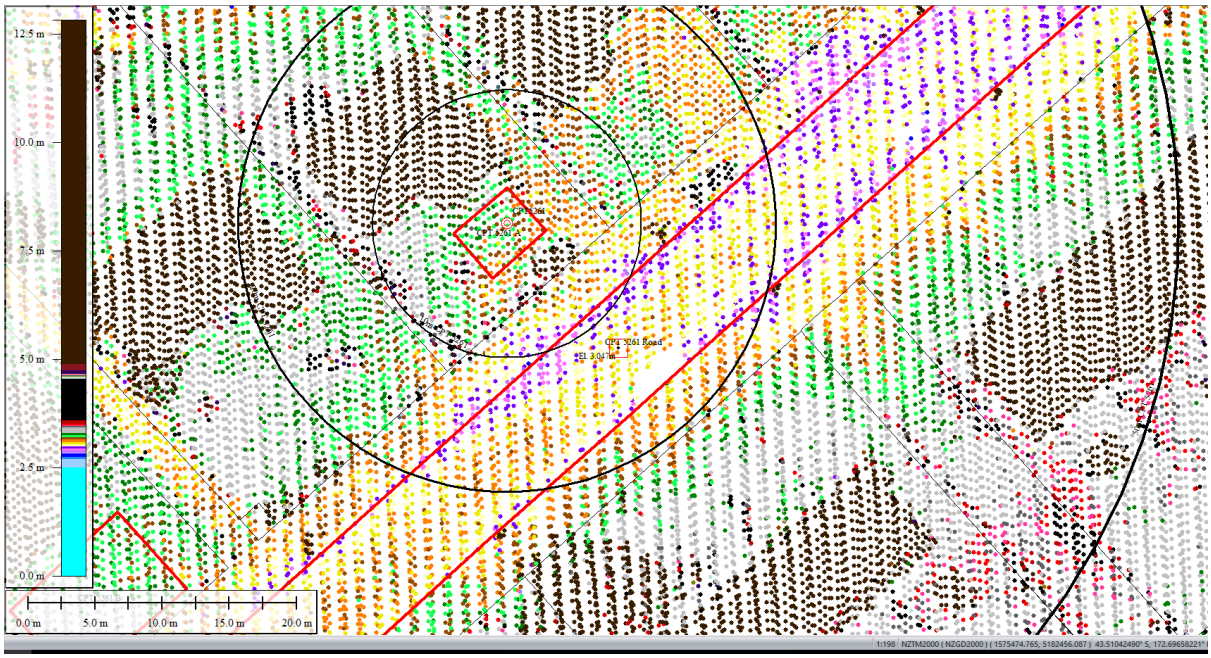

Figure 70: Ground surface elevation averaged over 20-m buffer for Road for Sep 2011 LiDAR survey.

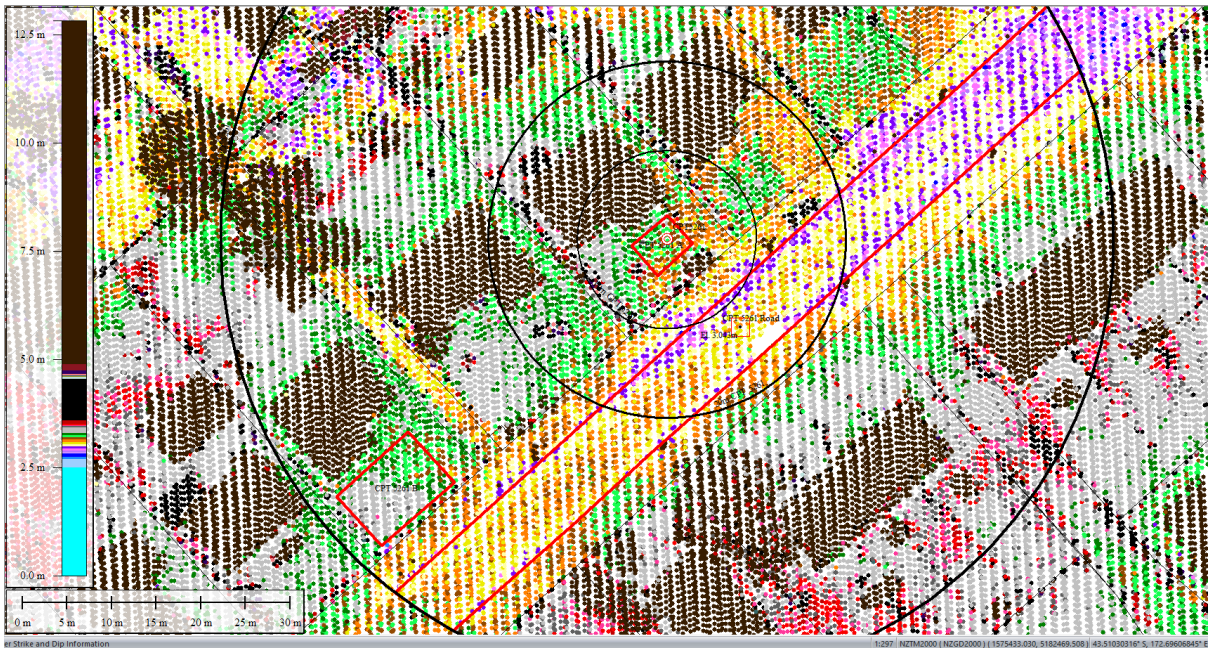

Figure 71: Ground surface elevation averaged over 50-m buffer for Road for Sep 2011 LiDAR survey.

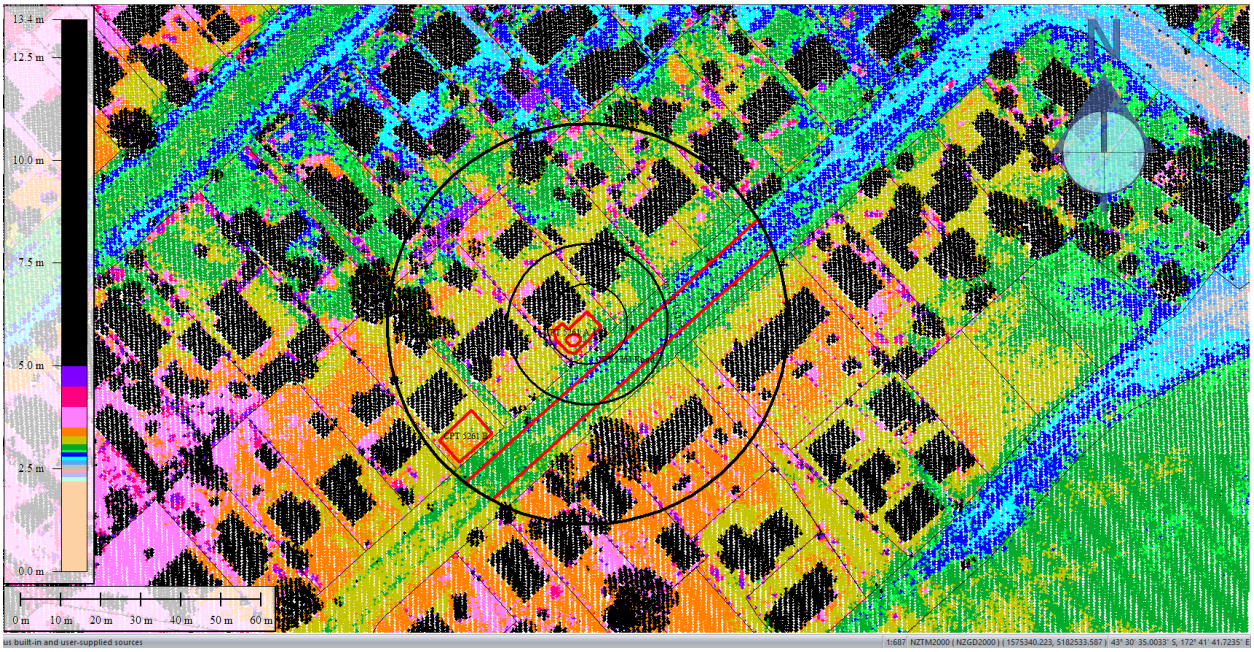

Figure 72: Feb 2012 LiDAR survey.

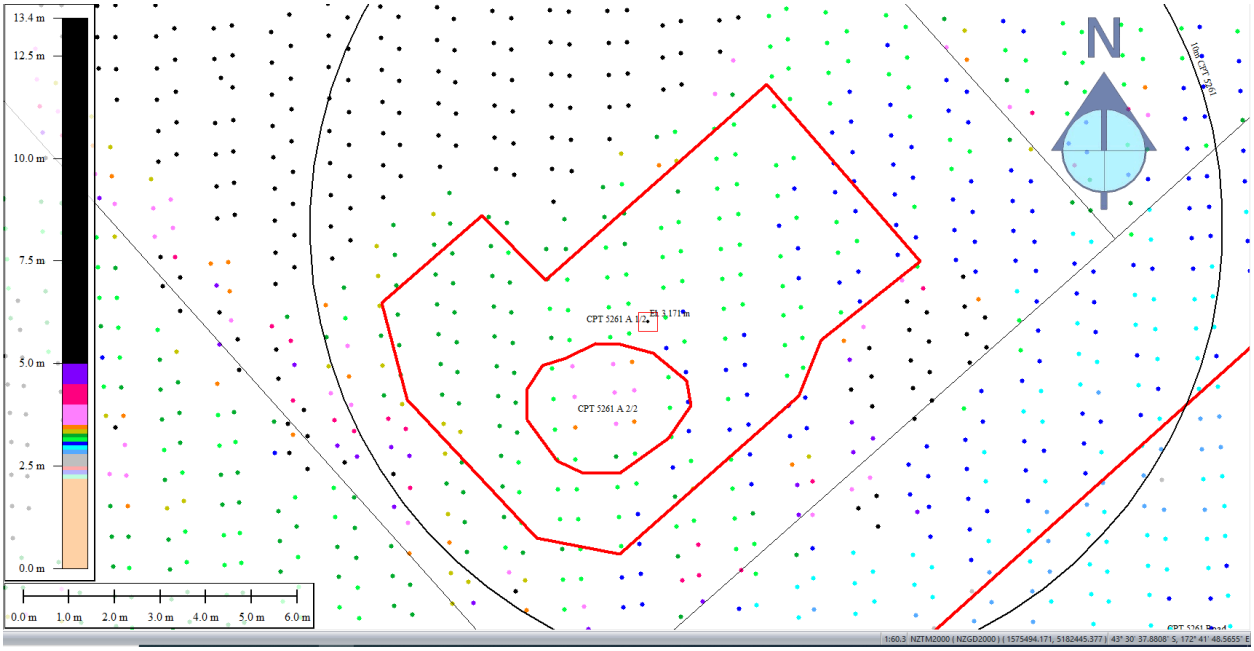

Figure 73: Ground surface elevation for Patch A for Feb 2012 LiDAR survey.

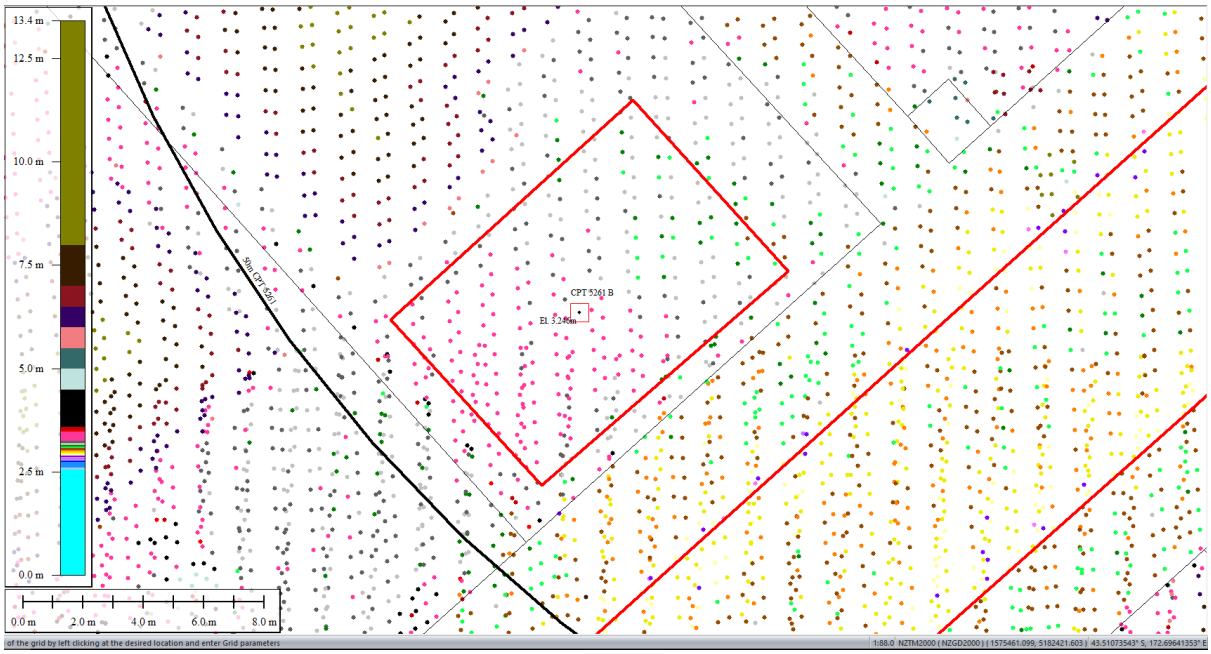

Figure 74: Ground surface elevation for Patch B for Feb 2012 LiDAR survey.

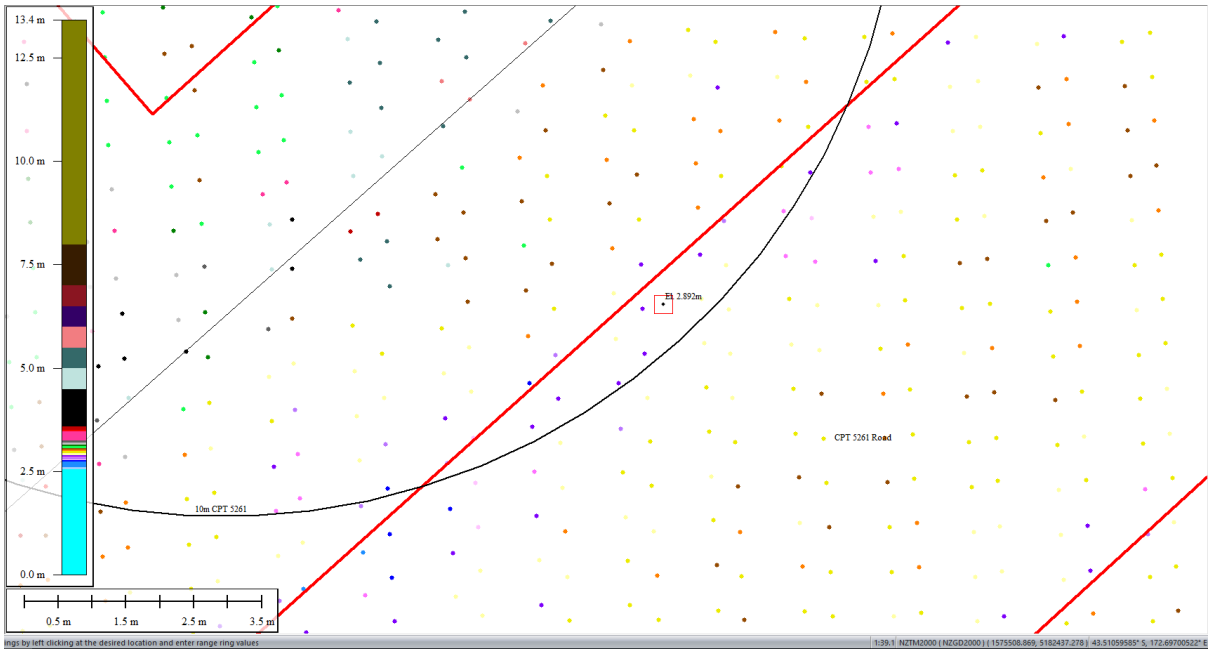

Figure 75: Ground surface elevation averaged over 10-m buffer for Road for Feb 2012 LiDAR survey.

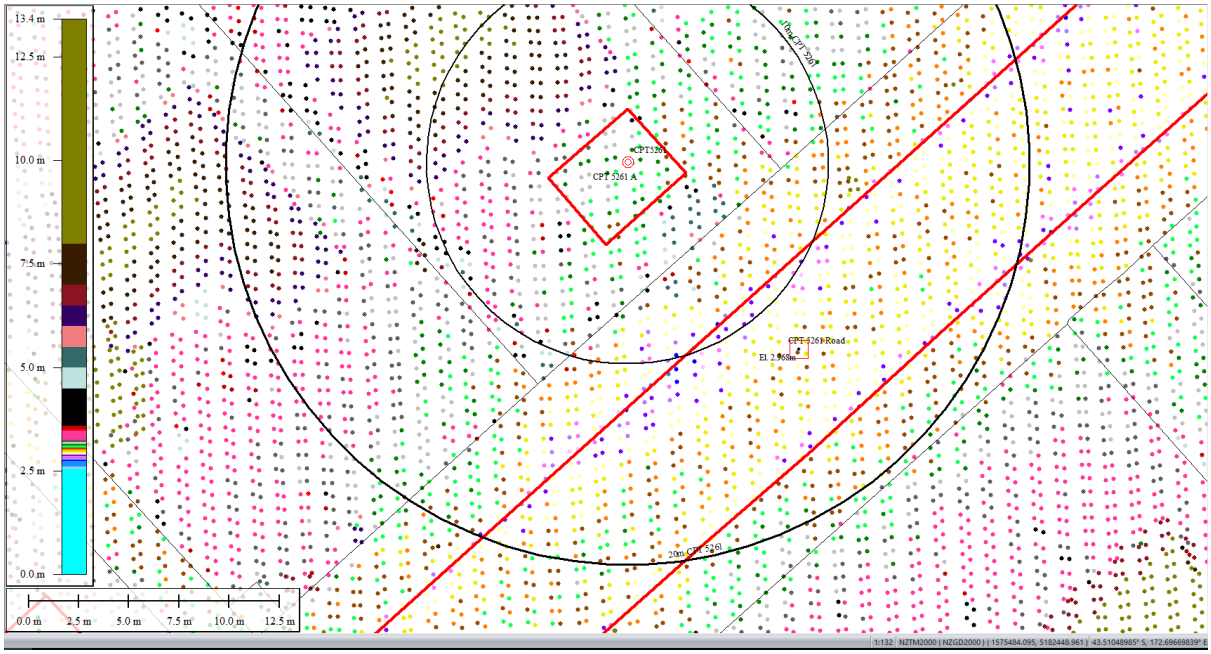

Figure 76: Ground surface elevation averaged over 20-m buffer for Road for Feb 2012 LiDAR survey.

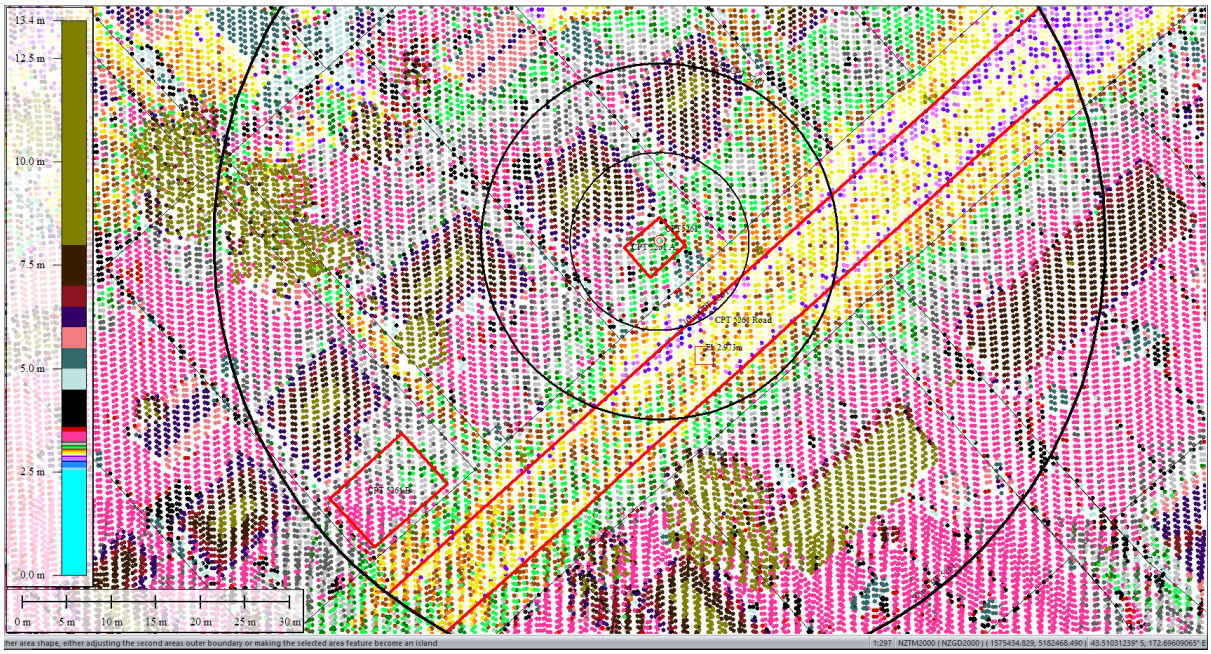

Figure 77: Ground surface elevation averaged over 50-m buffer for Road for Feb 2012 LiDAR survey.

Figure 78: Oct 2015 LiDAR survey.

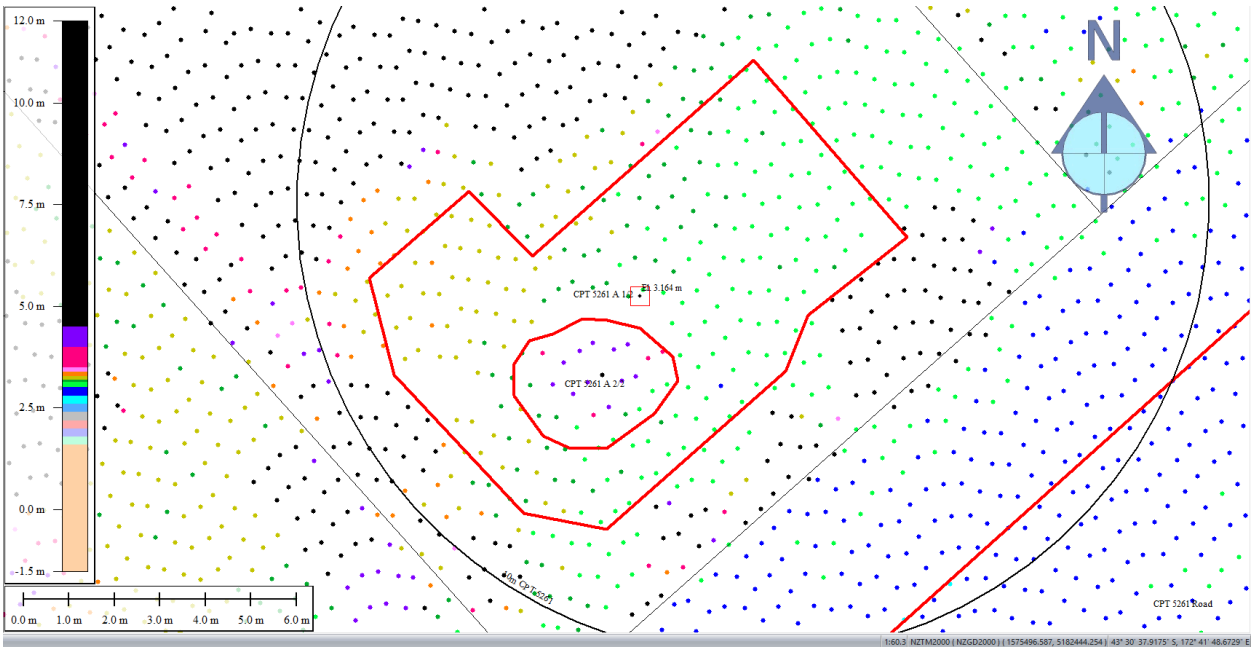

Figure 79: Ground surface elevation for Patch A for Oct 2015 LiDAR survey.

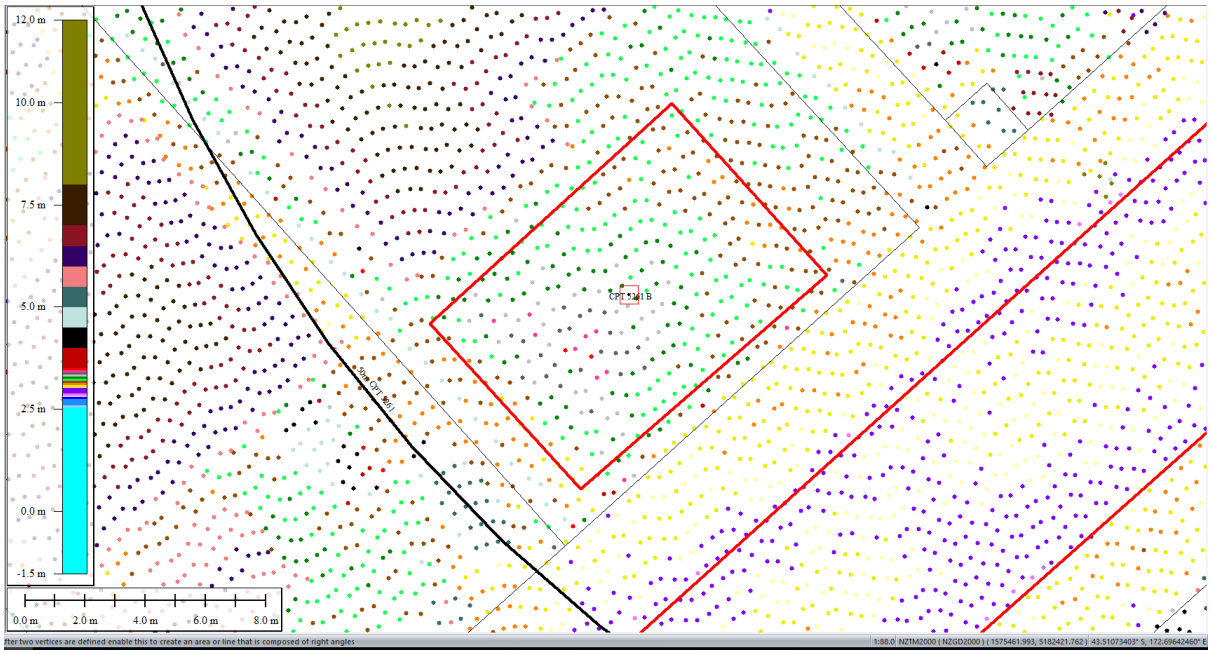

Figure 80: Ground surface elevation for Patch B for Oct 2015 LiDAR survey.

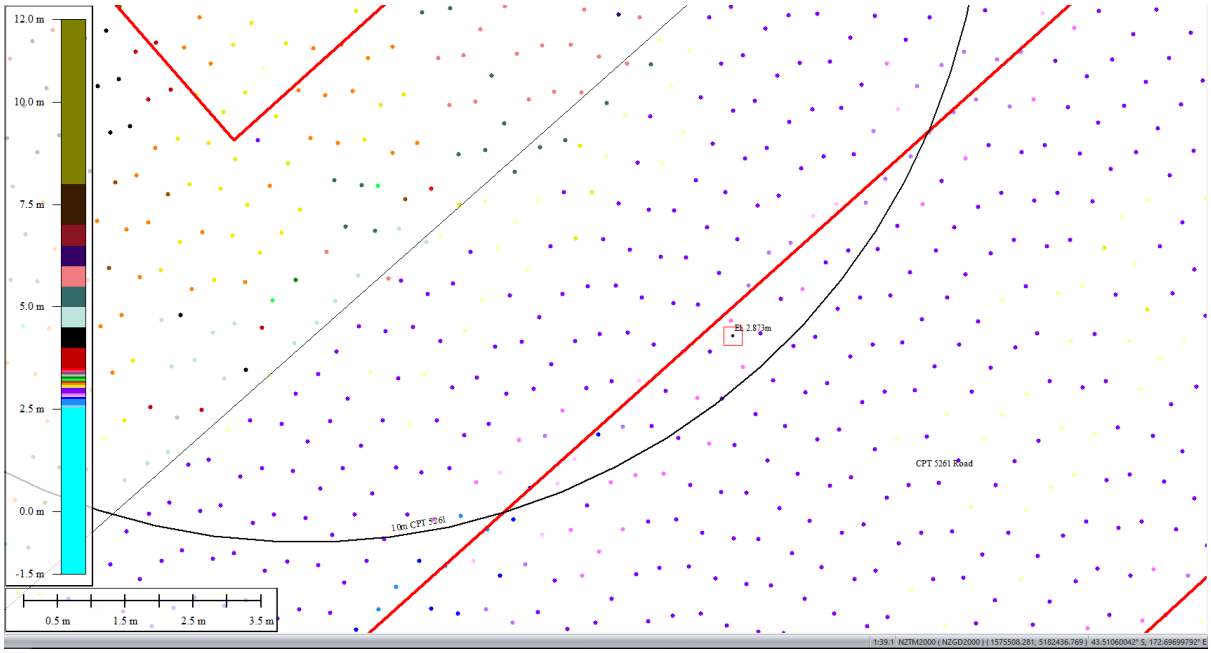

Figure 81: Ground surface elevation averaged over 10-m buffer for Road for Oct 2015 LiDAR survey.

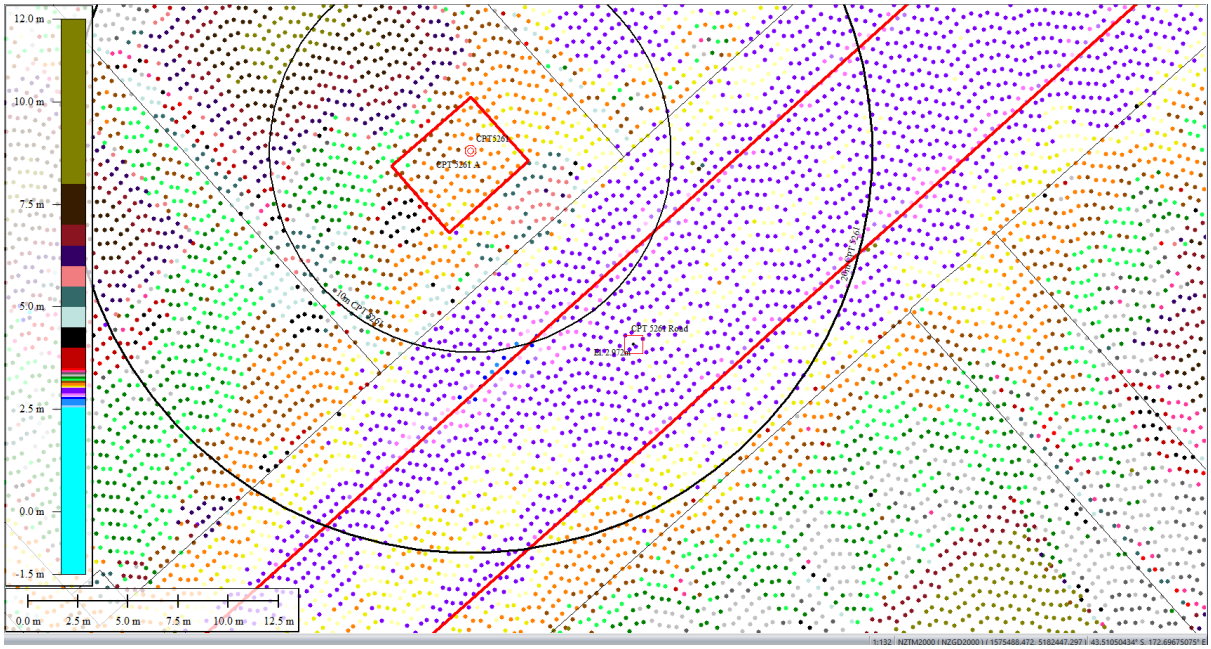

Figure 82: Ground surface elevation averaged over 20-m buffer for Road for Oct 2015 LiDAR survey.

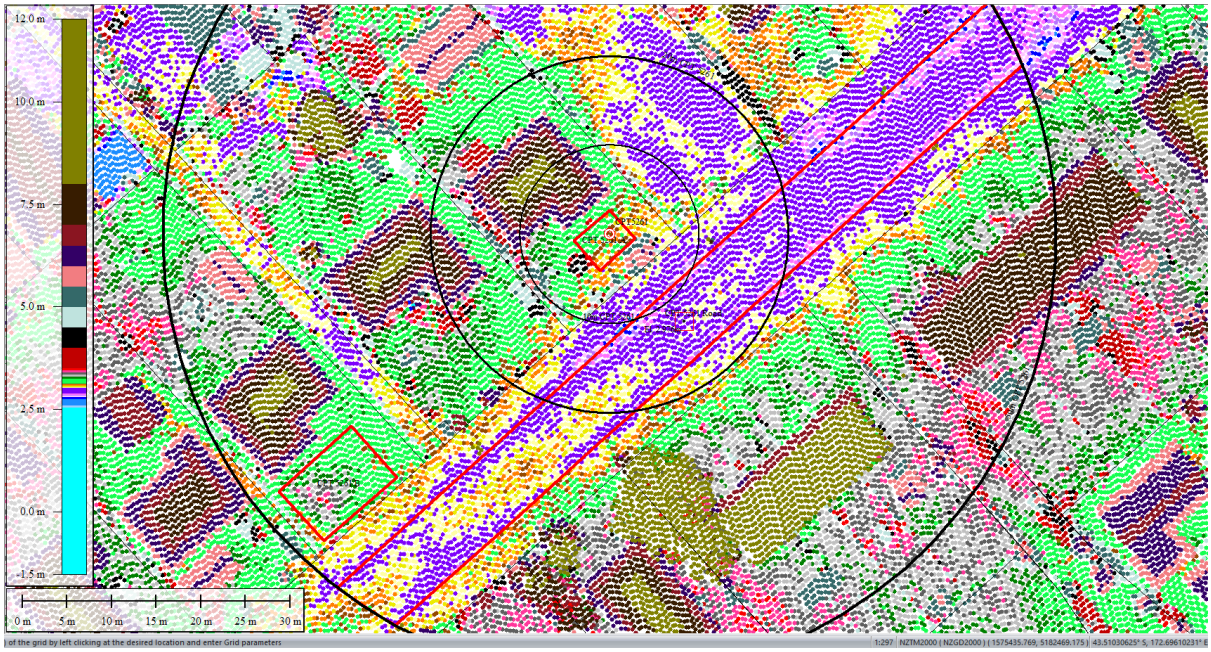

Figure 83: Ground surface elevation averaged over 50-m buffer for Road for Oct 2015 LiDAR survey.

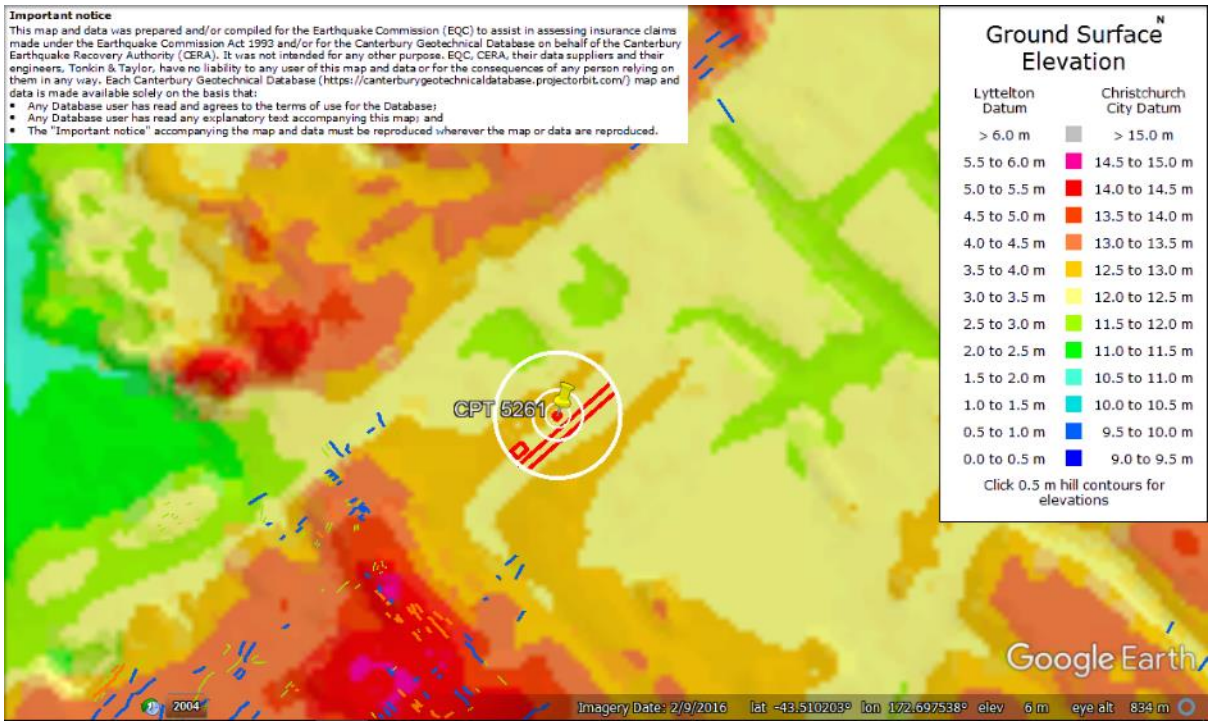

Figure 84: Ground surface elevation difference between the road and properties (LiDAR DEM for Sept 2010).

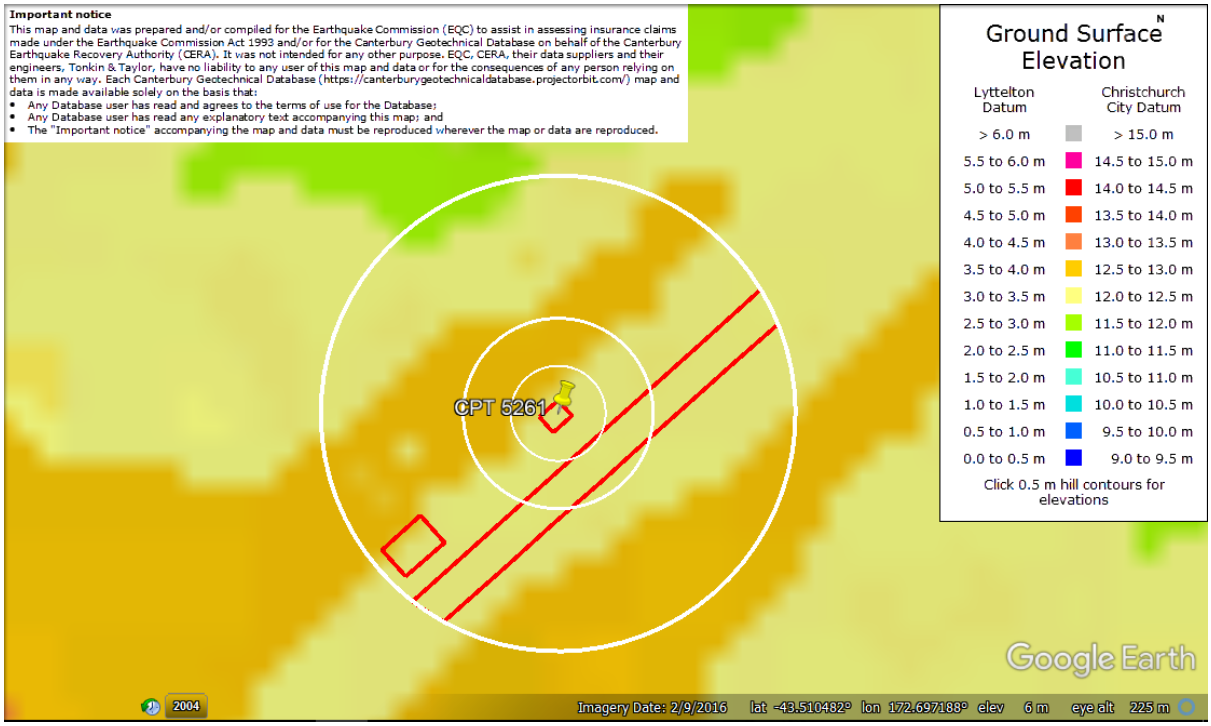

Figure 85: Enlarged view of ground surface elevation difference between the road and properties (LiDAR DEM for Sept 2010).

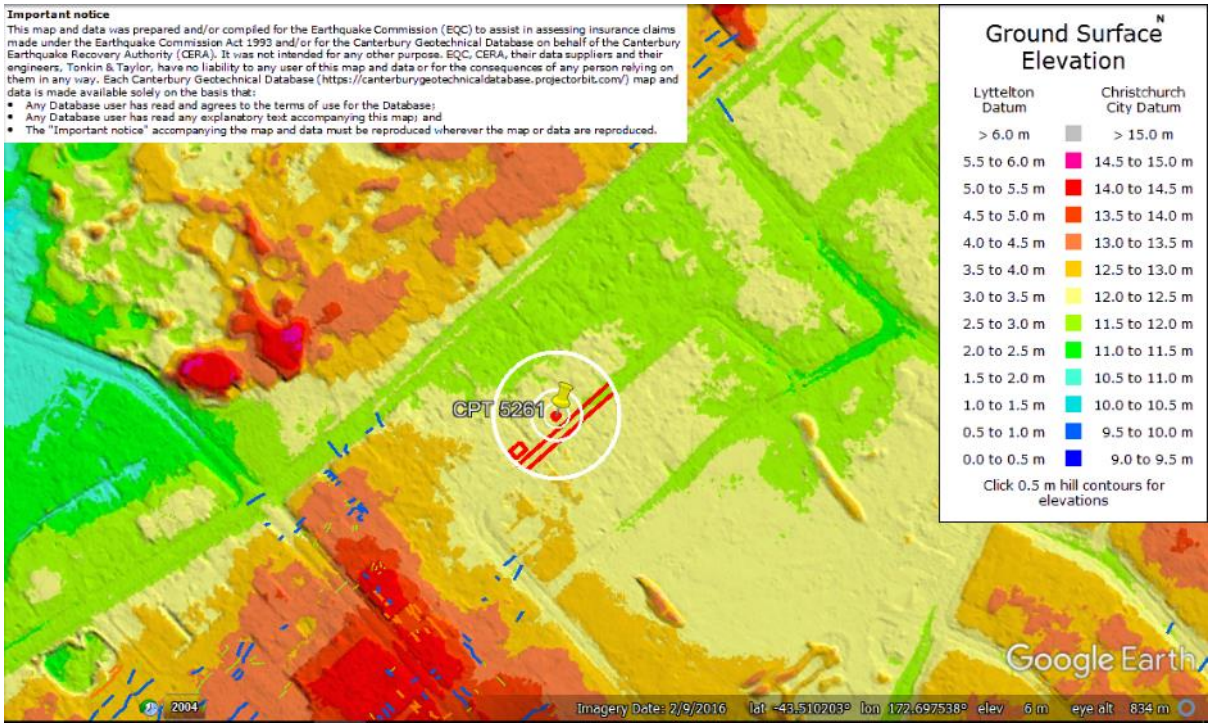

Figure 86: Ground surface elevation difference between the road and properties (LiDAR DEM for Sept 2011).

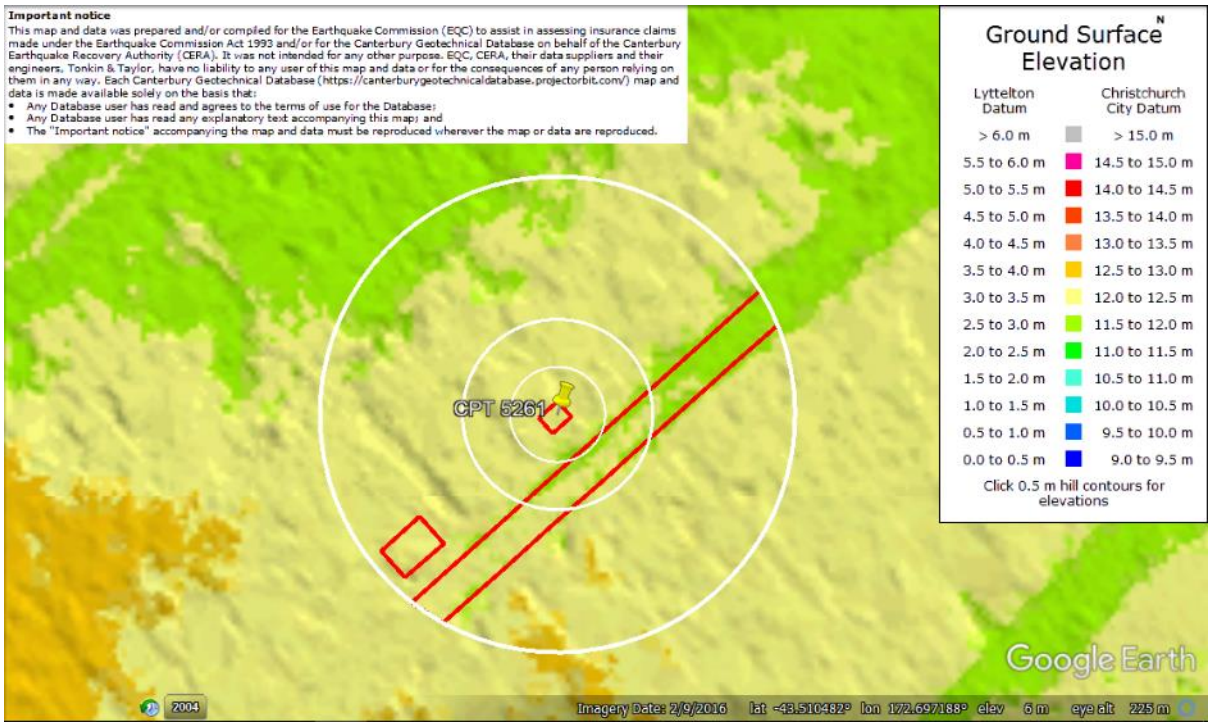

Figure 87: Enlarged view of ground surface elevation difference between the road and properties (LiDAR DEM for Sept 2011).

Figure 88: Absence of ejecta at the site for Sep-10 EQ.

Figure 89: Satellite image showing ejecta at the site for Feb-11 EQ.

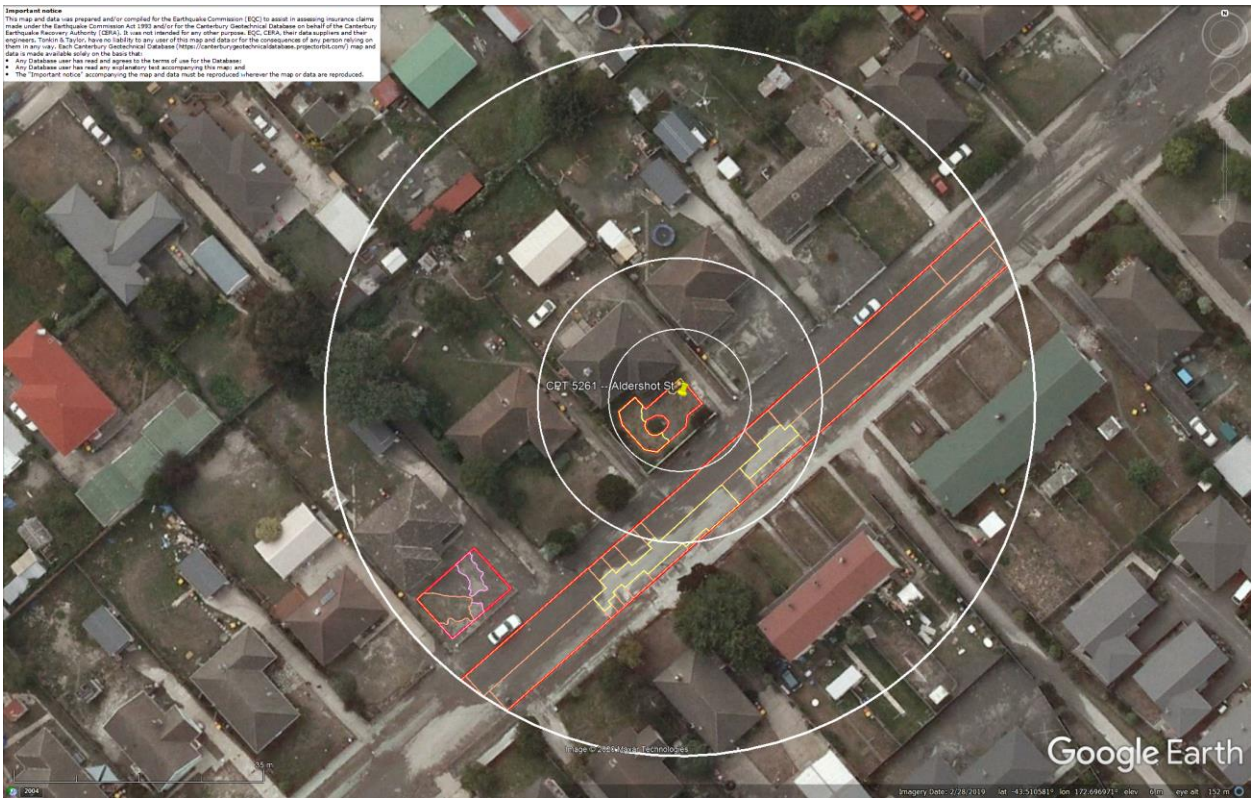

Figure 90: Ejecta outline for Feb-11 EQ.

Figure 91: Ejecta outline for Jun-11 EQ.

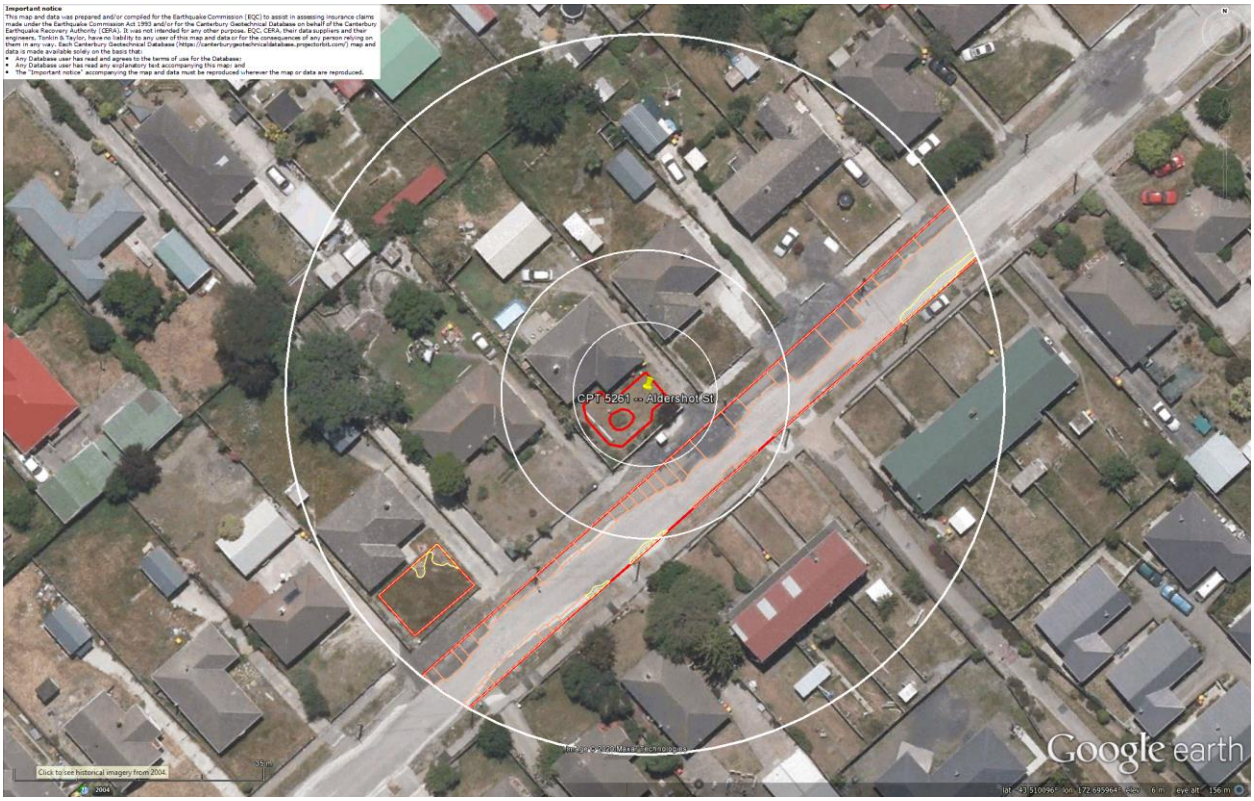

Figure 92: Ejecta outline for Dec-11 EQ.

Figure 93: Ground photographs of Patch A and ejecta remnants (photograph date: Sep 2011).

Contents of this figure cannot be shared as doing so is restricted by a Non-Disclosure Agreement.

Figure 94: LDAT property inspection notes for Patch A.

Figure 95: Ground photographs of Patch B and ejecta remnants (photograph date: Sep 2011).

Contents of this figure cannot be shared as doing so is restricted by a Non-Disclosure Agreement.

Figure 96: LDAT property inspection notes for Patch B.

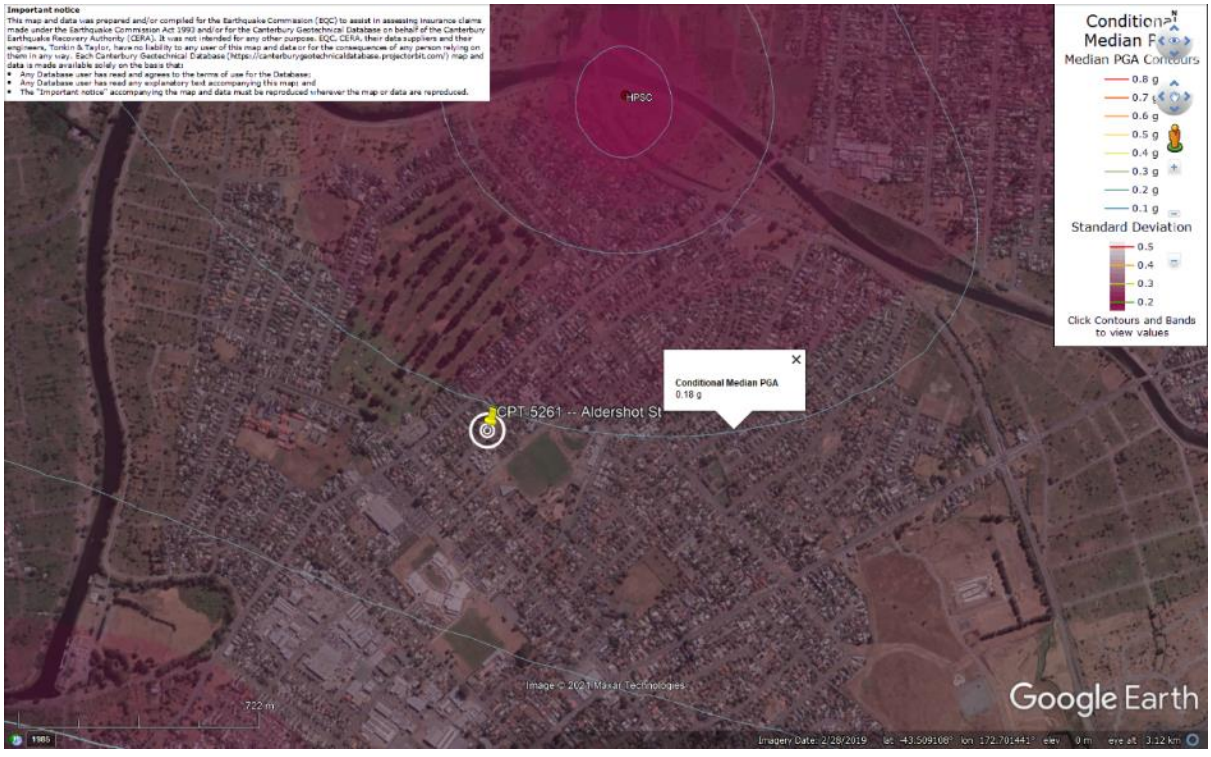

Figure 97: PGA for Sep-10 EQ (st. dev. = 0.300-0.325 ln units).

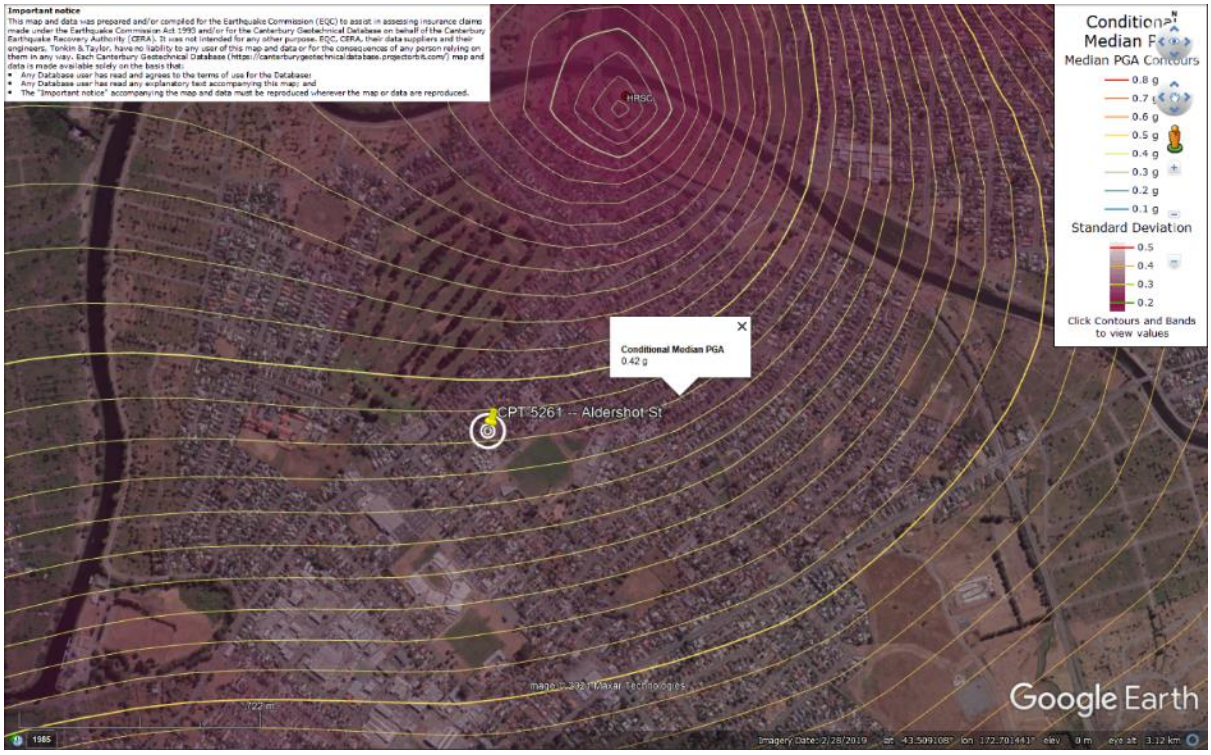

Figure 98: PGA for Feb-11 EQ (st. dev. = 0.300-0.350 ln units).

Figure 99: PGA for Jun-11 EQ (st. dev. = 0.325-0.350 ln units).

Figure 100: PGA for Dec-11 EQ (st. dev. = 0.350-0.375 ln units).

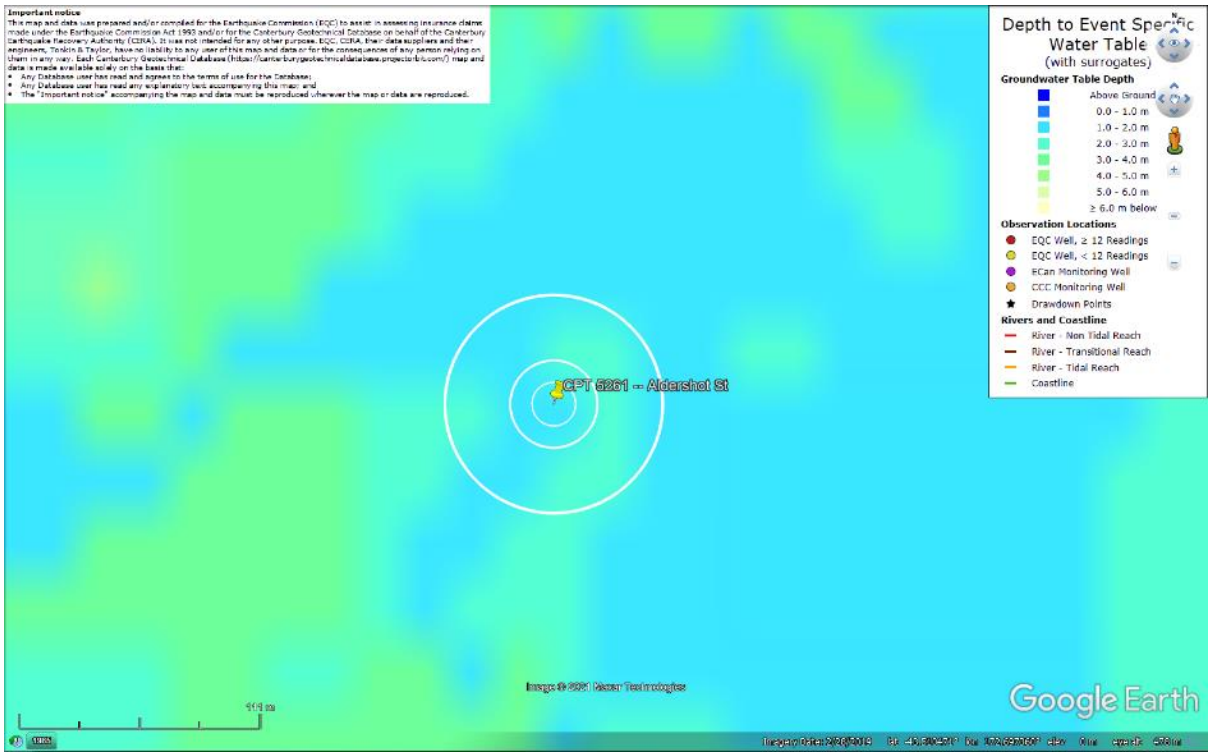

Figure 101: Depth to groundwater table for Sep-10 EQ.

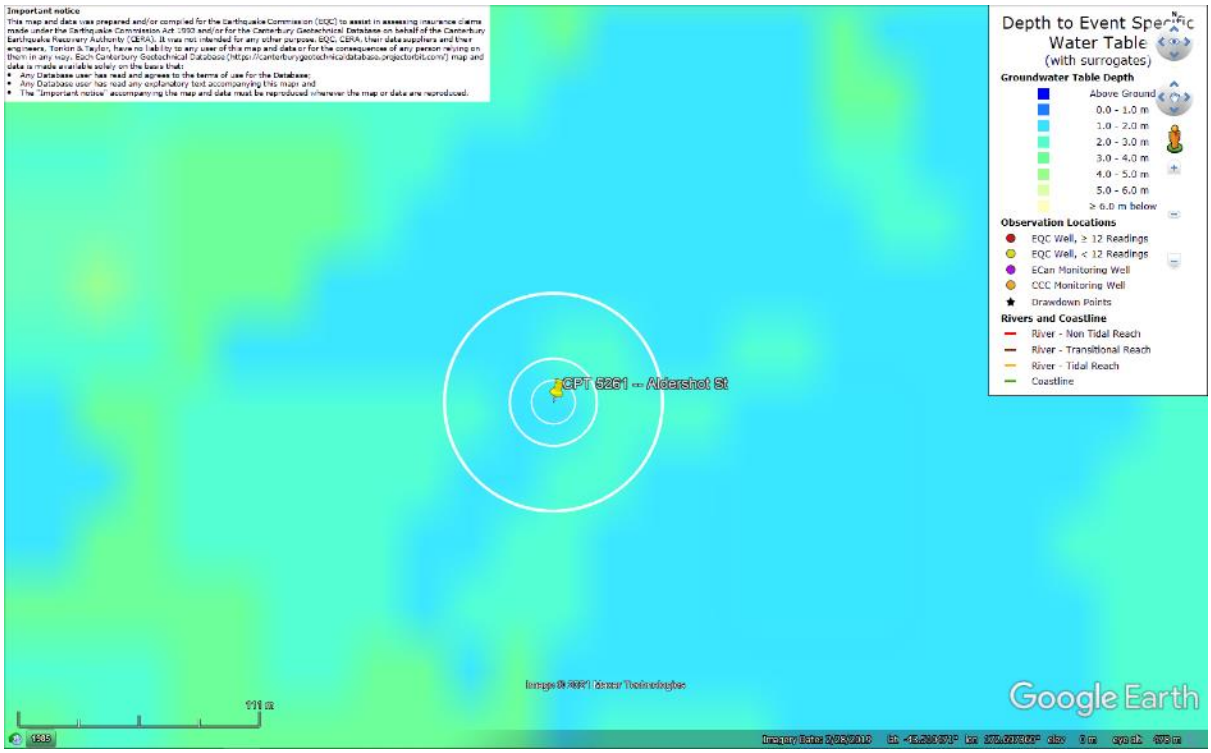

Figure 102: Depth to groundwater table for Feb-11 EQ.

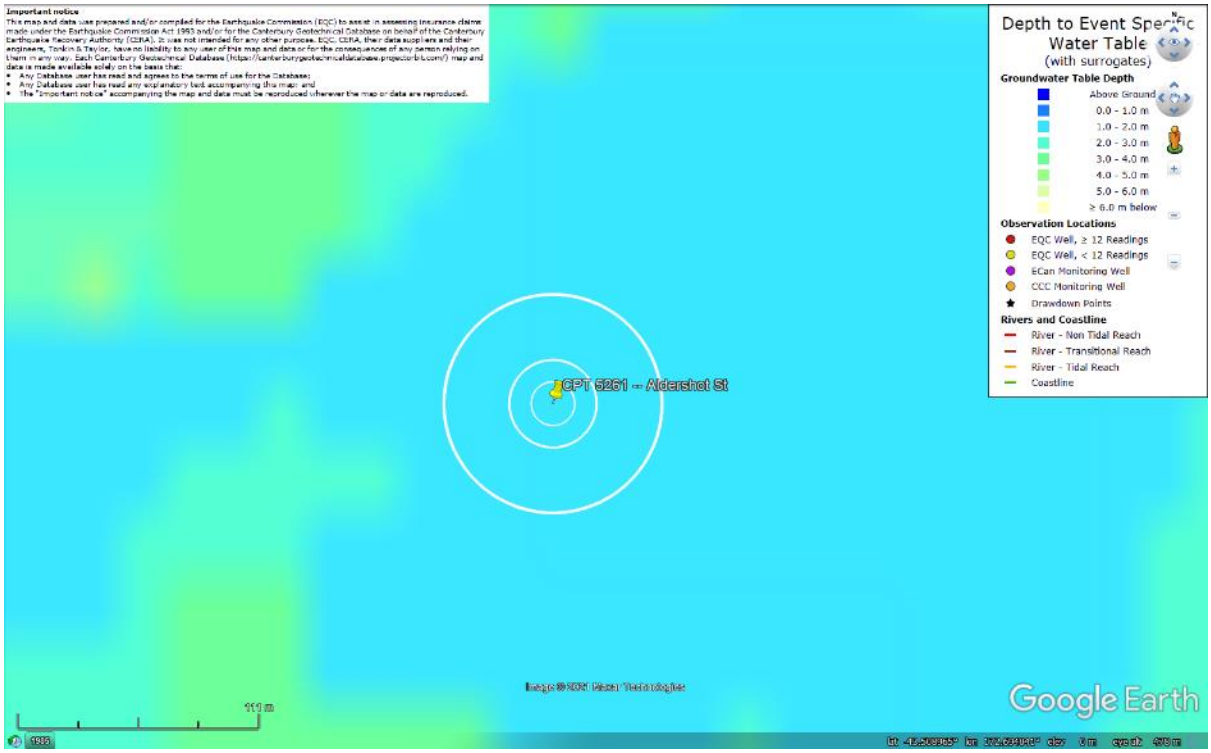

Figure 103: Depth to groundwater table for Jun-11 EQ.

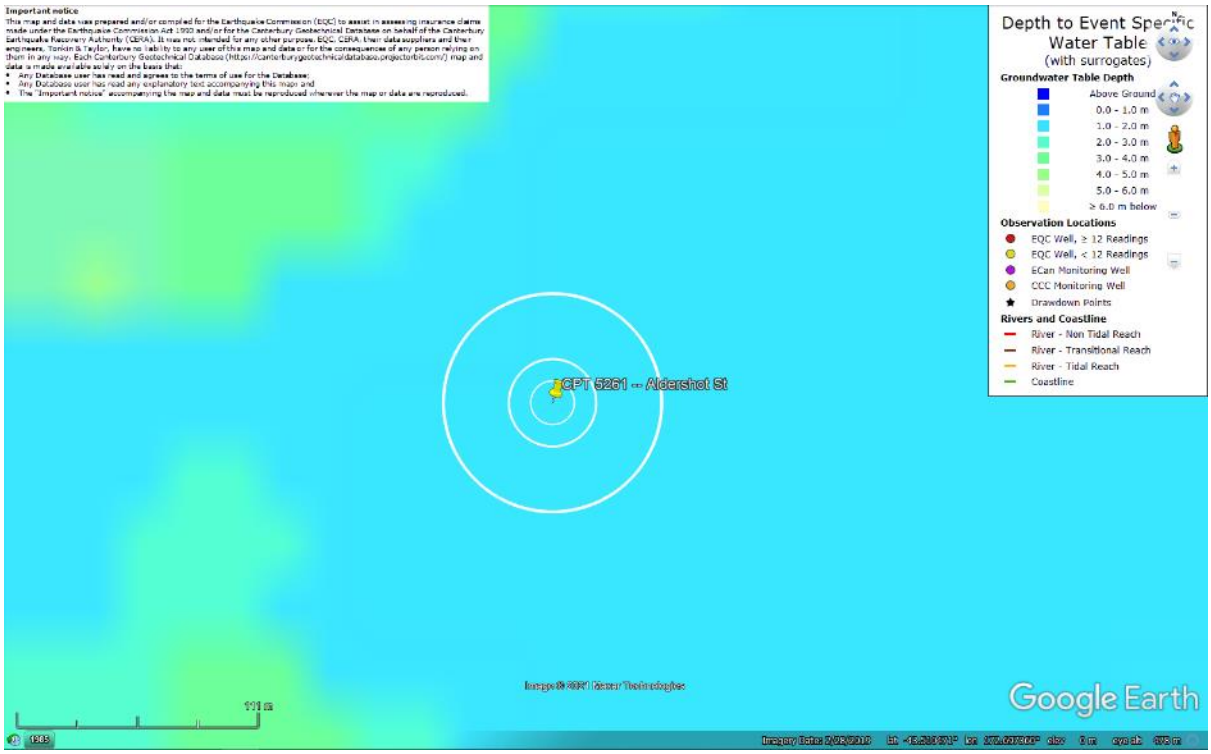

Figure 104: Depth to groundwater table for Dec-11 EQ.

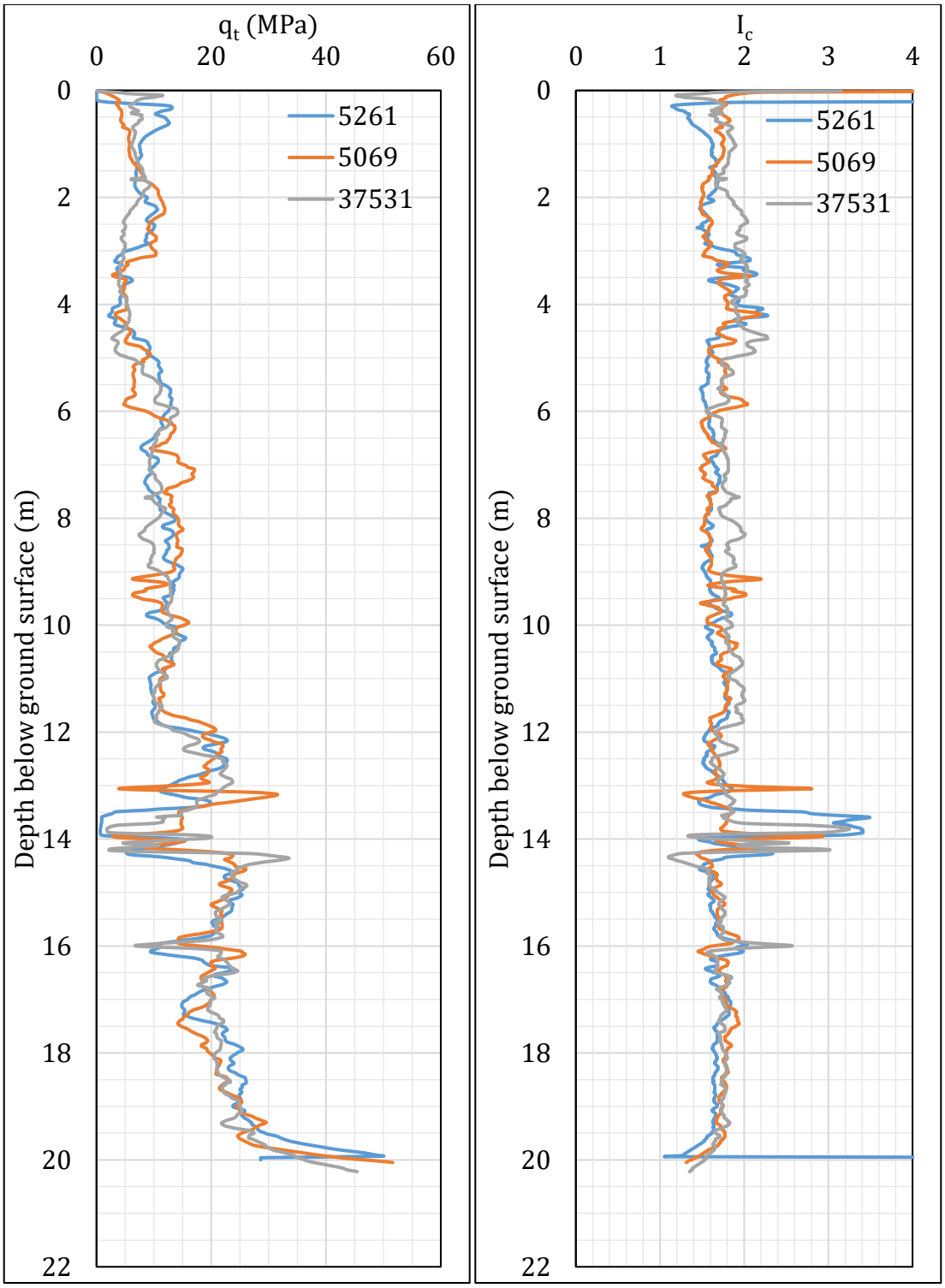

Figure 105: q_t and I_c profiles.

Note 9: The selection of CPTs for the area considered for settlement assessment (Figure 1) is based on the proximity of the CPTs to the considered areas. In accordance with that, the following table shows CPTs that were used for the volumetric settlement analysis in *Cliq v.3.0.3.2*, a CPT soil liquefaction software developed by GeoLogismiki. (The average volumetric settlements were reported in Table 8.)

Table 12: CPT profiles used in volumetric settlement analysis for areas selected for settlement assessment.

CPT ID No.	Patch A	Patch B	Road
5261	✓		✓
5069	✓		✓
37531		✓	✓

Table 13: CPT-based results.

		CPT ID		
EQ Event	Parameter	5261	5069	37531
Sep-10	S_{V1D} (mm)	20	17	5
	LSN	3	4	1
	LPI	0	0	0
	LPI_{ish}	0	0	0
	$D_{FS<1}$ (m)	undet.	undet.	undet.
Feb-11	S_{V1D} (mm)	152	111	83
	LSN	24	20	17
	LPI	15	12	7
	LPI_{ish}	9	5	3
	$D_{FS<1}$ (m)	2.9	3.12	2.59
Jun-11	S_{V1D} (mm)	80	67	32
	LSN	14	14	7
	LPI	4	5	1
	LPI_{ish}	0	2	0
	$D_{FS<1}$ (m)	3.09	3.26	3.47
Dec-11	S_{V1D} (mm)	99	77	42
	LSN	17	15	9
	LPI	6	6	2
	LPI_{ish}	3	4	0
	$D_{FS<1}$ (m)	3.02	3.14	3.20

Notes: $D_{FS<1}$ = Depth to the first liquefiable layer ($FS_L<1$) that is at least 200-mm thick, as determined by the Boulanger and Idriss (2016) liquefaction-triggering procedure (P_L=50%, C_{FC}=0.13, and $I_{c,cutoff}$ =2.6), and exported from *Cliq v.3.0.3.2*; undet. = the specified soil layer was not detected.

Note 10: Based on the borehole log (BH 13663, Figure 1), the groundwater table is at a depth of 1.5 m below the ground surface. The soil profile consists of (1) asphalt and gravelly fill to a depth of 0.2 m, (2) fine to medium sand, SP, of the Christchurch formation to a depth of 2.6 m, (2) sandy silt, ML, of the Christchurch formation to a depth of 4.1 m, and (3) fine to medium sand, SP, of the Christchurch formation to a depth of 20 m.

Note 11: The ejecta-induced free-field settlement provided in Table 11 is an areal average settlement due to ejecta, which is based on the total settlement assessment area, A_T (provided in Table 9 and repeated in Table 14). However, the considered area was not always covered completely with ejecta; thus, it is important to provide the localized ejecta-induced settlement, too. The localized settlement due to ejecta is estimated using photographic evidence only as

$$S_{E,P\_localized} = \frac{V_E}{A_E}$$

where V_E is the total volume of ejecta within A_T and A_E is the total coverage area of ejecta within A_T. Please note that the areal ejecta-induced settlement provided in Table 14 as S_{E,P_areal} is the same as $S_{E,P}$ in Table 11, which was estimated as

$$S_{E,P\_areal} = S_{E,P} = \frac{V_E}{A_T}$$

where V_E is the total volume of ejecta within A_T and A_T is the total settlement assessment area.

Table 14a: Areal and localized ejecta-induced settlement estimates for Patch A (10-, 20-, and 50-m buffers) based on photographic evidence.

Earthquake Event	A_T (m^2)	A_E (m^2)	V_E (m^3)	S_{E,P_areal} (mm)	$S_{E,P\_localized}$ (mm)
Sep-10	54.0	0	0	0	0
Feb-11	52.3	52.3	1.7-2.7	40±10	40±10
Jun-11	54.0	NA	NA	NA	NA
Dec-11	54.0	0	0	0	0

Notes: $S_{E,P\_areal} = S_{E,P}$ reported in Table 11 = areal ejecta-induced settlement; $S_{E,P\_localized}$ = localized ejecta-induced settlement; A_T = total settlement assessment area; V_E = total volume of ejecta within A_T; A_E = total area of ejecta within A_T; The estimates of both areal and localized ejecta-induced settlement are rounded to the nearest 5; Final plus/minus values are also rounded to the nearest 5; NA = Not available.

Table 14b: Areal and localized ejecta-induced settlement estimates for Patch B (50-m buffer) based on photographic evidence.

Earthquake Event	A_T (m^2)	A_E (m^2)	V_E (m^3)	S_{E,P_areal} (mm)	$S_{E,P\_localized}$ (mm)
Sep-10	81.2	0	0	0	0
Feb-11	81.2	81.2	5.9-9.0	90±20	90±20
Jun-11	81.9	23.2	0.9-2.3	20±10	70±30
Dec-11	81.9	81.9	1.5-3.0	30±10	30±10

Notes: $S_{E,P\_areal} = S_{E,P}$ reported in Table 11 = areal ejecta-induced settlement; $S_{E,P\_localized}$ = localized ejecta-induced settlement; A_T = total settlement assessment area; V_E = total volume of ejecta within A_T; A_E = total area of ejecta within A_T; The estimates of both areal and localized ejecta-induced settlement are rounded to the nearest 5; Final plus/minus values are also rounded to the nearest 5.

Table 14c: Areal and localized ejecta-induced settlement estimates for Road (50-m buffer) based on photographic evidence.

Earthquake Event	A_T (m^2)	A_E (m^2)	V_E (m^3)	S_{E,P_areal} (mm)	$S_{E,P\_localized}$ (mm)
Sep-10	730	0	0	0	0
Feb-11	698	698	41.7-66.5	80±15	80±15
Jun-11	717	717	26.2-45.8	50±15	50±15
Dec-11	730	316	13.7-20.3	25±5	55±10

Notes: S_{E,P_areal} = $S_{E,P}$ reported in Table 11 = areal ejecta-induced settlement; $S_{E,P\_localized}$ = localized ejecta-induced settlement; A_T = total settlement assessment area; V_E = total volume of ejecta within A_T; A_E = total area of ejecta within A_T; The estimates of both areal and localized ejecta-induced settlement are rounded to the nearest 5; Final plus/minus values are also rounded to the nearest 5.

Summary 2:

- **The best estimate of the localized ejecta-induced free-field ground settlement at the Aldershot St site for the SEP 2010, FEB 2011, JUN 2011, and DEC 2011 earthquake is 0 mm, 90±20 mm, 70±30 mm, and 30±10 mm, respectively.**
- **The best estimate of the localized ejecta-induced settlement of the road at the Aldershot St site for the SEP 2010, FEB 2011, JUN 2011, and DEC 2011 earthquake is 0 mm, 80±15 mm, 50±15 mm, and 55±10 mm, respectively.**